CYSTIC FIBROSIS: THE ROLE OF AIRWAY STEM CELLS IN SUSTAINED GENE EXPRESSION BY LENTIVIRAL DIRECTED GENE THERAPY

NIGEL FARROW

BMedSc Flinders University
BHSc Medicine (Hons) first class
The University of Adelaide

Submitted in fulfilment of the Degree of Doctor of Philosophy (PhD)

28 April 2015

University of Adelaide
School of Paediatrics and Reproductive Health
Robinson Research Institute

Declaration

I certify that this work contains no material which has been accepted for the award of any other degree or diploma in my name, in any university or other tertiary institution and, to the best of my knowledge and belief, contains no material previously published or written by another person, except where due reference has been made in the text. In addition, I certify that no part of this work will, in the future, be used in a submission in my name, for any other degree or diploma in any university or other tertiary institution without the prior approval of the University of Adelaide and where applicable, any partner institution responsible for the joint-award of this degree.

I give consent to this copy of my thesis when deposited in the University Library, being made available for loan and photocopying, subject to the provisions of the Copyright Act 1968.

The author acknowledges that copyright of published works contained within this thesis resides with the copyright holder(s) of those works.

I also give permission for the digital version of my thesis to be made available on the web, via the University's digital research repository, the Library Search and also through web search engines, unless permission has been granted by the University to restrict access for a period of time.

Signed:

Date: 28 April 2015

This Thesis is dedicated to my daughter

Ella Farrow.

My very special little girl, your determination to enjoy life to its fullest despite having the insidious disease Cystic Fibrosis is a source of inspiration which drives me every day. Darling this is for you.

Acknowledgements

Publications and awards

Publications arising from this work

Cmielewski, P, **Farrow, N**, et al, Transduction of ferret airway epithelia using a pre-treatment and lentiviral gene vector. BMC Pulm Med, 2014. 14 (1): p. 183. DOI:10.1186/1471-2466-14-183.

Cmielewski, P, and **Farrow, N**, were equal contributing first authors.

N. Farrow, D. Miller, P. Cmielewski, M. Donnelley, R. Bright, D. Parsons, "Airway gene transfer in a non-human primate: Lentiviral gene expression in marmoset lung", Scientific Reports, 3, 2013. P.4. DOI: 10. 1038/srep01287.

Kaye S. Morgan, Martin Donnelley, **Nigel Farrow**, Andreas Fouras, Naoto Yagi, Yoshio Suzuki, Akihisa Takeuchi, Kentaro Uesugi, Richard C. Boucher, Karen K. W. Siu*, and David W. Parsons*. "In vivo x-ray imaging reveals improved airway surface hydration after Cystic Fibrosis airway therapy" American Journal of Respiratory and Critical Care Medicine 2014, 190, 4.

Martin Donnelley, Kaye S. Morgan, Karen K. W. Siu, **Nigel R. Farrow**, Charlene S. Stahr, Richard C. Boucher, Andreas Fouras & David W. Parsons, "Non-invasive airway health assessment: Synchrotron imaging reveals effects of rehydrating treatments on mucociliary transit in-vivo", Scientific Reports, 4, 2014. DOI: 10.1038/srep03689.

Martin Donnelley, Kaye S. Morgan, Karen K. W. Siu, Andreas Fouras, **Nigel R. Farrow**, Richard P. Carnibella and David W. Parsons "Tracking extended mucociliary transport activity of individual deposited particles: longitudinal

synchrotron X-ray imaging in live mice" Journal of synchrotron radiation, 21, 2014. DOI: 10.1107/S160057751400856X.

Abstracts Presented At National and International Conference Meetings

2014

Patricia Cmielewski, **Nigel Farrow**, Chantelle McIntyre, Harsha Padmanabhan, Martin Donnelley, Tim Kuchel, and David W Parsons." Lentiviral airway gene transfer in normal ferrets" American Society for Gene and Cell Therapy, Washington, USA.

Nigel Farrow, Martin Donnelley, Patricia Cmielewski, Ivan Bertoncello , David Parsons. "Gene therapy for CF: is long term expression a consequence of transducing conducting airway endogenous respiratory stem cells?" presented at the North America Cystic Fibrosis Conference, Atlanta, Georgia, USA, 2014.

2013

Nigel Farrow, Jonathan L McQualter, David Parsons, Ivan Bertoncello. "Endogenous stem/progenitor cell compartments of conducting airways differ in cystic fibrosis and normal mice, presented at the British Society for Gene and Cell Therapy conference, Royal Holloway, University of London, London.

Nigel Farrow, Jonathan L McQualter, David Parsons, Ivan Bertoncello' "Analysis of endogenous airways stem/progenitor cell types in CF and normal mice and the role of basal cells in sustained gene expression following airway gene transfer"**,** presented at the Cystic fibrosis Australia conference, Auckland, New Zealand, 2013

Martin Donnelley, Kaye Morgan, Karen Siu, Andreas Fouras, **Nigel Farrow**, Richard Carnibella and David Parsons, "Advances in airway surface imaging for cystic fibrosis: extended monitoring of individual particle mucocilary clearance" presented at the Cystic fibrosis Australia conference, Auckland, New Zealand, 201 Ivan Bertoncello, **Nigel Farrow**, Jonathan McQualter, David Parsons.

Evidence of an Expanded and Dysregulated Airway Epithelial Stem Cell Compartment in Cystic Fibrosis Mice, Stem Cells and Cell Therapies in Lung Biology and Diseases conference, Vermont, Burlington, USA, 2013.

2012

Martin Donnelley, Kaye Morgan, Karen Siu, **Nigel Farrow**, Charlene Chua, Andreas Fouras and David Parsons, "Non-invasive airway health assessment: Synchrotron imaging reveals effects of therapeutics on mucociliary transit function" presented at the Medical Applications of Synchrotron Radiation conference, Shanghai, China, 2012.

K. Morgan, M. Donnelley, D. Paganin, A. Fouras, **N. Farrow**, Y. Suzuki, A. Takeuchi, K. Uesugi, N.Yagi, D. Parsons, K. Siu, "Assessing new treatments for cystic fibrosis using micron-scale live phase contrast x-ray imaging of the airway surface liquid", presented at the Medical Applications of Synchrotron Radiation conference, Shanghai, China, 2012.

Jonathan L McQualter, **Nigel Farrow**, David Parsons, Ivan Bertoncello, "Endogenous Lung Epithelial Stem/Progenitor Cell Compartments Differ In Cystic Fibrosis and Normal Mice", presented at the North America Cystic Fibrosis Conference, Orlando, Florida, 2012.

2011

D Parsons, **N Farrow**, D Miller, S Le Blanc, R Bright , P Cmielewski and D S Anson, "One Year Persistence From a Single HIV-1 Lentiviral Vector Delivery Into Marmoset Lung: LacZ and Vector Gene Presence" presented at the American Society of Gene & Cell Therapy conference, Seattle, North America, 2011

Awards Received

Robinson Research Institute, research travel award 2014

Adelaide University Post Graduate Conference Best Poster Presentation 2012

MS McLeod Foundation PhD scholarship 2011-2014

Cystic Fibrosis Australia PhD scholarship 2011-2014

APA PhD scholarship (declined) 2011

Letter of Commendation from Lord Mayor of Adelaide, South Australia 2010

Golden Key Honour Society 2009

Flinders University Chairperson's Letter of Commendation 2008 and 2009

Synopsis

In this thesis transduction of airway stem cells (basal cells) in the nasal and tracheal airways was investigated to determine the causality of sustained transgene expression following a gene therapy protocol that utilised an LPC pre-treatment and a HIV-1 VSV-G pseudotyped lentivirus vector treatment, as previously published. To assess stem cell transduction and epithelial regrowth a forced-injury model was employed at a number of time points after the gene therapy protocol.

Epithelial remodelling in cystic fibrosis and normal airways of mice was also assessed. Airway stem cell hyperplasia and goblet cell hyperplasia and hypertrophy, and epithelial mucin content were assessed in the trachea and in some instance the nasopharynx in the nasal airways of CF and normal mice.

Additionally, the effectiveness of the LPC / lentiviral gene therapy protocol was assessed in lung airways of normal ferrets and the marmoset, a non-human primate, to determine if airway transduction of both differentiated ciliated cells and stem cells reflected observations noted in previously-published mouse-based studies. These ferret and marmoset animal studies have been published prior to thesis submission.

Airway stem cells transduction was confirmed in the trachea and nasal airways of mice following pre-treatment with LPC and subsequent treatment with a HIV-1 VSV-G pseudotyped lentiviral vector carrying the LacZ marker gene. A forced injury model was employed to force regeneration of the airway epithelium after vector treatment. Following the ablation and subsequent regeneration of the airway epithelium, clusters of LacZ positive were observed in both the trachea and nasal airways suggesting transduction of the airway stem cells and the passing of the

transgene to their progeny upon differentiation.

Airway epithelial remodelling was demonstrated in both airway stem cells and goblet cells in CF mice. Hyperplasia of airway stem cells and goblet cells in CF mice was observed. Hypertrophy and change in mucin acidity of goblet cells was also observed. Additionally, remodelling of the cartilage rings in the trachea was observed in CF mice. This is the first study to demonstrate the presence of goblet cell hyperplasia, hypertrophy and change in mucin acidity in the presence of airway stem cell hyperplasia. Importantly, the hyperplasia of airway stem cells in CF airways had previously been proposed however, this is the first study to directly quantitate the airway stem cell compartment using a novel flow cytometry and clonogenic assay approach.

Finally, the transduction of airway stem cells and ciliated cells is shown in normal ferrets and marmosets, a non-human primate. Validation of transducing relevant airway cell type in these animals adds to the gene therapy proof of principle foundation previously demonstrated in the airways of mice.

Contents

Figure list

1 Introduction

1.1 Cystic fibrosis: A historical perspective

Cystic fibrosis (CF), a lethal monogenic disorder is the most common chronic autosomal recessive disease within the Caucasian population affecting approximately one per 2500 newborns [1]. The first documented scientific history of CF did not appear until well into the 1930's in a paper written on the disease by a Swiss paediatrician [2], however there are previous writings which hint at the presence of this disease dating back as far as the 16th century. In what is possibly the earliest accurate medical description of insufficiency and lesions of the pancreas, associated with CF can be found in an autopsy report of an 11 year old girl by Pieter Pauw in 1595. This report documented his observations that "the child was meagre with a swollen, hardened, gleaming white pancreas"[3], a description consistent with today's observations of pancreatic deficiency associated with CF. Furthermore there is anecdotal evidence from the 1600s that suggests the CF hallmark of excessive salt loss in sweat was associated with early mortality. In 1606, a professor of medicine in Henares, Spain, Alonso y de los Ruyzes de fonteca wrote "that it was known that the fingers tasted salty after rubbing the head of the bewitched child" [3]. There is also similar reference within German folklore from the middle ages "Woe to that child, which when kissed on the forehead tastes salty; he is 'bewitched' and soon must die" [4]. These writings suggest that while in modern medicine CF wasn't formerly classified until the 20th century, Europeans had recognised much earlier the symptoms of the disease and associated it with early mortality.

With the turn of the 20th century observations began to associate lung disease with diarrhoea and abnormal familial steatorrhea [5], however the disease still remained

nameless and was often thought of as a form of coeliac disease. It was in 1936 that Fanconi recognised the disease was unconnected to coeliac disease and referred to it as "cystic fibromatosis with bronchiectasis" [2] and in 1938, Andersen used the term cystic fibrosis of the pancreas [6] . In 1945 due to Andersens focus on the pancreas and the belief by Farber [7] that the cause of the disease was a thickening of the mucus, he coined the term mucoviscidosis and this name for the disease is still widely used today outside English-speaking European countries [7]. In the ensuing years Andersen and Hodges refined the observations and provided the first evidence of a genetic basis of the disease and correctly identified it as a result of an autosomal recessive mutation [8]. It was at this time that Andersen noticed a high increase in heat prostration in patients at Columbia Hospital during a heat wave in New York [9], furthermore 50% of those effected were known to have CF. Intrigued by the salt loss that had precipitated the heat prostration, a colleague of Andersen's, di Sant'Agnese, set about determining the cause for the high incidence amongst CF patients. His findings concluded that the abnormally elevated electrolyte content of sweat in CF patients was due to a disturbance in the sweat glands themselves. Furthermore, and more importantly, he pointed out that it was a hallmark of those inflicted with this disease [10]. Indeed the elevated electrolyte content soon became (and still is) a common method of diagnosis of CF in the form of the sweat test [11] and thus 20th century CF medicine and the observations of medieval Europe had come full circle.

In the 1950s the life expectancy of infants with CF improved with the introduction of pancreatic enzyme supplements and at this time the respiratory manifestations of the disease became more perceptible. The first detailed report discussing the detrimental effects of CF on the lungs had recently been published [12] and the use of antibiotics

2

to treat the common infections of the lung had begun [13, 14]. It was also at this time that pulmonary function tests were introduced to monitor the decline of lung health in CF patients [15] and such tests remain in use today.

1.2   Mapping, isolating and sequencing of the CF gene

While there had been a breakthrough in the understanding, identification and naming of CF as a disease unto itself in the first half of the 20th century it became clear that to gain further insights into the mechanisms behind the disease required exploration on a genetic and molecular level. The first step was realised in 1985, with the aid of the polymorphic marker DOCRI-91, the CF gene was first localised and mapped to chromosome 7q31.2 [16, 17]. The gene was subsequently isolated and sequenced in 1989 using the technique of positional cloning [18-20]. Following sequencing it was revealed that there are approximately 180,000 base pairs in the CF gene encoding 1480 amino acids [21].

1.3   The CFTR protein

 The product of the CF gene was determined to be a membrane protein of 168,173 daltons involved in ion transport and regulation, thus it was named the cystic fibrosis transmembrane conductance regulator (CFTR) [22]. The CFTR protein is a cAMP-dependant ATP-gated ion channel and as such belongs to the ATP binding cassette transporter superfamily of proteins [19, 23], which are involved in the ATP–dependent transport of large molecules across the cellular membrane (Figure 1-1)
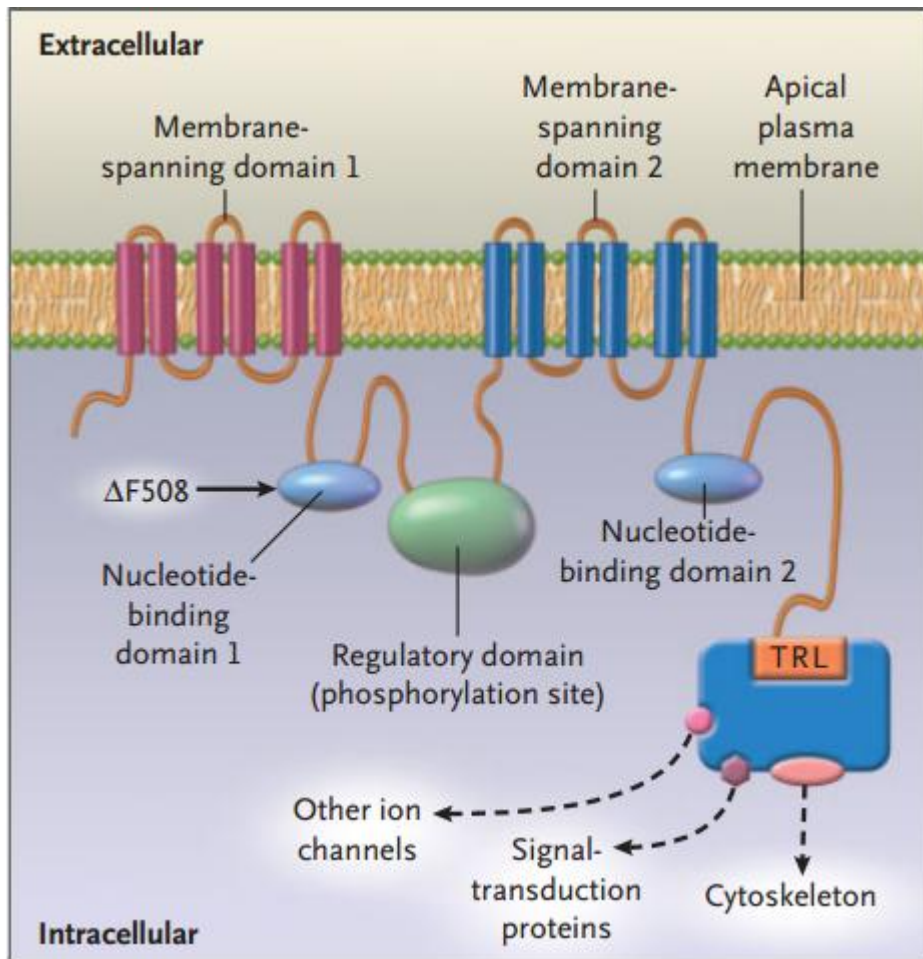
Figure 1-1: The CFTR channel.

The CFTR protein consists of 1480 amino acids, folded into globular and transmembrane domains [21]

1.3.1 Genetic mutations of the Cystic fibrosis gene

The relation between CF genotype and phenotype is complicated by the existence of over 2000 different CF mutations [21] and possible interactions among these mutations, the environment, and other genetic modifiers [24]. The Mutations can be grouped into six classes on the basis of CFTR protein alterations: Class I: no synthesis; Class II: block in processing; Class III: block in regulation; Class IV: altered conductance; Class V: reduced synthesis and Class VI: decreased CFTR stability (Figure 1-2).

	Normal	I	II	III	IV	V	VI
CFTR defect		No functional CFTR protein	CFTR trafficking defect	Defective channel regulation	Decreased channel conductance	Reduced synthesis of CFTR	Decreased CFTR stability
Type of mutations		Nonsense; frameshift; canonical splice	Missense; aminoacid deletion	Missense; aminoacid change	Missense; aminoacid change	Splicing defect; missense	Missense; aminoacid change
Specific mutation examples[11]		Gly542X Trp1282X Arg553X 621+1G→T	Phe508del Asn1303Lys Ile507del Arg560Thr	Gly551Asp Gly178Arg Gly551Ser Ser549Asn	Arg117His Arg347Pro Arg117Cys Arg334Trp	3849+10kbC→T 2789+5G→A 3120+1G→A 5T	4326delTC Gln1412X 4279insA

Figure 1-2: CFTR class mutations.

Schematic diagram illustrating the classes of defects in the CFTR gene, their locations within the cell and the consequence on the mutations within the different classes [25].

Although there are over 2000 different mutations only a small number are prevalent and even less result in severe lung disease and pancreatic insufficiency (PI) (Table 1-1). The most common CF mutation termed ΔF508 is characterised by both severe lung disease and PI and is present in approximately 70% of defective CFTR alleles [21]. ΔF508 is a class II mutation caused by an in-frame deletion of phenylalanine at position 508 in exon 10 on chromosome 7, resulting in a temperature sensitive folding defect. The result is retention of the CFTR in the endoplasmic reticulum and degradation by the proteasome [26], producing a loss of chloride channels in the lipid bilayer on the apical surface of the epithelial cells [27].

Haplotype analysis of CF chromosomes carrying the ΔF508 CF gene mutation has suggested that a founder event (single mutation event) is responsible for the prevalence of this mutation rather than a series of multiple events [18]. While the incidence of other CFTR mutations is relatively low such founder events can

increase the frequency within specific ethnic populations. As an example the class 1 mutation W1282X represents ~ 2% of CF mutations worldwide however, it is present in 60% of CFTR mutations in the Ashkenazi Jewish group [21]. Furthermore the W1282X mutation is an example of a premature truncations or nonsense alleles [21] which are responsible for approximately 5 to 10 percent of all CFTR mutations.

Table 1-1: List of common CF mutations, classes, ethnic incidence and symptoms.

Mutation	Class	Ethnic incidence	symptoms
W1282X*	I	60% Ashkenazi Jews (2.0% worldwide)	Severe lung disease PI
G542X*	I	3.4% worldwide	PI
R553X*	I	1.3% worldwide	PI
N1303K*	II	1.8% worldwide	PI
ΔF508	II	70 – 75% North America 82% Denmark 32% Turkey	Severe lung disease PI
G551D*	III	2.4% worldwide	PI
A455E*	IV	8.3% French Canada 1% Dutch < 1% worldwide	Variable lung disease PI
3849 + 10 kb C→T*	V	< 1% worldwide	Variable lung disease PI

* Compound heterozygotes (i.e. one copy of the mutation noted and one copy of ΔF508). PI = pancreatic insufficiency. [28] [29, 30].

1.4 **Pathophysiology of Cystic Fibrosis**

As previously mentioned CF is due to the defective CFTR channel either malfunctioning or in some instances being absent altogether. These abnormalities lead to a disruption in transepithelial Cl- and Na+ ion transport and the subsequent dysfunction of the epithelium within the respiratory system, pancreas, the sweat glands and the submucosal glands [23, 31]. Foremost is the disruption to the respiratory tract which becomes enveloped with thickened mucus due to an osmotically driven reduction in airway surface liquid (ASL) volume, thus reducing mucociliary clearance [31, 32] (Figure 1-3)
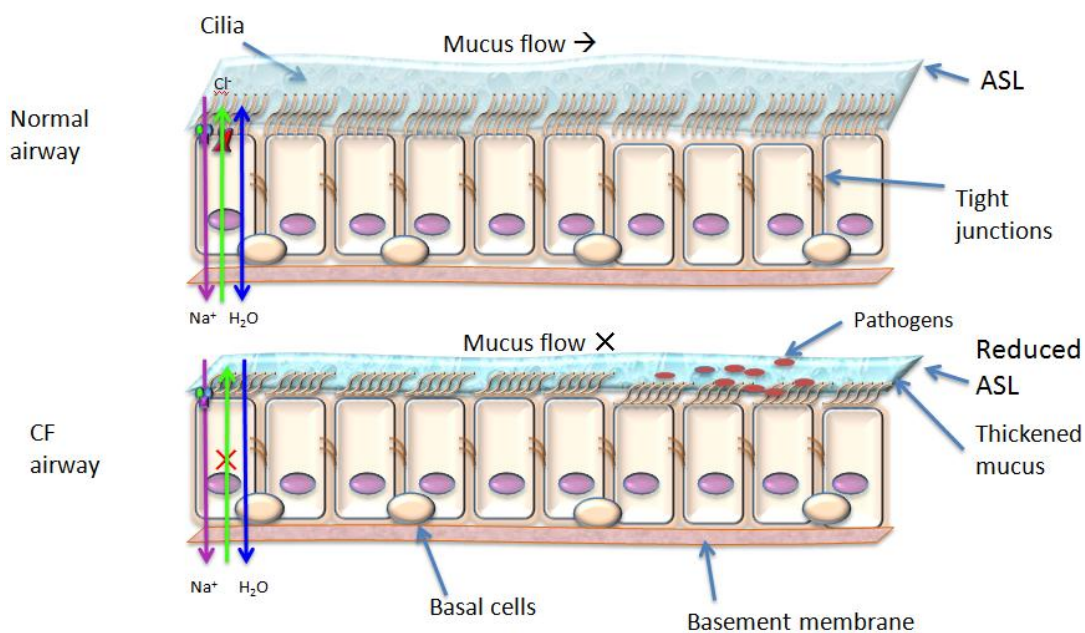
Figure 1-3: Schematic diagram of the reduced ASL theory.

The ASL layer in the CF airway (bottom) is reduced as a consequence of the osmotically driven cellular retention of Chloride and hyper absorption of Sodium.

This abnormal environment is ideal for colonisation by pathogenic organisms such as *Staphylococcus aureus, Haemophilus influenzae* and *Pseudomonas aeruginosa*

and the enteric organisms *Klebsiella pneumoniae* and *Escherichia coli*. However, airway disease in CF is pathologically characterised by inflammation and airway remodelling beginning in infants, with neutrophilic airway inflammation being observed prior to obvious infection [33]. There is supportive evidence that neutrophil elastase leads to an increase in mucus forming MUC5AC mRNA and protein expression in the airways [34] which may account in part for the overproduction and release of mucins. Subsequently, an increase in inflammation is in turn associated with an increase in infection as pathogenic bacteria proliferate in the thickened mucus of the conducting airways. Importantly, while there is a failure to clear thickened mucus there also appears to be a lack of, or dysfunction in, an auto feedback mechanism preventing goblet cells from continually over producing mucins leading to mucus plugging and plaques [35]. Tarran and colleagues further demonstrated that a reduction in ASL volume as opposed to salt content leads to goblet cell hyperplasia and/or metaplasia in the nasal airways of CF mice [32].

There have also been reports of tracheal cartilage ring remodelling in CF knockout mice, however while there is a consensus by researchers in some areas of cartilage ring remodelling there is also a discrepancy. The discrepancy reported is that Bonvin *et al* observed no change in cartilage ring numbers between CF knockout mice and controls while in contrast Wallace *et al* observed there was a statistical difference [36, 37].

1.4.1 Current treatments

Current treatments for the respiratory tract are restricted to daily chest physiotherapy, hypotonic saline inhalation and aggressive antibiotic regimes which although productive are inadequate at halting the inevitable respiratory failure [38, 39]. With

the discovery of the CF gene in 1989, came a shift in CF research towards genetic therapies, and with the premise that a single gene defect is responsible for the disease, CF became one of the first targets for a monogenetic gene therapy in an effort to deal with the morbidity and early mortality caused by respiratory tract disease and its complications.

1.4.2 Emerging treatments

Current treatments focus on CF disease manifestations by treating the phenotype of the mutated genotype. However there has in recent years been an emergence of novel treatments that aim to correct the underlying CFTR protein defect in an attempt to prevent or reduce the phenotypic expression of CF disease.

1.4.2.1 Potentiators

Potentiators are a class of small molecules which have shown promise in treating gating malfunctions of the CFTR protein. One such molecule the compound VX-770 known as Ivacaftor has been shown to restore lung function in CF patients with the G551D mutation [40, 41]. The mechanisms behind the action of VX-770 are thought to be a modification of the incorrect phosphorylation, ATP binding, and/or hydrolysis of the CFTR protein. The result is a return to function of the gating mechanism of CFTR with a net result of restoring the ASL to a normal state [40] .

1.4.2.2 Correctors

Correctors are aimed at the cellular processing of the CFTR protein and more specifically as the name suggests correcting the block in processing of the protein seen in class II mutations. This class includes the ΔF508 mutation which is present in 70 − 75% North Americans, 82% Danish, and additionally ~90% of CF patients carry at least one allele [41]. The ΔF508 mutation impairs processing of the CFTR

protein within the endoplasmic reticulum, reduces protein stability at the plasma membrane, and alters chloride channel gating [42-44]. Given the multiple components associated with this mutation, finding a single compound to correct the defect(s) presents a greater challenge than for the potentiators. It is more plausible that a combination of correctors which act on the different underlying problems such as processing, stability, and gating with a synergistic effect may be the answer [45]. If this is the case, and given the very high cost of potentiators, treating the ΔF508 mutation with a combination of correctors or even correctors with potentiators may result in a financial burden on the health care system that is unrealistic in the long term. Additionally correctors and potentiators are by design targeted to specific mutations underlying CF. In contrast; a gene therapy approach that corrects the absent or malfunctioning gene using a correctly functioning CFTR gene, will target all mutations with a single approach.

1.5 Gene Therapy

The development of technologies for introducing genes into eukaryotic cells paved the way for the development of gene therapy as a new approach to treating human disease. The concept of gene therapy was originally developed with regard to the treatment of lack of function monogenic inherited diseases, where there had been limited or no success in treatment using more conventional approaches [46]. Within this paradigm, gene therapy can be defined as the use of nucleic acid as a means by which the expression of therapeutic genes can be facilitated. The principle mechanism behind gene therapy is to introduce therapeutic genes into defective somatic cells. In the most straightforward example, once introduced into somatic cells, the gene can then direct the synthesis of the desired protein product to facilitate

the restoration of normal cellular and bodily function.

There are three categories in which different approaches to gene therapy can be grouped according to the corrective mechanism by which they operate: (1) gene replacement (2) gene reprogramming and (3) gene repair [47]. The first category, gene replacement, aims to add a correct copy of a gene to overcome the problems caused by a defective inherited gene. Gene reprogramming however, aims to correct the RNA transcript product of a mutant gene, so replacing the defective gene product with the normal one. Gene repair has the same end goal as gene reprogramming, but with the mutant genomic DNA itself as the target of correction. At present gene replacement is the main focus of attention in regard to gene therapy targeting monogenic diseases. Monogenic diseases are considered ideal candidates for gene therapy as, by definition, a single defective gene is responsible so that only one gene needs to be targeted in a therapeutic approach [48].

To facilitate the transfer of genetic material to somatic cells requires the use of a vector as a transport vehicle. To date research has approached this using both non-viral and viral vectors in both *in vitro* and *in vivo* studies. In regards to non-viral vectors a further division into two subgroups; cationic lipids [49, 50] and molecular conjugates [51] can be applied. Both of these non-viral approaches have been devised as a simple measure to protect naked DNA from degradation by endonucleases but are inefficient in providing gene delivery and expression [52].

Viruses, however, are intracellular obligate parasites that evolved as efficient vehicles for the delivery of DNA or RNA to target cells and thus offer the greatest prospect in providing a functional vector for efficient gene transduction. To date a number of different virus types have been explored as possible gene delivery vectors

including adenoviruses (AdV), adeno-associated viruses (AAV), retroviruses, poxviruses, alpha viruses, and rhabdoviruses [53].

1.5.1 Adenoviruses and Adeno-associated viruses

Both AdV and AAV viruses have received a great deal of attention in the formulation of a vector for the respiratory tract. However, there are limitations that need to be addressed with each of these vector types. The foremost problem is that they have a relatively low efficiency of transduction to the targeted well-differentiated ciliated airway epithelium, necessitating repeated high dose application [54]. However, this elicits a problem on two fronts, the first being that a high dose elicits an immune response which in turn introduces the second problem, that the immune response is thereafter activated and elevated upon repeated administration of the vector [47]. Compounding this is the fact that the viral genome of AdV vectors remains episomal in the target cell [55]. As such there is a necessity for repeated treatment using the AdV vectors as there will be a dilution of the episomal viral genome upon mitotic cell division. Because of the limitations of AdV and AAV vectors, there is an increasing interest in using retrovirus vectors.

1.5.2 Retroviral Vectors

Retroviridae is a family of viruses that have been used in gene therapy vector research since the early 1980s [56, 57]. Maloney murine leukemia virus (MLV)-based vectors were the first of the retroviral vectors to be used and trialled and has shown some major advantages. These advantages include: (1) they lack viral proteins, which makes them less immunogenic in the sense that they don't elicit an immune response to the vector and (2) they have the ability to integrate into the host genome resulting in persistent gene expression [56]. However the MLV-based

vectors have also demonstrated limitations, the foremost being the inability to transduce non dividing cells [56, 58]. The inability to transduce non dividing cells is an extreme draw back in relation to gene therapy aimed at the epithelium of the respiratory system as most of these cells are terminally differentiated [47]. Therefore while retroviruses provided a promising direction further exploration of this virus family was undertaken and the sub group known as the lentivirus attracted particular attention.

1.5.3 Lentiviral Vectors

Lentivirus is a genus of retroviruses and as such integrate into the target cells genome [59] leading to the genetic stability of the vector in the target cell and daughter cells upon mitotic division. Furthermore lentiviruses have the ability to transduce both dividing and non-dividing cells [60-62] making them a valuable prospect for use as a vector in gene therapy studies focused on the respiratory epithelium. Lentiviruses can be divided into two groups: (1) primate lentiviruses and (2) non primate lentiviruses. Examples of the two groups include the human immunodeficiency virus (HIV) and simian immunodeficiency virus (SIV) for the former and the feline immunodeficiency virus (FIV), bovine immunodeficiency virus (BIV), caprine arthritisencephalitis (CAEV), equine infectious anemia virus (EIAV) and visnavirus for the latter [56].

The research presented in this thesis utilized a modified HIV-1 lentiviral vector to facilitate gene transfer to the airway epithelium, targeting both dividing and non-dividing cells.

1.5.4 HIV-1 Biology

The HIV-1 genome is a 9.3 kb RNA that encodes for 15 proteins from nine open reading frames (ORFs) (Figure 1-4) and three of these ORFs encode gag, pol, and env which are common to all retro viruses [63]. These polyproteins are subsequently cleaved into individual proteins as follows: Gag is cleaved into four proteins, matrix (MA), capsid (CA), nucleocapsid (NC), and p6; Pol is cleaved into the replication enzyme protease (PR), reverse transcriptase (RT), and intergrase (IN); and Env is cleaved to form the transmembrane (TM), and surface (SU or gp 120) glycoproteins which are required for viral budding and entry into the cell [64] (Figure 1-4). In addition to the gag, pol, and env genes HIV-1 also encodes for six regulatory and accessory proteins. Three of the accessory proteins, virion infectivity factor (Vif), the viral protein R (Vpr), and the negative factor (Nef) are also found in the viral particle (Figure 1-4), however they are not essential for viral replication but play a role in the virulence and pathogenicity of the virus [64]. The viral protein u (Vpu) provides two functions in the course of HIV-1 replication: (1) it enhances the release of virus particles and (2) promotes the degradation of the glycoprotein CD 4 [64]. There are two remaining accessory proteins, Tat which contains a number of regulatory elements important for RNA polymerase II transcription, and Rev which directly enhances the export of uncleaved mRNAs into the splicing pathway [63].
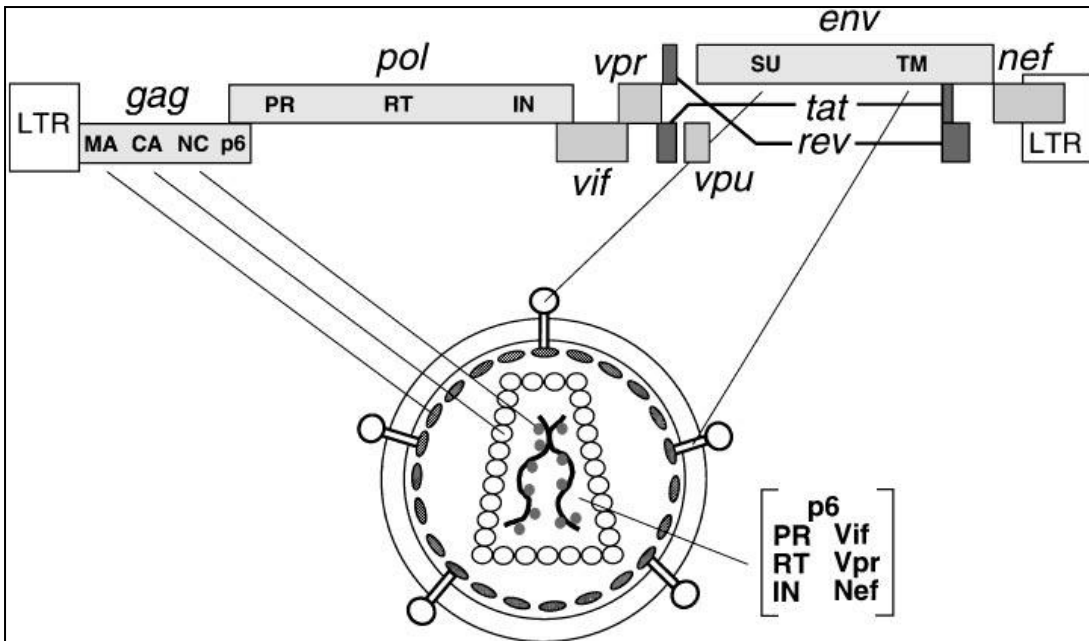
Figure 1-4: Organisation of the HIV-1 genome.

Organisation of the HIV-1 genome and its translation to the virion [63] Modified from Frankel and Young, HIV-1: Fifteen Proteins and an RNA, Annual Review Biochemistry 1998, Vol 67, 1-25

1.5.5 Trans and Cis Acting Elements

The trans-acting sequence elements are those that can operate at a distance and need to be expressed to function. In regards to HIV-1 this covers all of the 15 proteins mentioned and which are necessary for viral propagation.

The cis-acting sequence elements are those that do not require expression to have an effect and generally act locally. Examples of cis-acting elements include promoters, polyadenylation (pA) signals and transcription factor binding sites. In HIV-1 these cover the following elements: primer binding site (PB), encapsidation sequence (ψ), splice donor and acceptor sites (SD and SA), integrase binding sites (INT), long terminal repeats (LTRs), 3' polypurine tract (PPT), central polypurine tract (cPPT), and rev response element (RRE) (Figure 1-5). In addition there are also various cis-acting sequence elements required for RNA synthesis in the long terminal repeats

(LTR). The LTR is divided into three regions: U3 (unique 3' end), R (repeated), and U5 (unique 5' end) with transcription being initiated at the U3 and R junction where the transcription factor IID (TFIID) binds to the TATA box (Figure 1-5) [64].
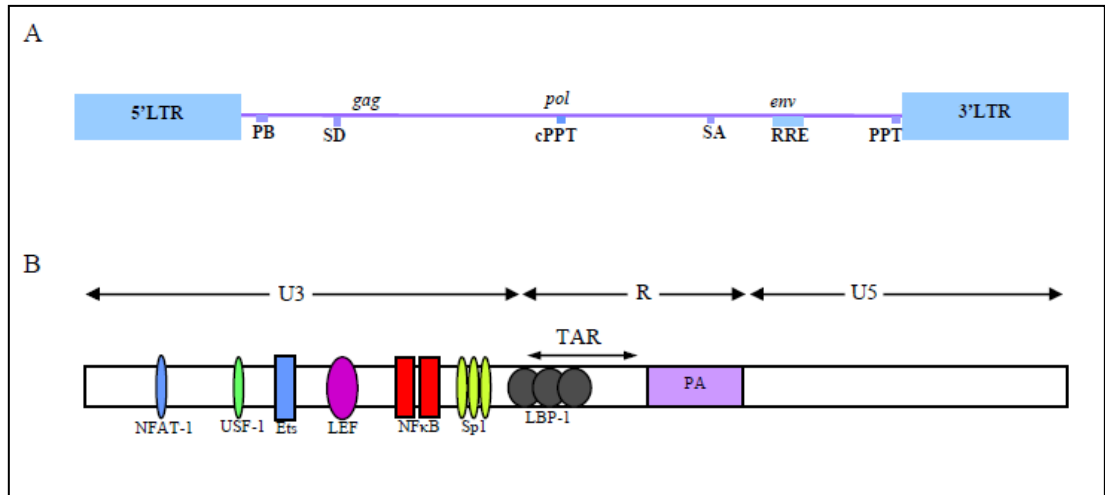
Figure 1-5: Cis-acting elements within HIV-1.

(A) Schematic representation of the cis-acting elements across the HIV-1 backbone (B) Schematic representation of the cis-acting elements within the 3' and 5' HIV-1 LTR showing the position of the binding sites for host factors (LBP-1, NFkB, LEF, Ets, USF-1, and NFAT-1) are shown 5' of the transcription start site.

1.5.6 HIV-1 as a Vector

The generation of replication-defective lentiviral vectors requires a segregation of the cis-acting sequences that are required for the transfer of the viral genome to target cells as well as the sequences that encode essential viral structural and enzymatic proteins onto separate plasmids. The transfer vector consists of the following cis acting sequences: The LTR's, PB, ψ packaging signal, PPT and the RRE linked to the transgene of interest in the context of a transcriptional unit [59]. The transfer vector is then co-transfected into a producer cell with the packaging and envelope expression plasmids which lack most, if not all, of the cis acting sequences and the viral proteins provided in trans assemble into virions encapsulating the

replication defective transfer vector RNA [59].

The first generation HIV-1 vectors appeared in scientific literature in the early 1990s [65] and by the middle of the decade there was a concerted effort to produce safety modified HIV-1 vectors. At that stage the first generation HIV-1 vectors typically comprised of three expression plasmids: (1) a transfer vector, (2) a packaging construct, and (3) an envelope gene [66]. The transfer vector contained the intact HIV-1 LTR's and all the cis acting sequences and the transgene was expressed from an internal human cytomegalovirus (CMV) immediate early region enhancer-promoter.

The packaging plasmid encoded all of the HIV-1 proteins except for Vpu and Env and consisted of HIV-1 genome with some minor modifications. Those changes were that the 5' LTR was replaced with CMV promoter to allow the expression of viral proteins required in trans, the ψ packaging signal, Env gene and ORF for the Vpu protein were all deleted, and the 3' LTR was replaced with a polyadenylation site from the insulin gene. In the envelope encoding plasmid a CMV promoter drove the expression of the G glycoprotein gene of the vesicular stomatitis virus (VSV-G). Using transient co transfection of human embryonic kidney 293T cells with the three plasmid combination resulted in a replication defective VSV-G pseudotyped HIV-1 particle capable of transducing non dividing cells [67]. It was subsequently demonstrated that the HIV-1 accessory proteins, vif, vpr, vpu, and nef were dispensable in the efficient generation of VSV-G pseudotyped HIV-1 particles [68].

This work paved the way for the second generation HIV-1 vector systems, which contained only the HIV-1 gag, pol, rev, and tat genes in a multiply attenuated packaging construct. Furthermore the level of transgene delivery by the second

generation HIV-1 vectors were as efficient as the first generation HIV-1 vectors which contained an almost full complement of HIV-1 wild type accessory genes [68]. The clear advantage is the deletion of the accessory proteins which contribute to virulence and are needed for viral replication added a further safe guard against the vector becoming replication competent. However it was soon realised that recombination events with a wild type retrovirus that may reside within a given system may lead to the HIV-1 replication incompetent viral particles becoming replication competent [68, 69].

In an effort to prevent the risk of replication competent viral particles from being created through recombination a third generation of HIV-1 vectors was created [59, 69]. The third generation vectors are also known as gutted vectors because even more of the wild type HIV-1 genes have been removed. This includes a deletion within the U3 region of the 3' LTR which serves as a template for both the 3' and 5' LTR in the provirus. This modification results in the 5' LTR of the integrated provirus to be almost completely inactivated [70]. The modification of the 3' LTR created what is now known as self-inactivating (SIN) HIV-1 vectors due to their inability to transcribe full length vector RNA [69], thus providing protection against the forming of replication competent viral particles through recombination. To further safe guard the reconstitution of U3 sequences within the deleted regions of the 3' LTR by homologous recombination with an intact 5' LTR during transient co-transfection, the U3 region of the 5' LTR has been replaced with the CMV promoter [59, 69]. The modifications which make the SIN HIV-1 vectors safer also provide greater control over the expression of the transgene utilizing an internal promoter. This reduces the likelihood of the expression of cellular coding sequences located adjacent to the vector integration site either due to the promoter activity of the 3'

LTR or through an enhancer effect. Furthermore, the potential for transcriptional interference between the LTR and the internal promoter driving the transgene is prevented by the SIN design [59, 71]. Additionally, the inactivation of viral transcription allows for the expression of cell type specific promoters, as well as the flexibility of finding the appropriate level of expression for the best therapeutic outcome.

With the development of third generation vectors, there was also further refinement aimed at increasing the odds against recombination leading to a replication competent HIV-1 vector. The packaging system was changed so that the gag-pol and rev genes are now expressed from two different non overlapping plasmids [69]. Furthermore the gag and gag-pol open reading frames have been codon optimised to reduce sequence homology with wild type retroviruses further insulating against recombination events [72, 73]. There are also additional genetic elements that stimulate transgene expression in a post transcriptional manner which have been added to many of the third generation retro viral vectors. The primary addition has been the woodchuck hepatitis virus post-transcriptional regulatory element (WPRE) which influences transgene expression by augmenting 3' end processing and polyadenylation [74]. Finally, the addition of the VSV-G pseudotyping of the HIV-1 envelope has given the vector a greatly expanded tropism due to the ability of the VSV-G protein to bind to a phosphatidyl serine component of the lipid bilayer present in the cellular membrane of most eukaryotic cells [75]   including undifferentiated stem cells [76, 77].

1.6 Stem cells in Gene Therapy

The targeting of adult multipotent stem cells as a source of a constantly self-

renewing and differentiating cell pool is of immense interest in relation to gene therapy for inherited diseases. This is due to the innate possibility of a single corrective treatment providing a lifelong therapeutic response through continual expression of the transgene, despite cellular turnover. In 1961 Till and McCulloch observed cells in bone marrow that were able to continually self-renew as well as differentiate [78]. Today these cells are known as hematopoietic stem cells (HSC) and through continual progressive research since their discovery, they have become the most characterised stem cell population [79, 80]. Briefly, a combination of fractionation methods, cell surface markers, *in vitro* and *in vivo* assays have been used to ascertain their capacity to self-renew and differentiate [81]. The results of these studies has led to what is now known as the classical stem cell hierarchy (Figure 1-6) were the HSC is a stem cell with an unlimited capacity for self-renewal, as well as the capacity to generate through differentiation all types of cells of the hematopoietic system. Additionally, the presence of a transit amplifying cell was shown to have the ability for limited self-renewal and the potential to differentiate into a limited number of cells of the hematopoietic system.
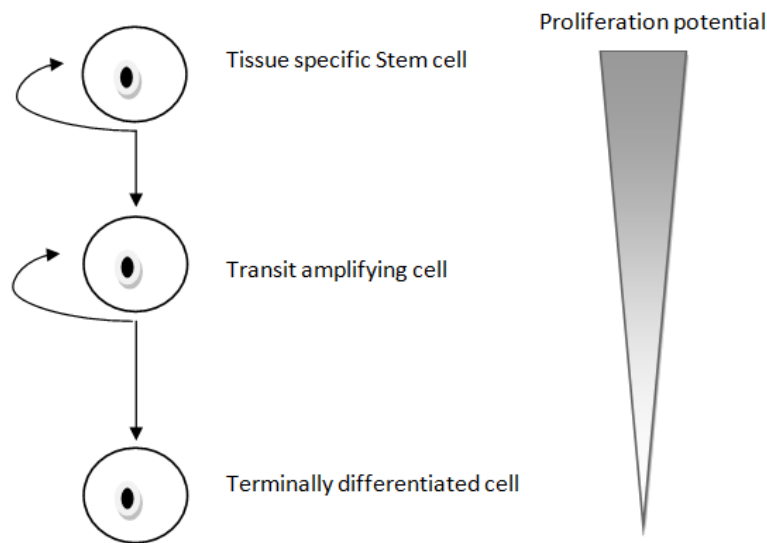
Figure 1-6: Classical stem cell hierarchy

1.6.1 Respiratory Stem Cells

The targeting of CFTR gene transfer to progenitor/stem cells within the respiratory epithelia was first raised over two decades ago [82, 83], after their existence was first demonstrated following research in the previous year's [83, 84]. The targeting of epithelia stem/progenitor cells (stem cells) for *in vivo* gene therapy is reminiscent of an earlier concept, the "magic bullet" proposed by Nobel laureate Paul Ehrlich over a century ago [85]. Ehrlich's postulate was that, ideally, a treatment would selectively target a specific cellular target came from his work on pathogenic organisms; however the same premise can be applied to the *in vivo* targeting of respiratory stem cells in a gene therapy setting. Specifically, if a stem cell can be targeted for transduction with a genomic integrating therapeutic gene, then all its progeny, both self-renewed and differentiated cells, will also carry the introduced gene as the cells turn over through epithelial repair and replacement.

Unlike HSC which have been extensively studied there is far less known in regards

22

to respiratory stem cells. Traditionally, adult organs are classified depending on their capacity to proliferate in the steady state or following injury and are classified as either continuously renewing (bone marrow, gut, skin), conditionally renewing (lung, kidney, liver) or non-renewing (nervous tissue, muscle) [86]. The small intestine and colon epithelium as part of a continuously renewing organ is replaced every 5 days [87]. As a conditionally renewing adult organ the airway epithelial cell turnover is comparatively slow (~1% per day) and the epithelium of the trachea-bronchiolar region is replaced approximately every 4 months [88]. With the considerable variation of epithelial life span between the tissues of these organs, there arises the possibility that cellular and molecular mechanisms distinct to their niche regulate maintenance during both the normal and injury state. To expand on this premise, the intestinal epithelium is in a state of rapid renewal negating need for dramatic change in cell cycle frequency due to perturbations or injury. In contrast, injury to the slowly renewing respiratory epithelium results in the acquisition of compensatory growth rapidly increasing the level of renewal to replace the damaged epithelium. It is this unique difference in requirements for tissue maintenance and repair that suggests differential use of regulatory mechanisms such as signalling pathways that regulate cell proliferation, self-renewal, and differentiation. The difference in requirements for tissue maintenance and repair in the conditionally renewing respiratory tract is demonstrated by the Club cell. The Club cell in its differentiated state contributes to respiratory epithelium homeostasis through apoproteins A, B, and D, proteases, anti-microbial peptides, several cytokines and chemokines, and mucins that are within the airway surface liquid [89]. In response to epithelial injury Club cells may re-enter the cell cycle and proliferate/differentiate in order to maintain the ciliated cell population, as well as their own. The ability for

Club cells to re-enter the cell cycle and act as a facultative progenitor is not in accordance with the classical stem cell hierarchy (Figure 1-6) but instead proposes a non-classical stem cell hierarchy (Figure 1-7).
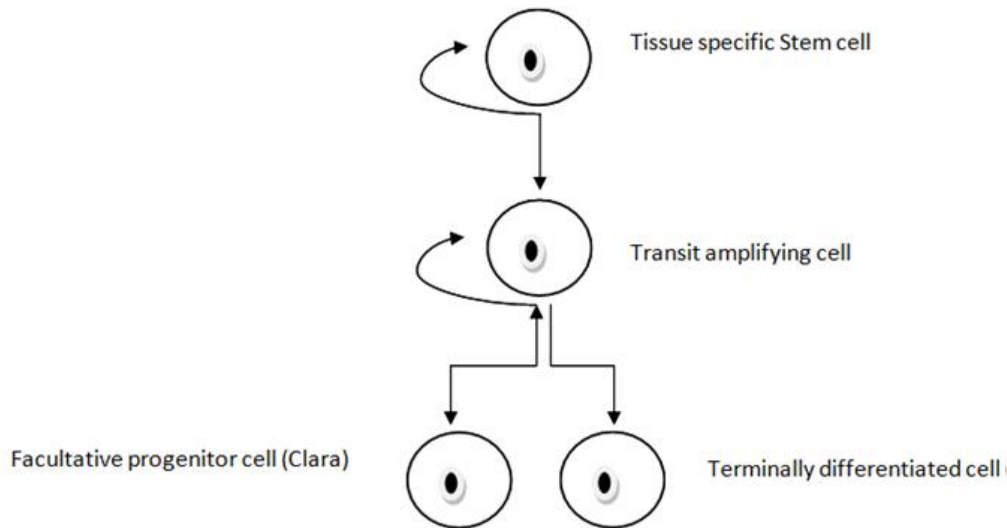
Figure 1-7: Non-classical stem cell hierarchy

1.6.2 Respiratory Stem Cell Transduction

As previously mentioned the respiratory stem cell pathway is far less understood as the hematopoietic stem cell pathway and its niche environment and the respiratory stem cell pathway may comprise of a non-classical hierarchy. To compound matters further there is a disparity amongst researchers in the allocation of members of the different levels of the respiratory stem cell hierarchy. As an example, researchers have given the title of *stem cell* to the basal cells of the tracheal epithelium [90, 91] positioning it at the root of the hierarchy. In contrast the basal cells of the bronchial epithelium have been labelled as *progenitor cells* [92] delegating them to a position further down the stem cell hierarchy. The inconsistency in allocation of the basal cell to a position in the stem cell hierarchy is at first an obstacle, however while there

may be some contention as to where it fits in the hierarchy, there is a consensus that the basal cell is a multipotent stem cell capable of both self-proliferation and differentiation into all cell types of the respiratory pseudostratified epithelium [84, 91, 93, 94]. While this has been observed in the trachea and bronchial regions there as yet has been no definitive study demonstrating the function of basal cells in the uppermost portion of the conducting respiratory pathway; the nasal passage. At first, this omission seems logical in that research into the stem cell pathways of the respiratory system is not solely aimed at an academic understanding but also clinical relevance. That is to say there are many diseases affecting the lungs such as CF that may in the future clinically benefit from an academic understanding of the respiratory stem cell pathway and the process's involved in the regulation and regeneration of the respiratory conducting epithelium. Furthermore, current research into gene therapy for CF is often trialled in the murine nasal epithelium [95-98]. This is due to the region containing very similar cell types to the epithelium of the trachea and bronchioles. In addition, mouse models for CF display the hallmark phenotype of the disease in the nasal region but this is not recapitulated in the murine trachea and bronchioles. Therefore a lack of completeness in the study of the respiratory stem cell pathway, to include nasal epithelium, has left a gap in knowledge that may have diminished the capacity to assess the full implications of gene therapy for CF at a fundamental level. As an example, Limberis *et al* reported that a single gene transfer treatment to the murine nasal epithelium facilitated by a HIV-1 VSV-G pseudo type lentiviral vector was sufficient to produce expression of a marker gene (LacZ) for at least 92 days [96]. Interestingly, not all cell types displaying positive marker gene expression at day 92 were present at earlier time points (days 7 and 28). In another example, Stocker *et al* showed that a single dose of the same vector was

sufficient to produce expression of a marker gene (LacZ) for 24 months and a therapeutic gene (CFTR) for at least 12 months [98]. Importantly it has also been shown that the epithelium of this region has a cellular turnover of approximately 4 months [88]. Together these studies suggest the outgrowth and differentiation of transduced cells of the stem cell linage has sustained ongoing expression of the transgene. However without knowledge of the stem cell compartment or niche of the nasal epithelium this remains conjecture. A further study in this area has shown more compelling evidence of stem cell transduction in the murine nasal airway. In this study another lentivirus was used the F/HN pseudotyped SIV vector in conjunction with an epithelium forced injury model [95]. The forced injury model facilitated by the instillation of polidocanol following gene transfer results in the ablation of the respiratory epithelium leaving the basal cells residing on the basement membrane intact. While the premise of the study was to explore the possible transduction of the basal cells it also importantly provided an additional piece of evidence. That is, that the basal cells could regenerate all the cells of the nasal respiratory epithelium and may provide the same function as they do in the trachea and bronchioles. Importantly, the study successfully demonstrated that following transduction of the basal cells with an integrating lentiviral vector the transgene was passed on to its differentiated progeny upon regeneration.

1.7 **Conclusion**

Therapies for treating CF have improved significantly over the last century; however an effective treatment to prevent CF related lung disease remains elusive. Gene therapy for CF lung disease holds great potential; however despite ongoing research for approximately 20 years, clinical application has not been realized. The

development of a therapeutically effective vector has in part delayed the progress of CF gene therapy. The ongoing research to produce an effective vector utilizing the HIV-1 lentivirus has shown great promise [73, 96, 98-100] and has the potential to bring gene therapy for CF airway disease to fruition. However, there remains aspects of the HIV-1 lentivirus vector that requires further research to gain a more succinct understanding of the potential it holds.

Note. Given the lack of a definitive nomenclature for the airway stem cell hierarchy and the absence of clear agreement whether basal cells are tissue specific airway stem cells or facultative progenitor cells, for simplicity of expression basal cells of the airway epithelium will be referred to from here on in this thesis as airway stem cells.

1.8 Aims of Thesis

To gain further insight into the potential of a HIV-1 lentiviral vector and lysophosphatidylcholine (LPC) pretreatment to treat CF airway disease, the thesis presented here was designed to address the following aims: (1) Establish if long term transgene expression following treatment with the HIV-1 viral vector and LPC pretreatment is a consequence of transducing airway stem cells. (2) Isolation and quantification of airway stem cells and goblet cells in the airways of CF mice to determine if possible remodeling of the cells in terms of hyperplasia is present. (3) Determine if the HIV-1 vector can transduce the relevant cells types including stem cells in the airways of the normal ferret. (4) Determine if the HIV-1 vector can transduce the relevant cell types including stem cells in the airways of a non-human primate.

2 Materials and methods

2.1 Materials

2.1.1 Chemicals and Supplies

Agarose, type C, gelling T° 40-43°C   Calbiochem (USA) Cat # 121852

Alexa Fluor 647-conjugated anti-mouse EpCAM (clone G8.8)   Biolegend (Australian biosearch) Cat # 118212

Anti-CD31 antibody [390] (Pe)   Biolegend (Australian biosearch) Cat # 102407

Antisedan® (atipamazole HCl 5 mg/ml)   Pfizer (USA)

Bacto™-Agar   Becton, Dickinson (USA) Cat # 214010

Bacto™-tryptone   Becton, Dickinson (USA) Cat # 211705

Bacto™-yeast extract   Becton, Dickinson (USA) Cat # 212750

Brilliant Violet 421-conjugated anti-mouse CD24 (clone M1/69) Biolegend (Australian biosearch) Cat # 101825

Bromophenol Blue   BDH Chemicals (USA) Cat # H3392-2

Calcium chloride ($CaCl_2$)   Sigma Aldrich (USA) Cat # 223506

CD45 Antibody (30-F11) (Pe)   Biolegend (Australian biosearch) Cat # 103105

ColonLyetly®   Dandy Pharmaceuticals (AUS)

Dimethylformamide (DMF)   Sigma Aldrich (USA) Cat # D4551

Dulbecco's Modified Eagle Medium (DMEM)   SAFC Biosciences (USA) Cat # 51441C

(DMEM/F-12)   Gibco (USA) Cat # 10565-018

Domitor® (medetomidine HCl 1 mg/ml)   Pfizer (USA)

D.P.X mounting medium   Sigma Aldrich (USA) Cat # 317616

Ethylenediaminetetraacetic acid (EDTA)   Sigma Aldrich (USA) Cat # E5134

Eosin Y	ProSciTech (AUS) Cat # C097
Ethanol	Ajax Chemicals (AUS) Cat # 1045
Ethidium Bromide	Sigma Aldrich (USA) Cat # E7637
Fetal calf serum (FCS)	JRH Biosciences (USA) Cat # 12103-500M
FITC-conjugated anti-mouse CD104 (clone 346-11A)	Biolegend (Australian biosearch) Cat # 123605
Formalin	Fronine Laboratories (AUS) Cat #JJ018B
β-Galactosidase from E.Coli	Sigma Aldrich (USA) Cat # G5635-1KU
Gentamycin (1mg/ml)	Sigma Aldrich (USA) Cat # 48757
D-Gluconic acid	Sigma Aldrich (USA) Cat # G9005
L-Glutamine (200mM)	SAFC Biosciences (USA) Cat # 59202C
Glutaraldehyde, grade II (25%)	Sigma Aldrich (USA) Cat # G6257
Growth factor reduced Matrigel	Corning (USA) Cat # 354230
Haematoxylin (Mayer's)	ProSciTech (AUS) Cat # AMH
Hydrochloric acid (HCl, 37%)	Sigma Aldrich (USA) Cat # 258148
Hank's Balanced Salt Solution	Life Technologies (AUS) Cat # 14025092
Hepes	Sigma Aldrich (USA) Cat # H3375
Indian Ink	Windsor and Newton (UK) Cat # 1005754
Ketamine (100 mg/ml)	Parnell Laboratories (AUS)
Liberase TM research grade	Roche (USA) Cat # 5401119001
Lysophosphatidylcholine (LPC)	Sigma Aldrich (USA) Cat # L4129
Magnesium Chloride hexahydrate ($MgCl_2$)	Sigma Aldrich (USA) Cat # M9272

Millicell cell culture inserts, 0.4 μm pore size, hydrophilic PTFE, 30 mm

Diameter	Merck Millipore (AUS) Cat # PIPH03050
Mlg 2908 mouse lung fibroblast cell line	ATCC Cat # CCL-206
OptiPro SFM	Invitrogen (USA) Cat # 12309-019
Paraformaldehyde	Sigma Aldrich (USA) Cat # P6148
Penicillin G (5000 U/ml)/Streptomycin (5mg/ml)	Sigma Aldrich (USA) Cat # P4458
Phosphate Buffered Saline Tablets (PBS)	MP Biomedicals (USA) Cat # 2810305
PBS without calcium and magnesium	Sigma Aldrich (USA) Cat # D8537
Polybrene (Hexadimethrine bromide)	Sigma Aldrich (USA) Cat # H9268
Potassium Chloride (KCl)	Sigma Aldrich (USA) Cat # P1597
Potassium Ferricyanide ($K_3Fe(CN)_6$)	Sigma Aldrich (USA) Cat # P8131
Potassium Ferrocyanide ($K_4Fe(CN)_6$)	Sigma Aldrich (USA) Cat # P3289
Potassium Phosphate monobasic (KH_2PO_4)	Sigma Aldrich (USA) Cat # P9791
Potassium Phosphate dibasic (K_2HPO_4)	Sigma Aldrich (USA) Cat # P3786
Propidium iodide	Life technologies (AUS) Cat # P1304MP
Proteinase K	Promega (USA) Cat # V3021
Red Cell ASK lysis buffer	Life technologies (AUS) Cat# A10492-01
Safranin O	ProSciTech (AUS) Cat # C138
0.9% Sodium Chloride (Saline)	Baxter Healthcare (AUS)
Sodium Chloride (NaCl)	Sigma Aldrich (USA) Cat # S1679
Sodium Hydroxide (NaOH)	Sigma Aldrich (USA) Cat # S5881
Sulphuric Acid (H_2SO_4)	Sigma Aldrich (USA) Cat # 320501
TE Buffer	Usb Corp (USA) Cat # 75834

Trypsin	SAFC (USA) Cat # 59430
Water for Irrigation (H_2O)	Baxter Healthcare (AUS)
Xgal	Progen Industries (AUS) Cat # 200-0191
Xylene	Merck (Germany) Cat # 410234

2.1.2 Consumables and Suppliers

Cell culture plates and flasks	Costar (Corning Scientific, USA),
	NUNC (Nalgene, USA),
	Sarstedt (Germany),
	Greiner Lab (Germany)
	Becton Dickinson (USA)
40 µm Cell strainer	Fisher scientific (AUS) Cat # 08-771-1
EIA/RIA 96 well plates	Corning Scientific (USA) Cat # 3590
GELoader Tips	Eppendorf (USA) Cat # 0030.001.222
Histology Cassettes	ProSci Tech (AUS) Cat # RCH40-G
Microscope Coverglass slips	Menzel-Glazer (Germany) Cat # CS22401GP
Microscope Slides	Menzel-Glazer (Germany) Cat # S41014A
Optical Adhesive Cover	Applied Biosystems (USA) Cat # 4311971
Optical Caps	Applied Biosystems (USA) Cat # 4323032
Optical Tubes	Applied Biosystems (USA) Cat # 4316567
Optical 96 well reaction plates	Applied Biosystems (USA) Cat # N8010560
Ultrafine insulin syringes	Becton, Dickinson (USA) Cat # 326725

6 Well flat bottom tissue culture plate   Sigma Aldrich (USA) Cat # CLS3516

2.1.3 Bacterial Strains and Media

Broth1% (w/v) Tryptone, 0.5% (w/v) Yeast extract, 0.5% (w/v) NaCl in dH_2O.

LB Agar 1% (w/v) Tryptone, 0.5% (w/v) Yeast extract, 1.5% (w/v) Agar, 0.5% (w/v) NaCl in dH_2O.

E. coli   E. coli DH10

2.1.4 Cell Lines

293T cells   American Type Culture Collection, CRL 11268

NIH3T3 cells   American Type Culture Collection, CRL 1658

2.1.5 DNA Plasmids

2.1.5.1   Plasmid Kits and Buffers

Agarose Gel 1.2% (w/v) agarose in TBE buffer

Endofree Plasmid Mega Kit   Qiagen (Germany) Cat # 12381

2 x HeBS 0.28 M NaCl, 0.05 M Hepes, 1.5 mM Na_2HPO_4, pH 7.04

TBE Buffer 89 mM Trizma base, 89mM Boric acid,

2mM EDTA

2.1.5.2 DNA Plasmids

Gagpol   pHCMVgagpolmllstwhv

Rev   pHCMVRevmlwhvpre

Tat   pcDNA3Tat101ml

VSV-G   pHCMV-G

$LacZ_{Co}$ pHIV-1SDMPSv-nlsLacZCo

2.1.6 Real Time qPCR Assay

2.1.6.1 PCR Kits

TaqMan Universal PCR Master Mix   Applied Biosystems (USA) Cat # 4304437

TaqMan MGB Probe (50,000 ρmol)   Applied Biosystems (USA) Cat # 43016032

Wizard SV Genomic DNA System   Promega (USA) Cat # A2361

20 x Assay Mix   18 μM forward primer, 18 μM reverse primer, 5
μM probe in TE buffer

2.1.6.2 Primers and Probes

Gag Forward 3'primer   AGC TAG AAC GAT TCG CAG TTG AT

Gag Reverse 5'primer   CCA GTA TTT GTC TAC AGC CTT CTG A

Gag Probe   6FAM-CCT GGC CTG TTA GAA AC-NFQ

mTransferrin Forward 3'primer   AAG CAG CCA AAT TAG CAT GTT GAC

mTransferrin Reverse 5'primer   CGT CTG ATT CTC TGT TTA GCT GAC A

mTransferrin Probe   6FAM-CTG GCC TGA GCT CCT-NFQ

NLS-LacZ 3' primer   GCC ACT TCT TGA TGG ACC ACT T

NLS-LacZ 5' primer   CCG CCA CCG ACA TCA TCT

NLS-LacZ Probe   FAM-CAC GCG GGC GTA CAT-NFQ

GAPDH 3' primer   CAT CCG GTG TAC CTT TCC TT

GAPDH 5' primer   CCA GGA AGA CAG GGA GAG TG

GAPDH probe   GCA CTG CTG CCA TGC

All primers and probes were ordered from (GeneWorks, Australia).

2.1.7 Animal Models

C57Bl/6

Laboratory Animal Services, University of Adelaide, SA (AUS) ARC, Perth, WA (AUS)

CF

$cftr^{tm1unc}$ CF colony stock, Animal Care Facility, WCH,

SA

$cftr^{tm\,1\,unc}\,Tg^{(FABPCFTR)}$ CF colony stock, Animal Care Facility, WCH,

SA

2.1.7.1 Anaesthesia

Domitor:Ketamine Mix   0.1 mg/ml Medetomidine, 7.6 mg/ml Ketamine in sterile H_2O

Antisedan Reversal   0.5 mg/ml Atipamazole in sterile H_2O

2.1.8 Processing of Mouse Heads

Carnoy's Fixative   60% (v/v) Ethanol, 30% (v/v) Chloroform, 10% (v/v) Glacial acetic acid

Decal 7% (v/v) HCl in 1.5% EDTA (w/v) in dH_2O

10% NBF 10% (v/v) Formalin, 0.22 M NaH_2PO_4, 0.45 M Na_2HPO_4 in dH_2O

PFA /Glut 2% (w/v) PFA, 0.5% (v/v) Glut in PBS

Pre-Xgal   5 mM $K_3Fe(CN)_6$, 5 mM $K_4Fe(CN)_6$, 1 mM $MgCl_2$ in PBS

Xgal 20 mg/ml Xgal in DMF

2.1.9 ELISA Assay

2.1.9.1 p24 ELISA

HIV-1 p24 ELISA Kit   Perkin Elmer Life Sciences (USA) Cat #
NEK050

2.2 **Methods:** *In Vitro*

2.2.1 **Vector Plasmid Preparation**

All plasmids were prepared using the Endofree Plasmid Mega-Kit (Qiagen, Germany) according to the manufacturer's instructions.

2.2.1.1 **Agarose Gel Electrophoresis**

Confirmation of plasmid preparations were performed via gel electrophoresis. Various appropriate DNA restriction enzyme digestions were visualized on 1.0% - 1.8% (w/v) agarose in 1 x TBE buffer gel, with the addition of GelRed Nucleic acid Gel Stain (Biotium USA). The gel was submerged in 1 x TBE buffer and run at 100 volts, maximum 400 mA, and maximum 100 watts. The purified plasmid was digested in the appropriate buffer and enzyme according to the manufacturer. 300ng/ml of DNA was loaded on to the gel in the presence of bromophenol blue dye. Fluorescence was measured under UV light and photographed (Bio-Rad EZ System). DNA fragment sizes were compared to the Standard DNA molecular weight marker SPP1/*Eco*RI (Geneworks, AUS).

2.2.1.2 **Spectrophotometry**

Quantification of plasmid preparations was performed via Spectrophotometry (Amersham Biosciences Ultra Spec 2100 pro).

2.2.2 **Cell Culture**

2.2.2.1 **Initiating cell culture**

All cell cultures were initiated in T 75 flasks from frozen (-80) stocks at passage 15. Vials were thawed rapidly in water bath at 35°C. Thawed cells were transferred to pre-warmed DMEM containing 10% fetal calf serum (FCS) and mixed gently by

inversion. A sample was taken and cell count performed to assess viability. Cells were then spun down in a centrifuge at 5000 RPM at 4°C for 10 minutes, supernatant then aspirated and cell pellet resuspended in 5 ml of pre-warmed DMEM/10% FCS media. Cell count to ensure viability was again performed. 5 ml cell suspension transferred to a T 75 flask containing DMEM with 10% FCS and allowed to seed in a 37°C incubator with 5% CO_2 until 90% confluent.

2.2.2.2   Cell Culture Maintenance and Expansion

Cells at 95% confluence were sub cultured to maintain or expand cells. Existing media was aspirated and washed with PBS to remove all DMEM/10% FCS. Trypsin was then added to cell flask(s) and incubated for ~ 2 minutes to detach adherent cells. Light microscopy was used to confirm detachment and DMEM/10% FCS was transferred into the flask to neutralise the trypsin. Cells were then spritzed to obtain a single cell suspension. Sub cultures were established at appropriate dilutions: 1:2 when required in 24 hours and 1:4 when required in 48 hours. Cells were incubated at 37° C and 5% CO_2 for the appropriate time. Cells were expanded over 5 days until confluent 6 x 150mm round dishes were obtained. Cells were then harvested and the concentration of live cells was obtained via an electronic haemocytometer and diluted to a final working concentration of 4.5 x 10^5 cells/ml in DMEM/ 10% FCS containing penicillin and streptomycin (Penn/Strep) (1/100). 110 ml of cell suspension were transferred into each 8 x 245 mm square plates and incubated at 37° C and 5% CO_2 for 24 hours.

2.2.3 Lentiviral Production

LV vector production was performed via transient transfection of a 5 plasmid system in 293T cells using calcium phosphate precipitation. Briefly, a DNA mix was

obtained and the ratio of plasmids used was 170 µg of the transgene 1SDmMPSV LacZnlsco, 3.16 µg of pcDNA3 Tat, 3.16 µg of pHCMVRev, 1 µg pHCMVgagpol, 7.9 µg pHCMV-G mixed with 320 µl of $CaCl_2$. For each plate, 3.2 mls of the DNA mix was then mixed by vortexing drop wise into 3.2 mls of 2 x Hepes buffered saline (HeBS) by pipette for 15 seconds, mixed for a further 30 seconds and allowed to sit for a further 75 seconds. The DNA-$CaPO_4$ precipitate was then transferred by pipette slowly and evenly onto the 245mm square plate and gently mixed by rocking. The plates were incubated for 8 hours at 37° C, 5% CO_2 and then the media changed to serum free medium with glutamine and Pen/Strep and incubated at 37° C, 5% CO_2 for a further 40 hours.

2.2.3.1 Lentiviral Purification and Concentration

For purification, approximately 1 L of vector supernatant was collected, passed through a 0.45 um filter (polyethersulfone membrane) and then onto two MustangQ Acrodiscs connected in series (Figure 2-1). During filtration the supernatant was passed through the filters at a flow rate of 10 ml/min. After loading, the MustangQ Acrodiscs were immediately flushed with 30 ml of PBS using a 30 ml syringe at the completion of filtration. The viral particles were then eluted with 4 ml of 1.5 M NaCl into a sterile tube containing an equal volume of 2% (v/v) mouse serum in H_2O. For further purification, the virus was then pelleted by ultracentrifugation at 20,000 $\times$ rpm for 90 minutes at 4°C and then resuspended in 50-500 µl of 0.9% (w/v) NaCl /0.1% (w/v) mouse serum albumin and stored at -80 °C.
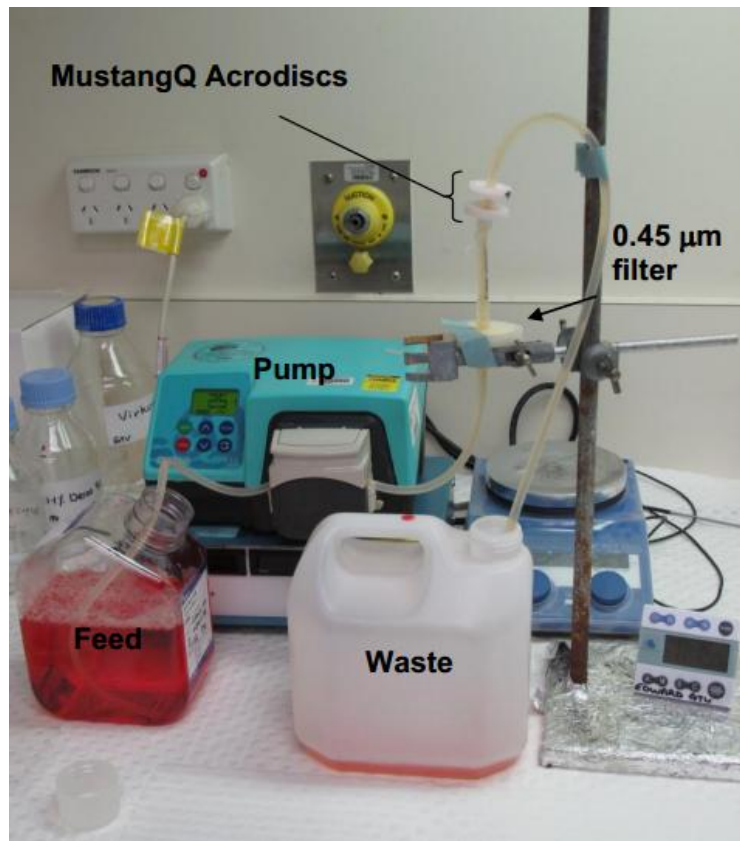
Figure 2-1: Lentivirus harvest system.

2.2.4 Establishing Viral Titre by qPCR

2.2.4.1 Obtaining Viral Genomic DNA

The infectious units of lentivirus per ml were determined by quantifying proviral DNA in transduced NIH 3T3 cultured cells. Briefly, cells were plated in DMEM 10% FCS on a 24 well plate at a density of 0.25×10^6 cells per well and incubated at 37 °C, 5 % CO_2 for 3 hours. Media was then aspirated and replaced with DMEM, 10% FCS, 4 μg/ml polybrene and 2 μg/ml gentamicin. Viral samples (20μl per well) at a dilution of 1:1000 were then added and incubated for a further 24 hours. The following day media was changed with pre-warmed (37 °C) DMEM / 10 % / FCS / 2 μg/ml x gentamicin and incubated at 37 °C, 5 % CO_2 for 24 hours. Cells were then split in each well 1:4 into a fresh 24 well plate using fresh medium containing gentamicin and continue to split 1:4 to maintain the cells under standard conditions

for a further 4 weeks.

Cells were harvested using 0.5 mL 10 % trypsin in PBS and trypsin neutralised by adding the cell suspension to 2.5 mL 1 % FCS in PBS. A Cell pellet was obtained by centrifugation (5 min at 2000 rpm), supernatant aspirated and resuspend in 3 mL of PBS. Cells were resuspended in 3 mL of PBS, pellet and aspirate supernatant.

Genomic DNA was isolated using the Wizard SV Genomic DNA isolation kit as per manufactures instructions and store DNA at -80.

2.2.4.2   Real Time PCR

To determine titre of virus each sample was analysed using rtPCR. Each assay contained a sample for detecting the Gag sequence and the control mTransferrin gene. Each (1 x) reaction contains:

20 x assay mix (gag or transferin)	1 µL
2 x TaqMan Universal PCR Master Mix	10 µL
H_2O	4 µL
gDNA sample	5 µL

All samples were performed in triplicate including a non-template control and a standard. Samples were analysed on a CFX Connect Real Time thermocycler (Bio Rad). The fluorescence of each reaction was read at the end of each cycle and the amplification plot was constructed using the 7300 system software. Cycle threshold (Ct) bar was set in the linear part of the graph and the Ct for each sample calculated. To determine LV titre the following formulas were applied:

ΔCt = Ct of gag – Ct of mTransferrin for a sample

$\Delta\Delta$Ct = ΔCt – 1 (or average of Standard)

$1/2^{\Delta\Delta Ct}$ = copy number per cell

Titre = (number of cells initially plated x copy number per cell x 1000 volume in µl)/dilution factor = infectious units/ml

2.2.5 Lentiviral Vector Instillations

Female C57Bl/6 mice, 8-10 weeks of age, were anaesthetised with 10 µl/g body weight of medetomidine (domitor) (0.1 mg/ml, Orion Corporation, Finland) and ketamine (7.6 mg/ml, Parnell Laboratories, AUS) mixture, delivered by an intraperitoneal (i.p.) injection. Mice were kept warm in a small temperature controlled cabinet at 32°C between nasal instillations and during the recovery period after reversal of the anaesthetic.

2.2.5.1 Nasal and Tracheal Instillations

Instillations were made into the right nostril *via* a micropipettor with a gel-loading tip (Eppendorf, USA), as previously described [96-98]. Pre-treatment with 0.3% LPC was instilled *via* a 4 µl aliquot one hour prior to a 20 µl bolus of the LV vector, delivered in 2 x 10µl aliquots over 2-3 minutes, *via* passive (inhalation-driven) fluid uptake. The tracheal instillations were performed via a fluid dose instilled in the trachea through a fine pipette tip inserted through a 20 gauge polyethylene cannula inserted into the trachea by oral-tracheal intubation. Anaesthesia was reversed with 2 µl/g i.p. injection of atipamazole (0.5 mg/ml, Orion Corporation, Finland).

2.2.6 Assessing *In vivo* Vector Dissemination

To assess the dissemination of vector particles following treatment blood samples were collected daily and processed to obtained sera for P24 presence by ELISA assay. ELISA was performed as per manufacturer instructions (Perkin Elmer Life Sciences USA Ca# NEK050).

2.2.7 Cell Sorting and Clonal Culture of Respiratory Airway Stem Cells

2.2.7.1 Cell Sorting via Flow Cytometry

To obtain airway stem cells from the total tracheal airway cell pool flow cytometry was employed on the basis of EpCAM+, CD 104hi, CD45-, CD31- cells as previously published [101]. Briefly, cells were first sorted on the basis of CD45^{neg} (leukocytes), CD31^{neg} (endolethial), then, EpCAM^{pos} (epithelial cell adhesion molecule), and CD104^{hi} (cell adhesion molecule) markers and grown on matrigel along with Sca-1^{pos}EpCAM^{neg} mesenchymal cells and mesenchyme-derived growth factors to establish the colony forming efficiency of the isolated tracheal airway stem cells.

2.2.7.2 Tracheal Cell Preparation and Flow Cytometry

Tracheas were dissected from mice and rinsed in sterile PBS and transferred to sterile PBS/2% glucose. Mouse trachea cell suspensions were prepared by liberase digestion. Low-density cells were then isolated by density gradient centrifugation (Nycoprep 1.077A; Nycomed Pharma) and then resuspended and incubated in 2% vol/vol FCS or newborn calf serum (5×10^7 cells/mL, 20 min on ice) in an optimally pre-titred [101] mixture of antibodies, including antiCD45, anti-CD31, anti-Sca-1, anti-EpCAM, anti-CD49f, anti-CD104, and relevant isotype controls (Biolegend).

Labelled cells were washed in PBS-2% serum, resuspended at $5–10\times10^6$ cells/mL, and held on ice until flow cytometric analysis and sorting. Sorting was performed using an Influx cell sorter (Becton Dickinson). Analysis was performed on a BD LSRII bench top analyzer (Becton Dickinson) and FlowJo (Tree Star).

2.2.7.3 Cell Culture for Clonal Assays

Sorted airway stem cells were centrifuged at 400 x g, 4°C for 5 min and the cell pellet resuspended in 1ml chilled CFU-Epi medium. Airway stem cells were mixed with Mlg 2908 cells at a final concentration of 2×10^4 and 2×10^6 cells per ml respectively and centrifuged at 400 x g at 4°C for 5 mins. Cell pellet was resuspended in Matrigel diluted with CFU-Epi medium: DMEM/F12, penicillin, streptomycin, glutamax (Gibco), insulin, transferrin, selenium, 10% FBS, 2 μg/mL Heparin sodium salt (STEMCELL Technologies) at a ratio of 1:1 and placed into a 30 mm Millicell insert in a six well culture plate. Three x 25 μl drops of Matrigel cell suspension was placed on top of the Millicell filter membrane and incubated for 5 mins at 37°C to set the Matrigel. 1200 μl of CFU-Epi medium was then placed around the insert of each well and the cell culture was then incubated at 37°C, 5% O_2, 10% CO_2, 85% N_2 with media changes performed 3 times weekly.

3 Airway stem cell transduction by a VSV-G pseudotyped HIV-1 lentiviral vector

3.1 Introduction

Gene therapy has the potential to correct the underlying gene and subsequent protein defects associated with all mutation classes of CF. Both non-viral and viral vectors have been explored with encouraging results from studies using integrating viral vectors such as lentiviruses [95, 96]. Furthermore, lentiviral vectors have the advantage of transducing both dividing and non-dividing cells [60-62] raising the potential of achieving stable lifelong integration of a transgene into airway stem cells, leading to a single treatment providing lifelong benefit. Research by Limberis et al [96] utilizing a MPSV promoter driven HIV-1 VSV-G pseudotyped lentiviral vector (LacZ) in the respiratory epithelium has shown that not all cell types displaying positive marker gene expression at day 92 were present at earlier time points (days 7 and 28). In addition, Stocker et al [98] showed that a single dose of the same vector in the respiratory epithelium was sufficient in some cases to produce expression of a marker gene (LacZ) for 24 months (life time of mice), and a therapeutic gene (CFTR) for at least 12 months. Together these studies strongly suggest transgene insertion into airway stem cells within the respiratory epithelium which is passed on to their progeny through the normal ongoing mitotic division.

The advantages associated with transducing tissue specific airway stem cells *in situ* are: (1) a single airway stem cell has the potential of acting as a progenitor for ~ 8 x 10^3 cells per generation [91], (2) that although lentiviral vectors are less immunogenic upon re-administration than other viral vectors [102], the targeting of

airway stem cell transduction may provide a single effective treatment, alleviating the need for re-dosing, and (3) it is a more practical and less invasive method than removing the airway stem cells, correcting them *ex-vivo* and re-seeding into the respiratory epithelium.

The aim of the experiments reported in this chapter was to determine if airway stem cells can be transduced and are able to pass the transferred transgene to their progeny.

3.2 Methods

3.2.1 Animals

All studies in this chapter utilized C57bl/6 normal mice and were approved by both the Adelaide University and The Adelaide Women's and Children's Hospital Animal Ethics Committees.

3.2.2 Gene Vector

The MPSV nuclear-localised LacZ (LacZnlsco) VSV-G pseudotyped HIV-1 based LV vector was produced according to previously published methods with some minor modifications [73, 97]. Briefly, the LV vector was produced by transient transfection of 293T cells with a five plasmid system using calcium phosphate co-precipitation. The ratio of plasmids used for all virus preparation was as per methods section 2.2.3. Virus titre was 2 x 10^9 tu/ml as assayed by qPCR, see section 2.2.4.1 [97]. The vector dose in these studies was 20 μl as used in previous nasal studies [97, 98]

3.2.3 Nasal and tracheal gene transfer treatment

All reagents were delivered to the nasal airway via inhalation-driven instillation, as previously described [97]. Tracheal instillations were performed via a fluid dose that was instilled into the trachea through a fine pipette tip inserted through a 20 gauge cannula inserted into the trachea via the oral cavity (non surgical). Prior to dosing, all mice were anesthetised, see methods section 2.2.5.

Prior to instillation of vector, mice were given a 4 µl (nasal) and 10 µl (tracheal) pre-treatment of 0.3% L-α-lysophosphatidylcholine (LPC) (Sigma Aldrich (USA) Cat # L4129) in phosphate buffered saline (PBS). The LV vector was administered one hour later into the same nostril (2 ×10 µl aliquots over 2-3 minutes). Anaesthesia was reversed with an intraperitoneal injection of atipamezole hydrochloride (1µg/g). Mice were kept in a humidified incubator (37 °C) and monitored until recovery from anaesthetic was complete (generally 3-4 hours).

3.2.4 Induced regeneration of the respiratory epithelium via Polidocanol treatment

For ablation of the tracheal and nasal epithelium 10 µl of 2% (w/v) Polidocanol (PDOC-Polyoxyethylene 9 Lauryl Ether; SIGMA, St Louis, MO) (Figure 3-1) was delivered using the same method described by Borthwick *et al* and Mitomo *et al* [84, 95]. The presence of subsequent transient ablation and regeneration of the nasal and tracheal epithelium was confirmed in pilot studies. Briefly, the nasal tissue was treated with 10µl of PDOC as a bolus via nasal sniffing; and the trachea with 10µl of PDOC as a bolus delivered via the intubated 20 Ga cannula with the opening placed just below the epiglottis. Following PDOC treatment, mice were treated with Buprenorphine (2µg/g) every 4 hours for pain relief. Relevant tissue samples were collected 24 hours (n=3), 4 days (n=3) and 7 days (n=3) post PDOC treatment for

assessment of ablation and regeneration.

Figure 3-1: Polidocanol

Chemical structure of polidocanol used as an ablation agent in the forced injury model

To assess transduction of airway stem cells mice were first treated with the HIV-1-VSV-G pseudotyped vector containing the LacZ marker gene as described in Methods 2.2.5. Following vector treatment mice were separated into 4 groups of n=11 per group. Group 1: short term control, seven days following vector instillation group one was culled for histological analysis for the short term gene expression profile. Group 2: long term control, at 4 and 8 weeks following vector instillation, mice were treated with PBS and culled at 14 weeks for histological analysis. Group 3: 1 x ablation, 4 weeks following vector treatment, mice were treated with PDOC and at 8 weeks treated with PBS and culled at 14 weeks for histological analysis. Group 4: 2 x ablation, 4 and 8 weeks following vector treatment, mice were treated with PDOC and culled at 14 weeks for histological analysis.

Marker gene expression was confirmed initially by *en face* examination of nasal and tracheal tissue samples. To assess the cell types expressing the LacZ marker gene following vector treatment 5 μ wax sections of formalin-fixed nasal and tracheal tissue were mounted on glass slides, processed and histochemically stained using

48

Haemotoxylin and Eosin (H & E) or Alcian Blue/Periodic Acid Schiff (AB/PAS).

3.3 **Results**

3.3.1 **LPC pre-treatment and vector instillation**

Nasal airway instillation of the vector and pre-treatment was technically uneventful and all mice tolerated the treatment well. Tracheal vector instillation was tolerated well; however pre-treatment instillation of the 0.3% LPC into the trachea resulted in the death of 3 mice.

3.3.2 **Effect of PDOC-based ablation on epithelial integrity and regeneration**

Histological analysis (H & E) of nasal airway tissue from 3 groups of mice collected 24 hours (n=3), 4 days (n=3) and 7 days (n=3) post PDOC instillation revealed ablation of nasal airway epithelium was successful, when measured at the 24 hour time point (Figure 3-2: Assessment of PDOC on the airway epithelium. Four days following the PDOC instillation the epithelium had partially recovered with a complete epithelium of immature cells present (Figure 3-2: Assessment of PDOC on the airway epithelium. At 7 days post PDOC instillation the epithelium appeared repaired, had re-ciliated and histologically presented a normal appearance (Figure 3-2: Assessment of PDOC on the airway epithelium.. Confirmation of the intact basement membrane and airway stem cell integrity 24 hours following PDOC was confirmed morphologically (Figure 3-3: PDOC airway epithelium ablation on the basement membrane and airway stem cells.
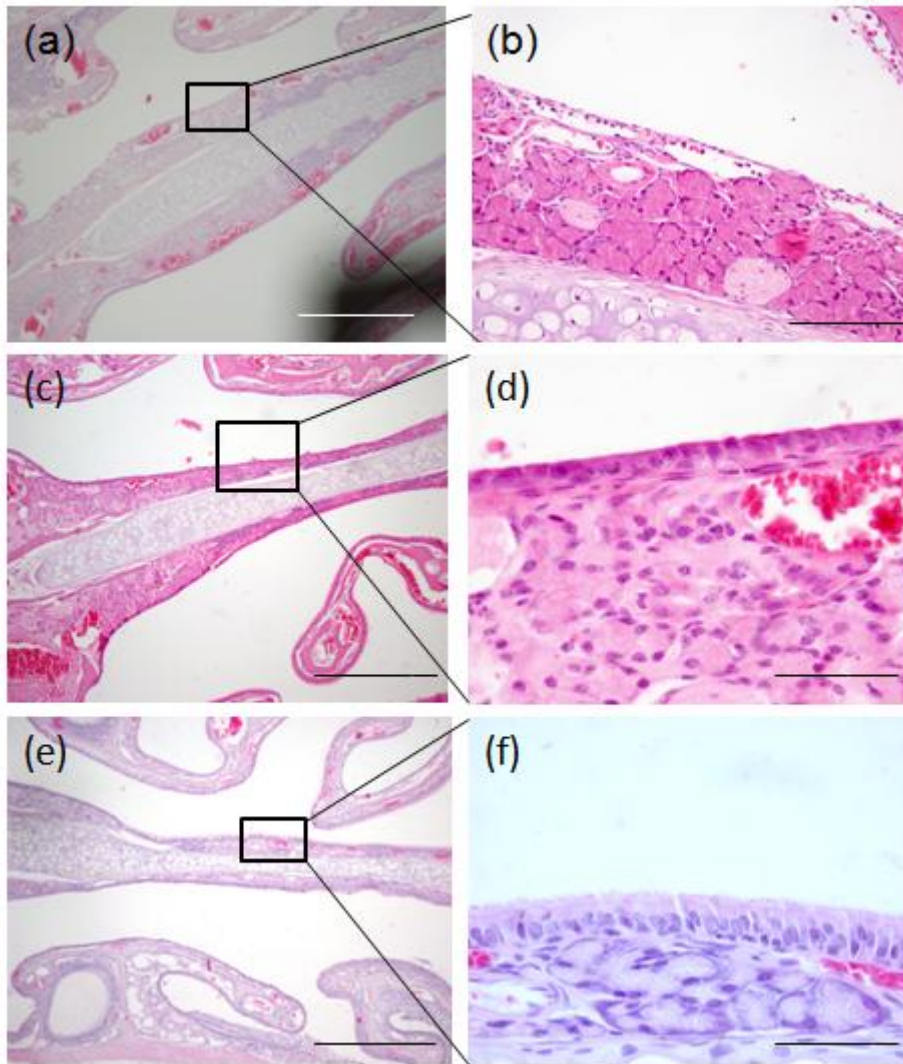
Figure 3-2: Assessment of PDOC on the airway epithelium.

(a & b) Nasal airways following PDOC ablation at 24 hours, (c & d) partial regeneration at 4 days and (e & f) regenerated at 7 days. (Scale bars 100 μm (a ,c & e) 50 μm b, d & f)
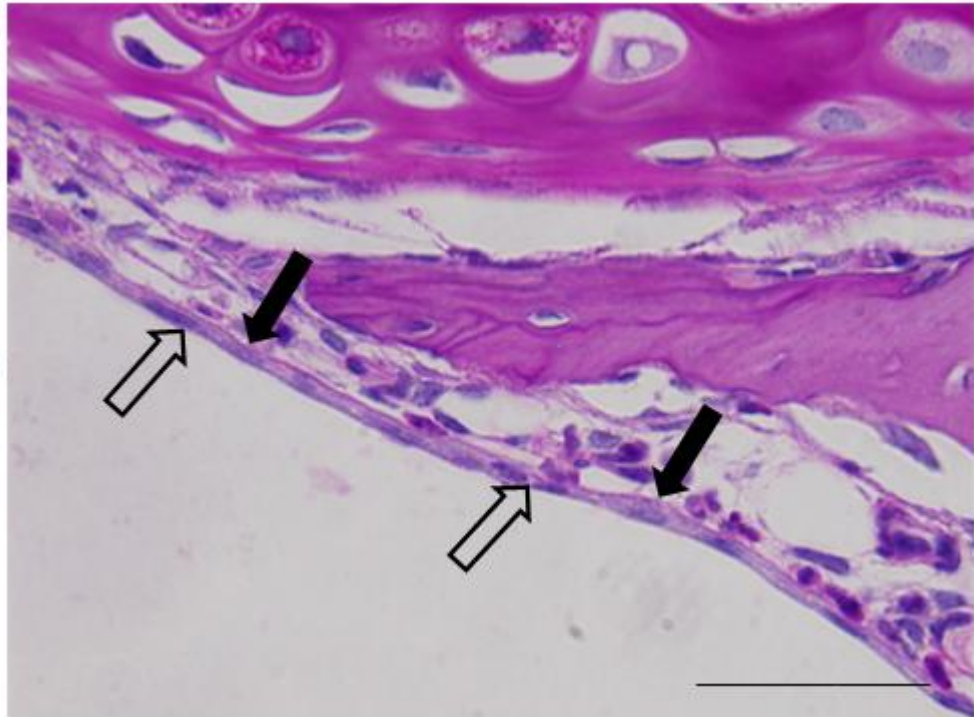
Figure 3-3: PDOC airway epithelium ablation on the basement membrane and airway stem cells.

Nasal airway following PDOC ablation showing an intact basement membrane (solid arrows) and presence of airway stem cells cells (open arrows show examples of airway stem cells) (AB/PAS) (Scale bar 50 μm)

3.3.3 Induced regeneration of the respiratory epithelium revealed clonal clusters of marker gene positive cells

To determine if chromosomal integration of a marker gene (LacZ) into airway stem cells in the respiratory epithelium by a HIV-1-VSV-G vector results in the passing on of that transgene to its progeny upon differentiation, regeneration of the respiratory epithelium was induced using PDOC treatment. After this treatment clusters of LacZ expressing cells were observed in both the nasal (Figure 3-4 d & e) and tracheal airways (Figure 3-5 d & e). In contrast the 7 day (no-ablation) controls displayed the typical finely speckled pattern of LacZ expression in both the nasal (Figure 3-4 a) and tracheal tissue sections (Figure 3-5 a). The 14 week no-ablation control displayed a similar speckled pattern but with some clusters also present in

both the nasal (Figure 3-4: Forced injury model in the nasal airway. In contrast, both PDOC ablation groups displayed numerous clonal clusters including instances of spotted and linear expansion in the nasal (Figure 3-4 c & f) and tracheal (Figure 3-5: Forced injury model in the tracheal airway.
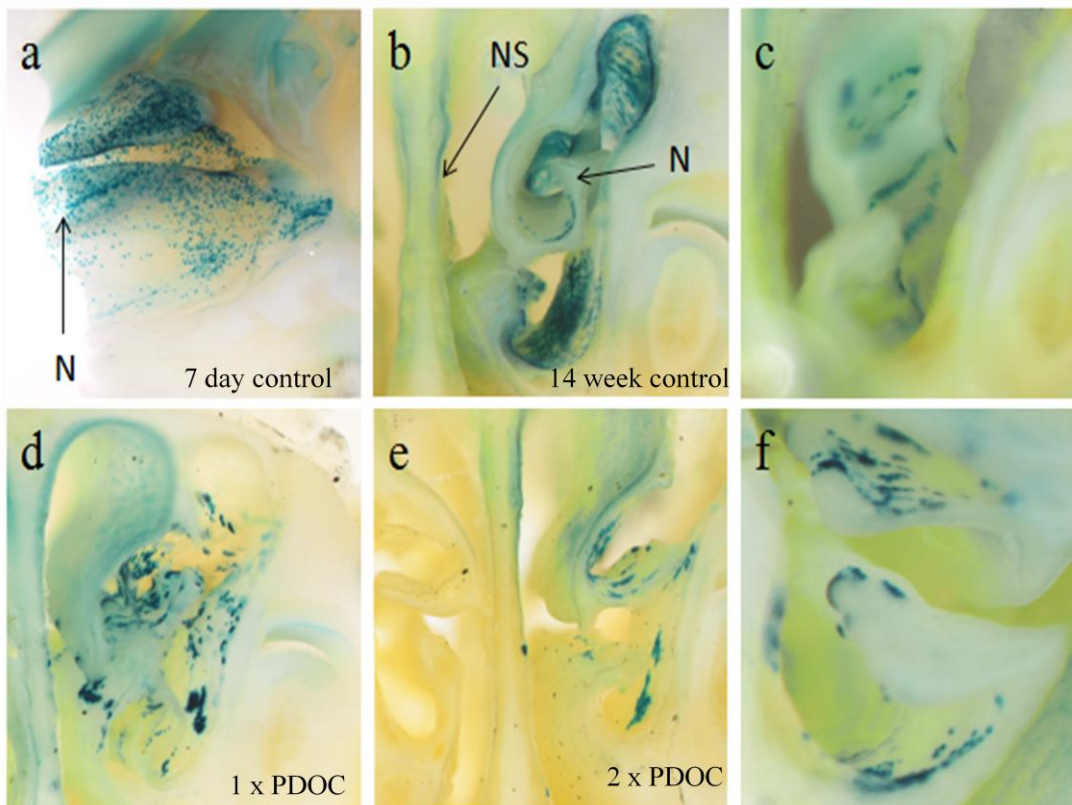
Figure 3-4: Forced injury model in the nasal airway.

(a-b) LacZ expression revealing the pattern of marker gene expression (nasal airway) in 7 day and 14 week controls and the presence of clustered LacZ positive cells in the forced injury models upon epithelial regeneration, (d) 1 x PDOC and (e) 2 x PDOC. (c & f) Clusters of LacZ positive cells were observed as both spotted clusters and linear clusters. NS = Nasal Septum, N = nasoturbinate. (a,b,d&e 20x) (c&f 40x)
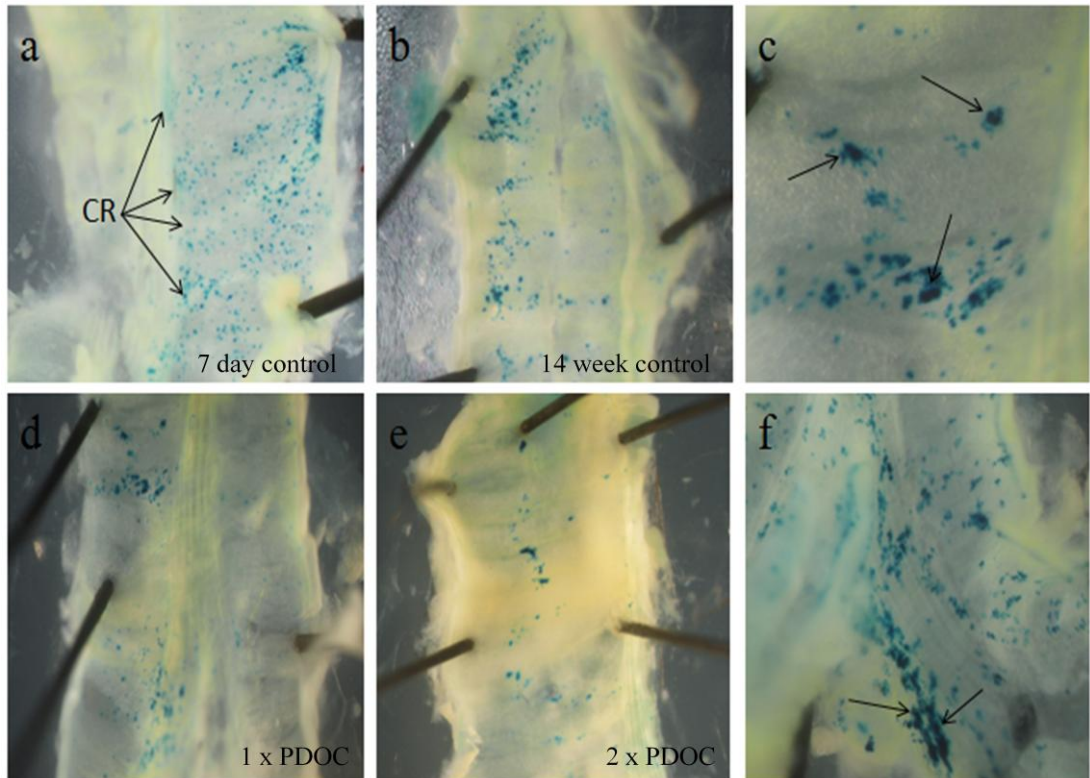
Figure 3-5: Forced injury model in the tracheal airway.

(a-b) LacZ expression revealing the pattern of marker gene expression (trachea) in 7 days and 14 week controls and the presence of clonal clusters in the forced injury models upon epithelial regeneration, (d) 1x PDOC and (e) 2x PDOC. Clonal regrowth was observed as both symmetrical clusters (c black arrows) and linear clusters (f black arrows). CR = cartilage rings (a,b,d&e 20x) (c&f 40x)

3.3.4 Identification of marker gene expressing cell types

Histological analysis of LacZ expressing cell types revealed the presence of transduced ciliated cells and airway stem cells in the no-ablation animals. The same cell types were also present in the ablation groups, but with the addition of LacZ-expressing goblet cells (Figure 3-6).
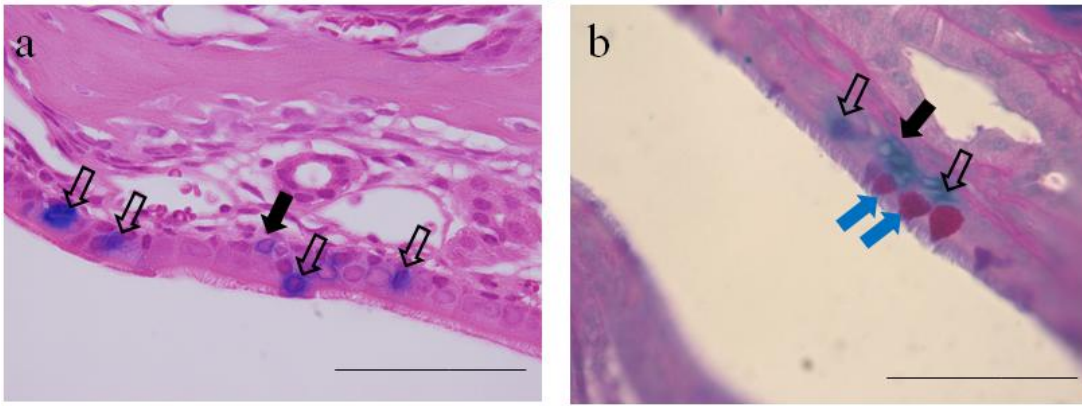
Figure 3-6: Forced injury model histology.

(a) Histology of non-ablation and (b) ablation airways revealed the presence of a marker gene expressing cell type (goblet) (blue arrows) in the regenerated airway (b) not observed in the non-ablated airway. Marker gene expressing cilliated and airway stem cells were observed in both the ablated and non-ablated airways (a & b). (AB/PAS) (scale bar 50 μm) Images 100x

3.4 **Discussion**

A gene therapy treatment to prevent CF related airway disease requires lifelong expression of an introduced CFTR transgene. Repeated dosing of a vector carrying the CFTR gene to maintain a therapeutic effect is at first an attractive option, however the ability to administer viral vectors repeatedly has proven to be limited [95]. It is commonly desirable for a therapeutic treatment to be a one-off procedure as opposed to one that must be a repeated treatment over time. It is proposed that a single dose of a viral vector capable of both chromosomal integration and transducing airway stem cells responsible for repair and regeneration of the respiratory epithelium may provide an effective treatment, or cure for CF airway disease.

Studies utilising a HIV-1 lentiviral vector have demonstrated sustained transgene expression following a single dose [96, 98]. In those studies the HIV-1 vector was pseudotyped with the VSV-G protein which targets receptors on the basolateral

surface of airway epithelial cells [103]. As these VSV-G receptors reside on the basolateral surface of epithelial cells, access to the HIV-1 VSV-G vector to the receptors is restricted. To allow access to the basolateral surface, Limberis *et al* and Stocker *et al* utilised a pre-treatment of LPC to transiently open the tight junctions present between cells allowing the vector access to the basolateral cell surface [96, 98]. The ability to access the basolateral cell surface following a pre-treatment with LPC also provides the opportunity to gain access to the airway stem cells that reside on the epithelial basement membrane. Taken together, access to airway stem cells following pre-treatment with LPC and the ability of the HIV-1 VSV-G vector to transduce dividing cells (airway stem cells) may be responsible for the sustained gene expression reported in both of these studies.

By using a PDOC forced injury model in the nasal and tracheal airways the airway epithelium can be ablated to assess the fate of potentially transduced airway stem cells.

Cells expressing LacZ were present following one ablation and two ablations and the subsequent epithelium regeneration in the nasal and tracheal airways. By comparing the pattern of LacZ expression to that present in the 7 days controls following pre-treatment and gene transduction, a different pattern of expression was observed, providing clues to the underlying mechanisms of sustained gene expression. The speckled pattern of LacZ expressing cells seen in the 7 day control was clearly different to the clustering of LacZ expressing cells in the epithelial forced injury and regeneration animals. The clustered appearance of LacZ expressing cells is consistent with a pattern of clonal expansion whereby transduced airway stem cells have passed the marker gene onto their progeny as they have differentiated during

the epithelium repair process.

Importantly, clusters of LacZ expressing cells were also observed following two PDOC treatments of the epithelium demonstrating that the clusters observed from the single ablation were unlikely to be a consequence from incomplete stripping of the epithelium during the ablation treatment

The pattern of LacZ expression observed in the long term (14 week) control group that did not receive PDOC, displayed both speckled and clustered LacZ- expressing cells. This finding is consistent with the speckled LacZ positive cells representing terminally differentiated cells that had been transduced at the time of vector treatment and the clustering of LacZ positive cells being progeny of airway stem cells that were transduced at the time of vector treatment.

Further evidence supporting airway stem cells passing the transgene on to their progeny can be seen in Figure 3-6 which shows that in the no ablation treatment group the presence of both LacZ expressing airway stem cells and ciliated cells. Following the regeneration of the airway epithelium after the ablation treatment the same LacZ expressing cells types were present; however, there was also the presence of mucin secretory cells expressing the marker gene. This suggests that transduced nasal airway stem cells have passed the marker gene to all their progeny upon differentiation, including those not targeted by the cell specific VSV-G pseudotype.

Clonal expansion from airway stem cells transduced with the LacZ marker gene was predicted to produce symmetrical LacZ positive clusters of cells upon epithelial repair and regeneration. These clusters were anticipated as the newly differentiated cells expanded out from the transduced parent airway stem cell (Figure 3-7) as previously reported [95].
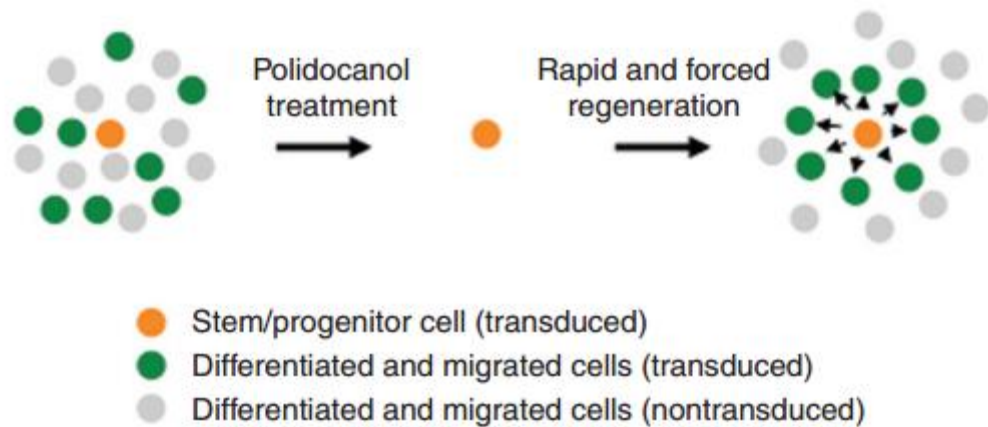
Figure 3-7: Pattern of clonal cluster.

Illustration demonstrating the outgrowth of differentiated cells from a transduced stem cell forming a symmetrical cluster. Adapted from Mitomo *et al* [95]

In the single and double ablation groups in both the nasal and tracheal airways, the clustering of LacZ positive cells was observed and confirmed. Unexpectedly though, in conjunction with the observation of symmetrical clustering of LacZ positive cells there were also linear clusters of cells present. There are several potential causes for the two distinct patterns of clonal expansion observed following repair and regeneration. Firstly, the pattern may have been a result from the fluid dynamics of the introduced doses during the instillation of the pre-treatment and vector. It is feasible that the nature of fluid delivery caused the vector to transduce airway stem cells along a linear track resulting in the pattern observed. However, if true the clusters within the linear expansion should be of approximately the same size as those in the symmetrical clusters, not smaller as observed. Secondly, epithelial disturbance caused by the ablation treatment could result in an altered airway cytokine expression leading to an abnormal linear outgrowth of cells from the airway stem cell parent.

Alternatively the two distinct patterns may be a result of the natural process of epithelial repair/regeneration. To the authors' knowledge these distinctively different clonal patterns have not been reported in airway stem cell literature and further studies are warranted to elucidate the mechanism(s) behind the differences, as this may gain further insight into the nature of airway stem cell repair and regeneration.

This demonstration of airway stem cell transduction in the airway epithelium provides a foundation that may be built on with further studies. Targeting the airway stem cell compartment may be a viable and promising option for elevating the level of sustained CFTR expression. One option is to consider the integrin profile of the airway stem cell, specifically integrins αvβ5 and α5β1 to target binding by the lentiviral vector and thereby enhancing transduction events. The integrins αvβ5 and α5β1 act as receptors for proteins that contain the Arg-Gly-Asp (RGD) attachment site [104].

Studies incorporating the integrin-targeting peptide RGD into vector envelopes have shown encouraging results. Morizono *et al* demonstrated increased transduction of a lentiviral vector in human umbilical vein endothelial cells following insertion of the RGD peptide into envelope proteins [105]. In addition they demonstrated that the RGD peptide could be incorporated into the lentivirus envelope without interfering with the VSV-G pseudotype [105], a possibility suited to the LV vector used in these thesis studies. Another group have used nanocomplexes containing the RGD peptide to target tumours, resulting in a 2 fold increase in transduction and also achieving delivery into the lungs [106]. Studies investigating the use of the RGD peptide to target specific integrins are encouraging. A detailed study designed to assess the ability of the HIV-1 VSV-G pseudotyped lentiviral vector to target airway stem cells

using this approach is an encouraging option for future studies.

While the proof-of-principle for sustained transgene expression has been presented in this chapter, there are a number of considerations to address. There has been substantial progress in the understanding of airway stem cell development, repair, and regeneration; however, there still remains an unknown factor involved that may impact the targeting of airway stem cells in a gene therapy setting.

The notion of targeting airway stem cells for sustained gene expression relies on the premise that a transduced airway stem cell will remain continuously throughout the lifetime of the patient, constantly passing on the inserted gene to its progeny upon epithelial repair. There are two models of tissue self-renewal that have been proposed that have yet to be resolved in the airways and depending on which model is correct will have an impact on the targeting of airway stem cells. The two proposed models are the division asymmetry model and the population asymmetry model. The division asymmetry model proposes that as stem cells divide they give rise to one stem cell (self-renewal) and one differentiated cell which may be terminally differentiated such as ciliated cell, secretory cell or a differentiated progenitor cell further down the stem cell hierarchy such as a Club cell. The important feature of this model is that a transduced stem cell would pass on its transgene through self-renewal; hence a transduced stem cell would potentially be present for life. The population asymmetry model proposes that a portion of stem cells in a niche will differentiate without self-renewal and the remainder will divide symmetrically to renew those that are lost. In this model, there is a chance that a transduced stem cell is lost through neutral drift and is replaced with a stem cell not carrying the transgene of interest.

To determine if the division population asymmetries model and neutral drift is a limiting factor in airway stem cell targeting for sustained gene expression, further studies are warranted. It is proposed that by transducing airway stem cells with the LV vector carrying a fluorescent gene the flow cytometric airway stem cell isolation technique presented in Chapter 4 may be used to provide insight into the question of neutral drift. Flow cytometry could be used to ascertain and quantify the number of airway stem cells expressing the fluorescent protein compared to the total number of airway stem cells sorted. This procedure could be performed over time points representing the life span of mice, to determine if the proportion of transduced stem cells changes over time. If the proportion remains stable over time it would suggest that neutral drift is not occurring, and that the division asymmetry model is more likely to explain the dynamics of airway stem cell activity.

3.5 Conclusion

The observations reported in this chapter support the notion that a HIV-1 VSV-G pseudotyped lentiviral vector when delivered with a pre-treatment of LPC can transduce airway stem cells. By utilising the ability of airway stem cells to pass on the transgene to their progeny upon differentiation, sustained transgene expression can then be produced without further airway gene transfer events.

.

4 Airway stem cells and epithelial remodelling in the conducting airways of CF mice

4.1 Introduction

Epithelial remodelling of the conductive airways in those afflicted with CF is poorly understood and a better understanding of the effect of CF on the epithelial phenotype is warranted. A more concise understanding of epithelial remodelling will potentially allow for the further development of approaches such as gene therapy to correct airway disease associated with CF.

Airway stem cell hyper proliferation in the CF airway has been reported [107, 108], Leigh *et al* showed the presence of cell hyper proliferation in CF compared to normal airways [107] and Voynow *et al* extended this finding to propose that airway stem cells were the responsible proliferating cell population [108]. However, the methods used to ascertain the state of cell proliferation in the CF airways have been restricted to antigen labelling, such as a proliferating cell nuclear antigen (PCNA) [107, 108]. Similarly, identification of proliferating cell types has been restricted to morphological and histological analysis [108]. There remains uncertainty as to whether an increase in respiratory cell proliferation is due to; (1) an increase in proliferation of the normal airway stem cell population, (2) is reflective of hyperplasia of the airway stem cell population, or (3) a combination of both.

The recent development of definitive cell surface markers now enables isolation of respiratory airway stem cells via flow cytometry, and an ability to subsequently measure their proliferative potential of specific subsets via a clonogenic colony

forming assay [101]. This approach provides for the first time a method to quantify and compare the airway stem cell compartment in CF and normal mice.

The pseudostratified epithelium of the murine tracheobronchial region is not fully reflective of that observed in humans: while both are comprised of airway stem cells, secretory cells and ciliated cells [109], goblet cells in mice are confined to the most proximal laryngeal region of the trachea, and to the nasal airways [110]. Nevertheless there remains sufficient similarity in cell types in humans and mice to allow the mouse animal model to assist in elucidating the potential presence of airway stem cell hyperplasia in the conducting airways of CF mice.

In addition to potential airway stem cell hyperplasia in the epithelium of CF airways, goblet cell hyperplasia has also been previously studied [32, 111]. *In vitro* studies assessing goblet cell hyperplasia in the differentiated epithelium of CF versus non CF airways have concluded there was no significant difference in goblet cell numbers [112, 113]. In contrast, *in vivo* studies have suggested goblet cell hyperplasia is present in the nasal airways of CF mice [32, 111].

It is currently unknown if the goblet cell hyperplasia in the airway of CF mice is present in conjunction with airway stem cell hyper proliferation and potential hyperplasia. Gaining a better insight into the possible dual presence of hyperplasic goblet cells and stem cells in the CF airways will provide a better understanding of the targeted epithelial environment which is the target of CF gene therapy.

In this chapter the remodelling of the CF respiratory epithelium was observed, quantified and compared across CF knockout mice and normal mice, using cell counts, histochemical analysis, and AB/PAS staining. An airway stem cell proliferation index was calculated using the staining of an antigen (KI-67) that is

only present in dividing cells. The number of airway stem cells and their proliferative capacity in CF knockout mice was compared to that in normal mice using flow cytometry and clonogenic assays.

4.2 Material and Methods

4.2.1 Mouse models

Three genotypes of mice from 2 colonies of CF mice were used in this study: (1) *Cftr*$^{tm\ 1\ unc-/-}$ and their litter mate controls *cftr*$^{tm\ 1\ unc+/-}$ (C57BL/6 background [114], termed CF UNC and UNC HET respectively). (2) *Cftr*$^{tm\ 1\ unc}$ Tg$^{(FABPCFTR)\ -/-}$ (mixed background [115], termed CF FABP) mice were bred from (-,-)homozygote's mating and therefore no littermates controls are produced. When comparison between CF FABP mice and non CF controls was required *cftr*$^{tm\ 1\ unc+/-}$ mice (UNC het) were used. All animals were anaesthetised using a mixture of 10 µl/g body weight of Domitor, 0.1 mg/ml, (Orion Corporation, Finland) and Ketamine, 7.6 mg/ml, (Parnell Laboratories Aust Pty Ltd), given as a single dose.

4.2.2 Processing of tissue

Animals were humanely killed via CO_2 inhalation. Tracheal tissue used for histochemistry and immuno-histochemistry were removed and fixed in 10% neutral buffered formalin (NBF). Mouse heads (for nasal airways) and trachea used to provide cells for flow cytometric analysis were removed from the body; the fur and skin was removed from heads and both tissue samples immediately washed with sterile PBS and placed into PBS with 2% glucose. Nasal septa were dissected free of the nose while submerged in PBS 2% glucose. Mouse head's used for counts of nasal airway goblet cell and airway stem cell numbers via immuno-histochemistry

were removed as above and placed into 2% (w/v) paraformaldehyde/0.5% glutaraldehyde (v/v) in PBS on ice for 2 hours, transferred to 10% neutral buffered formalin (NBF) for 24 hours before being decalcified in 1.5% (w/v) EDTA, 7% (v/v) HCL for 22 hours. Decalcified tissue was then rinsed in running water for 30 mins and stored in 70 % (v/v) ethanol. Following initial processing and decalcification of the head, the jaw was removed exposing the upper palate and gross sections made in locations at levels 6, 16, 24, and 30 described by Mery *et al* [116]. The four gross tissue sections were embedded in paraffin wax and 5 μm sections cut and mounted on glass microscope slides. A proliferation index was established via Ki-67 immuno-histochemistry in trachea were dissected from mice immediately following humane killing and subsequently placed into 10% NBF overnight.

4.2.3 Tracheal and nasal septum cell preparation and flow cytometry

Airway stem cells were FACS sorted from the processed respiratory airway epithelium of trachea to establish the incidence of this cell type in CF UNC, CF FABP and CF HET mice as described in Methods section.

4.2.4 Cell culture

Cell culture for clonal assays to gain the growth fraction of airway stem cells were performed in matrigel as described in Methods section.

4.2.5 Histochemistry and Immuno-histochemistry

To assess airway remodelling: (1) Nasal airway sections were stained with AB/PAS reagent, to identify goblet cells, quantify their numbers, measure the size of the mucin-stained cells and assess mucin acidity. (2) To establish a proliferation index

within the tracheal stem cell compartment, a nuclear proliferation antigen Ki-67 (MIB-1 clone) that is only present in cycling cells was employed.

4.2.6 Statistics

All comparisons between CF and controls were analysed for statistical significance using an unpaired t test with significance being set at $p < 0.05$.

4.3 Results

4.3.1 Goblet cell hyperplasia and hypertrophy in CF mouse nasal airways

Goblet cell hyperplasia and hypertrophy was assessed through AB/PAS staining in the nasopharyngeal airways sections from region 30 [116], were the airway is tubular and lined with ciliated respiratory epithelium. When standardised to goblet cells per 10 μm of nasal respiratory epithelium, CF UNC (6.6 ± 0.3 goblet cells) (n=5) showed a statistically significant (p<0.001, t-test) 2.02 fold increase compared to UNC het controls (3.2 ± 0.2) (n=5) (Figure 4-1). Goblet cell hypertrophy was also significantly increased (p<0.001, t-test) in CF UNC (3.5 ± 0.548 μm^2) (n=5) compared to controls (1.6 ± 0.115 μm^2) (n=5) that resulted in a 2.2 fold increase (Figure 4-1).
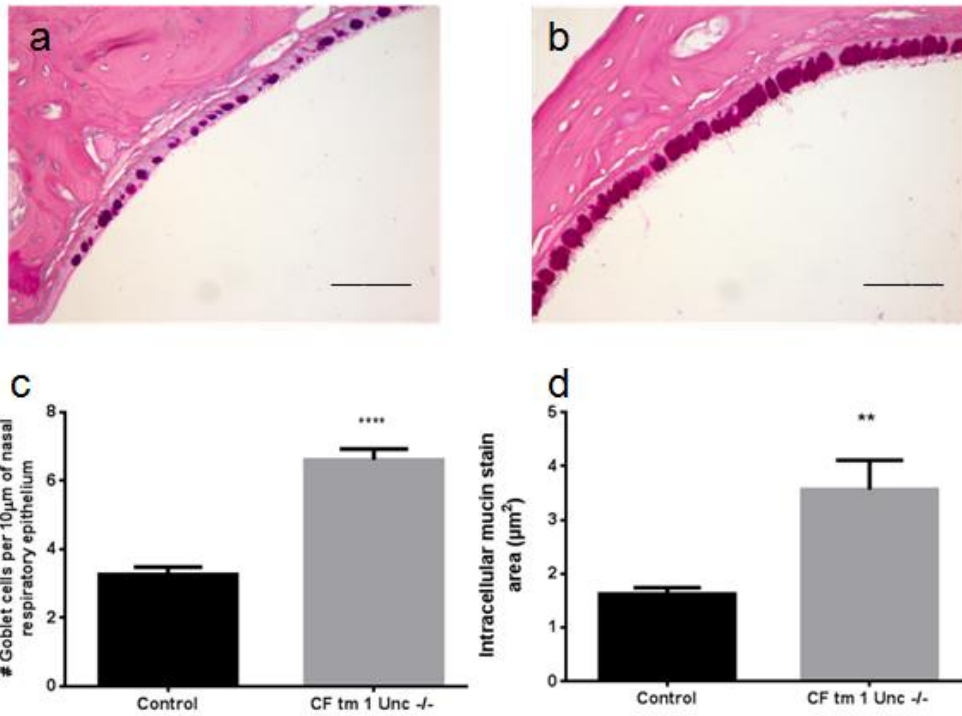
Figure 4-1: Goblet cell hyperplasia and hypertrophy.

(a) Goblet cell hyperplasia and hypertrophy in the non CF airway compared to the (b) CF UNC airway was statistically significant (****$p < 0.0001$) and (**$p < 0.01$) respectively. (AB/PAS) (Scale bar 50μm). Sections show typical examples from the same upper region of the naso-pharynx in normal and CF mice.

Histological examination of AB/PAS stained section revealed that the non CF mice had a more acidic mucin content (Figure 4-2 a) than the mucin content of the CF goblet cells (Figure 4-2 b).
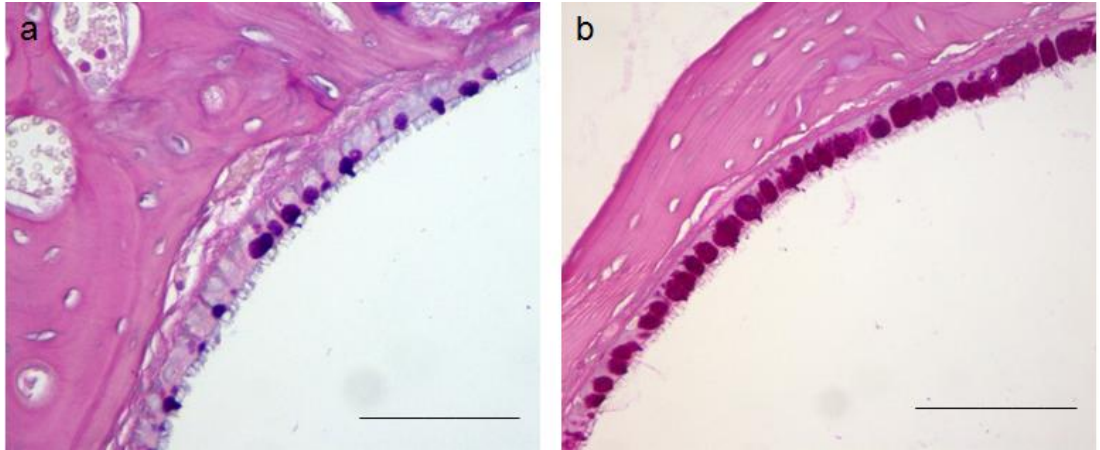
Figure 4-2: Goblet cell mucin content in CF mice compared to non CF.

(a) Mucin content in non CF airway goblet cells and (b) CF airway goblet cells A more neutral pH environment in CF goblet cells (purple staining) was present compared to the more acidic environment in the non CF goblet cells (blue). (AB/PAS) (Scale bar 50μm)

4.3.2 Proliferation index of airway stem cells

To quantify the proliferation of airway stem cells in CF mice and normal mice a proliferation index assay based on Ki-67 staining was used. Ki-67 is a nuclear antigen associated with the active G_1, S, G_2, and M phase of the cell cycle but is absent in resting cells or G_0 phase [108]. A 2.1 fold increase in actively cycling stem cells was found in CF FABP (59 $\pm$ 16 cells) (n=5) mice compared to CF HET controls (28 $\pm$ 4.2 cells) (n=5) (Figure 4-3). Most of the actively cycling cells were found at or close to the inter-tracheal cartilage zone of CF UNC control mice, but in CF FABP mice these actively cycling cells extended further into the tracheal cartilage zone.
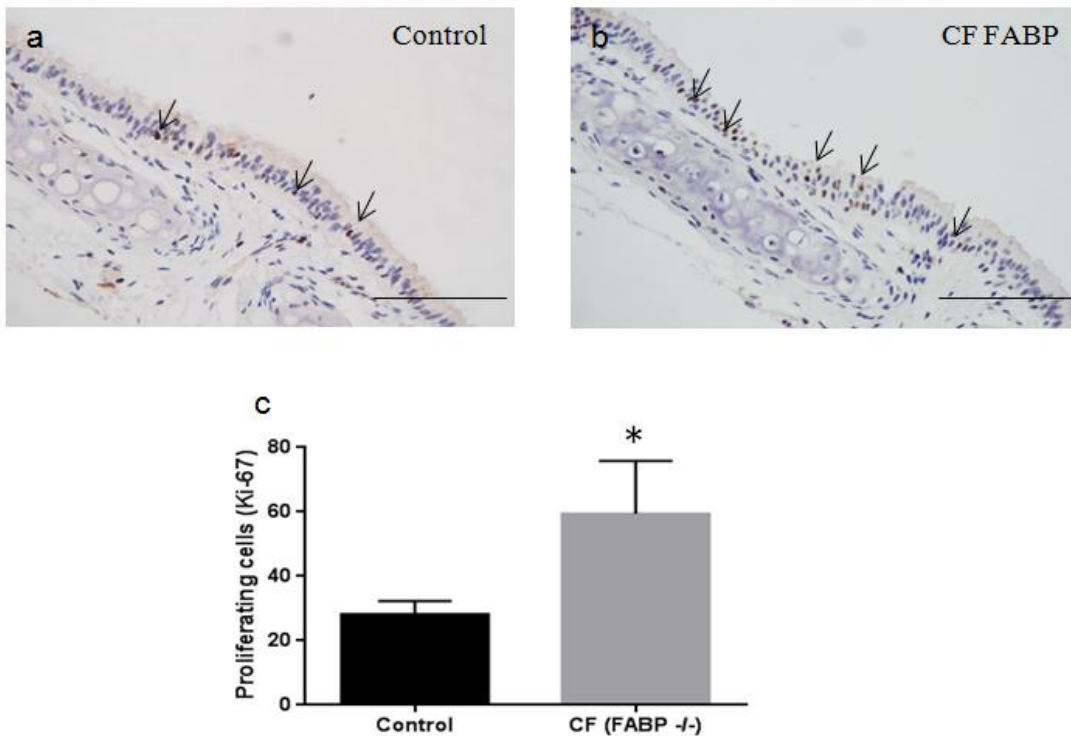
Figure 4-3: Ki-67 analysis of CF FABP trachea airway epithelium.

(a) Ki-67 analysis in CF control and (b) CF FABP trachea airway sections (c) showed a statistically greater number of proliferating cells positive for Ki-67 (black arrows) in the CF FABP mice (*p < 0.05). t test, (scale bar 50 μm)

4.3.3 Stem cell hyperplasia in the respiratory epithelium

To assess and quantify the relative abundance of airway stem cells within the respiratory stem cell compartment, a twostep flow cytometry cell sorting and clonogenic assay was employed (see methods section 2.2.7) in 2 separate studies.

To enable comparisons within each study and between the two studies it was necessary to normalize the data by calculating the relative abundance of airway stem cells obtained by the colony forming efficiency (Table 2: Study 1, relative abundance of isolated airway stem cells and their colony forming efficiency normalized. (Table 3: Study 2, relative abundance of isolated airway stem cells and their colony forming efficiency normalized.

Table 2: Study 1, relative abundance of isolated airway stem cells and their colony forming efficiency normalized.

Sample	Relative abundance (stem cells) x	Colony forming efficiency =	Normalized
UNC HET	36.0	0.38	13.68
CF UNC	24.0	2.30	55.2
CF FABP	27.0	0.97	26.19

Table 3: Study 2, relative abundance of isolated airway stem cells and their colony forming efficiency normalized.

Sample	Relative abundance (stem cells) x	Colony forming efficiency =	Normalized
UNC HET	33.6	0.62	20.83
CF UNC	43.5	0.67	29.14
CF FABP	29.4	0.65	19.11

Study one, showed that the level of functional airway stem cells present was increased in CF mice. CF UNC mice and CF FABP displayed a 4.0 and 1.9 fold higher levels of respiratory epithelium stem cells respectively when compared to the controls (Figure 4-4a). In study two, CF UNC mice displayed a 1.4 fold higher level of respiratory epithelium stem cells whilst CF FABP displayed no increase in airway

stem cells when compared to the controls (Figure 4-4 b).
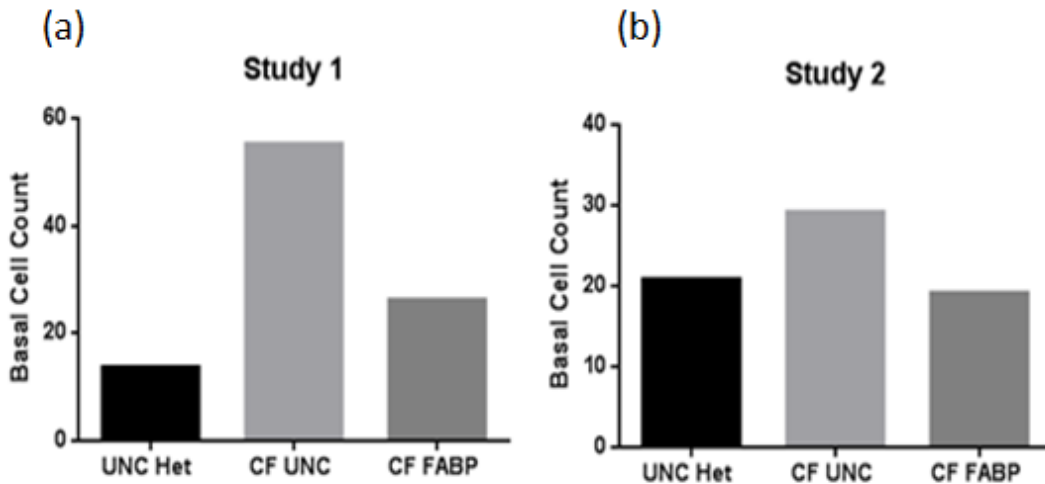
Figure 4-4: Quantification of airway stem cells.

The incidence of colony forming airway stem cells in UNC Het (normal), CF UNC, and CF FABP mice.
Normalised for relative abundance x colony forming efficiency to quantify stem cells.

4.3.4 Retrospective assessment of the ages of mice in the airway stem cell study

A retrospective assement of the available CF mice in study1 and study 2 revealed a statistical significant difference in ages, with the CF mice used in study 1 having an average of 7 months and study 2 the mean average was 4 ½ months of age (Figure 4-5).
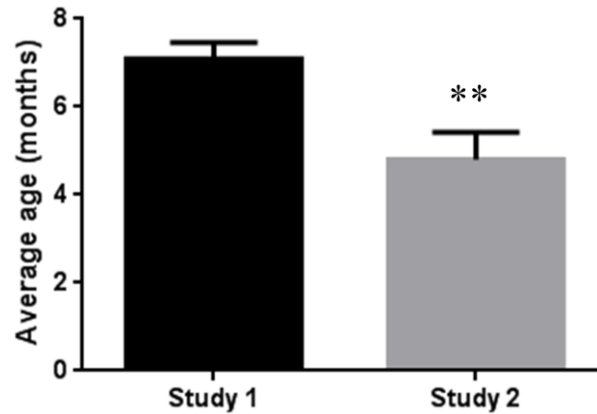
Figure 4-5: Average age of mice in the two airway stem cell studies

Analysis of the average age of mice in Study 1 compared to Study 2 showed there was a significant difference in average age between the two groups (**p <0.005, n=??). t test.

4.4 Discussion

There have been few studies characterising the conducting respiratory epithelium of the nasal and tracheal pathways in CF mice since their creation in the late 1990's. This is surprising as the nasal compartment of CF mouse models share an electrophysiological and histological profile which is similar to the epithelium of the CF nasal and lower airways in humans [117] and has been the preferred site for analysis of CFTR dysfunction in CF mice. The tracheobronchial epithelium in mice also shares some similarities with the same airway region in humans [109] although it does not share CF pathophysiological characteristics [118]. These similarities in airway phenotype have allowed researchers to explore and assess potential new therapies for CF airway disease, such as gene and cell therapies [119, 120].

It is unexpected that there have not been more studies in this area considering the implications from the findings of the few studies that have been published. Although goblet cell hyperplasia and airway remodelling in CF mice was first reported in 2001

and correlated to inflammation and infection of the respiratory airway [32], it was not until 2007 that goblet cell hyperplasia was independently reported in a CF animal model by Hilliard *et al* [111].

Prior to assessing the level of airway stem cell remodelling in the CF airways in this project it was important to verify if there was indeed a hyperplasia of airway goblet cells. This would allow for a more accurate assessment of relative influence of the stem cell compartment in a model with airway cellular phenotype changes similar to those seen in human CF airway disease.

In these thesis studies, the goblet cell hyperplasia in CF mice compared to normal mice (Figure 4-1) which is similar to that reported by Tarran *et al* who observed by morphometric comparison a 2-fold change in goblet cell numbers [32]. Although, Hilliard and colleagues demonstrated that CF goblet cell hyperplasia may occur independently from infection and inflammation [111], this conflicted with earlier reports that associated goblet cell hyperplasia in both the human airway [121] and CF mouse airways [32] with infection and inflammation.

In the current study, goblet cells in CF mice compared to controls displayed a 2.2 fold increase in the mucin-stained area within the goblet cells. This hypertrophy, together with the 2.0 fold increase in the number of goblet cells, represent a 4.4 fold increase in overall presence of mucin potentially able to be secreted into the airways.

The mucin within the CF airway goblet cells displayed a neutral pH, compared to the more acidic pH in non-CF airway goblet cells, as revealed by AB/PAS staining (Figure 4-2). This finding may reflect differences in key mucins that are found in the airway. Secretory cells in the mouse airway are known to express the mucin Muc5b at baseline conditions and these cells are a constitutive element of the homeostatic

mucosal defence [122]. Another mucin, Muc5a is up regulated in response to inflammation [34, 122] providing a possible explanation behind the change in mucin acidity. To clarify if an up-regulation of Muc5a produces the change in mucin acidity observed in the airway epithelial cells in CF mice, future studies should compare the levels of Muc5a mRNA in the goblet cells of the airway epithelium between non-CF and CF mice.

A different insight into the reasons for goblet cell hyperplasia in the respiratory epithelium of the CF airway may be provided by analysis of the airway stem cell compartment.

Studies that have examined the hyperplasia of the airway stem cell compartment in CF airways are limited. Hajj *et al* [112] have reported a 1.6 fold increase in proliferating airway stem cells in an airway epithelia regeneration study, using a model of humanized airway xenografts in nude mice. In addition, Voynow and colleagues [108] demonstrated a 5 fold increase in airway stem cells proliferation in human CF conducting airways compared to the normal airway. However, it is unclear if these rises in proliferative cells reflected an increase in the cell cycling rate in a normal airway stem cell population, or an increase in the total number of resident airway stem cell population undergoing cycling.

Until recently the analysis of airway stem cell pathophysiology in the CF airway conducting epithelium has lacked definitive assays to isolate, quantify, and index their proliferative capacity. The development of a robust airway stem cell sorting and clonal assay strategy to isolate and quantify the sub population of basal cells that act as stem cells in the respiratory airways of mice [101] was utilised in the studies presented here.

The hyperplasia of airway stem cells present in both CF mouse models at an average of age 7 months (Figure 4-4) which was not present in the CF FABP mice and substantially lower in CF UNC mice at an average age of 4.5 months indicates that the degree of hyperplasia maybe age/development dependent.

These preliminary data suggests that the airway stem cells of the conducting respiratory epithelium of the two CF mice models may not be hyperplasic at an early age but develops at a later stage in life. In addition, the statistically greater level of the airway stem cell hyperplasia observed in the CF FABP mice was correlated to a statistically different 2.1 fold increase in an actively cycling pool of airway stem cells. Together, the increase in proliferating cells correlates to the increase in colony forming airway stem cell numbers in CF FABP mice, suggesting that the increase in airway stem cell proliferation previously reported may be representative of an actively cycling hyperplasic stem cell population present in the CF airway.

The etiology of airway stem cell hyperplasia in the CF airway is unknown. The stem cell hyperplasia found in CF mice may be related to the hyperplasia of goblet cells in CF airways

It has been proposed that CFTR may function to regulate cell differentiation in the developing airway [111, 123], and the paradigm these authors proposed of a regulatory cascade, dependant on CFTR in the development and repair of the respiratory epithelium is logical. However, no further evidence to support this notion has appeared and the proposition is not supported by some of the knowledge gained from studies involving a mouse model that over expresses the epithelium sodium channel (ENaC). In those mice increased airway epithelium sodium absorption produces pathological changes that parallel those seen in CF, including severe

spontaneous lung disease, goblet cell metaplasia, neutrophilic inflammation and poor bacterial clearance [124]. One possible effect of this over expression of ENaC in an environment of an otherwise properly functioning CFTR channel, is that the elevated absorption of sodium can interrupt development of a normal airway epithelium and/or the epithelial repair cascade in airways that does not depend on CFTR dysfunction. It also suggests that elevated sodium absorption is more likely responsible for the initiation of CF-like lung disease, and importantly for these studies it may also underlie the ensuing respiratory airway remodelling such as goblet cell hyperplasia.

This elevated sodium absorption is associated with reduction in ASL depth, leading to poor mucus clearance and raised concentrations of neutrophil elastase [124] as occurs in CF. Neutrophil elastase has been linked to the release of pro inflammatory cytokine interleukin (IL)-8 which can support a self-perpetuating inflammatory process as the neutrophils present release neutrophil elastase into the airway epithelium to release IL-8, which then recruits more neutrophils to the airway surface [125], and so on.

Pro inflammatory cytokines such as IL-8 may also play a role in deregulating the Notch signalling pathway and its involvement in respiratory airway epithelium remodelling. The Notch pathway is an evolutionarily conserved signalling pathway that plays a role in integrating information cues from the extracellular environment to the cellular interior to enable appropriate developmental and physiological responses [126].

In the process of differentiation from airway stem cells into specific lineages, the Notch signalling pathway is important in determination of cell fate [127]. When the

Notch pathway is activated in the mature and developing lung epithelium the cell fate is pushed towards an increase in mucus cell production and a decrease in ciliated cell production [128] (Figure 4-6). This suggests that the Notch pathway could play an important part in the modelling of the lung epithelium in development. Similarly it also plays a role during repair of the mature lung epithelium [128].
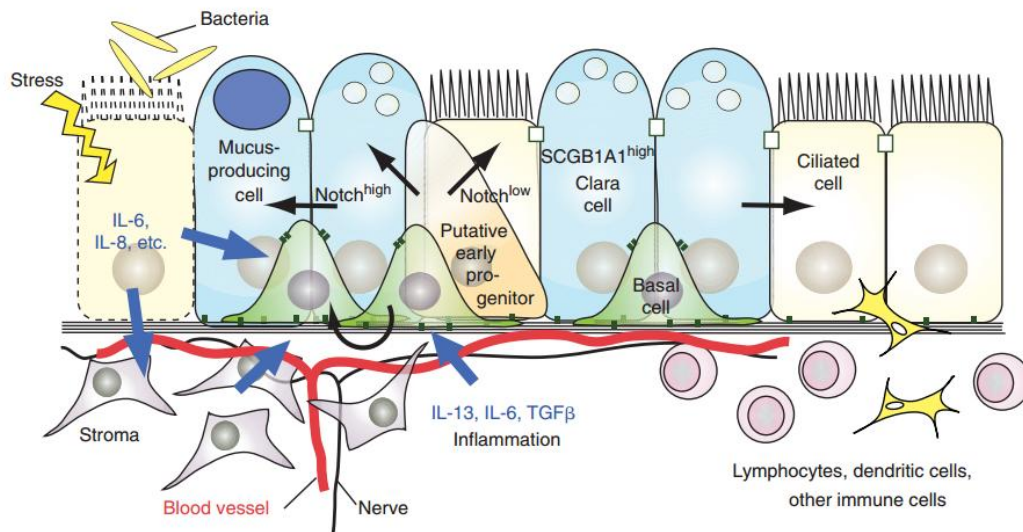
Figure 4-6: Schematic model of how signalling can effect airway stem cell (basal cell) behaviour.

A model depicting how signals including IL-8 influence airway stem cells (basal cells) and their progeny through interaction with the Notch signalling pathway [110].

The Notch pathway is modulated in part by signalling which includes cytokines such as IL-6 and IL-8 [110]. Expression mediators including cytokine IL-8 are altered in the CF airway and associated with a delay in repair [112]. As the Notch pathway plays a part in cell fate upon differentiation from airway stem cells, and activation of the Notch pathway suppresses the differentiation into ciliated cells [127], it may also lead to augmented self proliferation of airway stem cells.

An observation made during this study was that there was a statistically significant higher number of tracheal cartilage rings over a given distance in the proximal

trachea for normal mice, compared to CF UNC mice (see Appendix A). Whilst the tracheal ring observations were not the main focus of this study, it is already a known that tracheal ring remodelling is associated with decreased contractile responses from the smooth muscle surrounding the proximal trachea in both adult and new born CF mice [36]. Those structural and functional abnormalities could be viewed as a congenital malformation related to CFTR channel dysfunction during tracheal development. That is, the lack of properly functioning CFTR in development may contribute to intrinsic defects in the epithelial progenitor cell pool. If so, this could lead to dysregulation affecting cross-talk between the progenitors and the mesenchymal compartment during development, resulting in the changes observed in this study.

4.5 Conclusion

This study showed the presence of goblet cell hyperplasia in the respiratory epithelium of the CF mouse nasopharyngeal airway. Additionally, remodelling of the respiratory epithelium of the CF airway was found to extend to the airway stem cell compartment, with an increased proportion of actively-cycling hyperplasic airway stem cells present in CF mice at 7 months of age. These initial findings support the need for further studies able to elucidate the origins of pathogenic remodelling of the respiratory epithelium of the CF airway.

5 Airway gene transfer and stem cell transduction by a VSV-G pseudotyped HIV-1 lentiviral vector in the Ferret (*Mustela putorius furo*) and common Marmoset (*Callithrix jacchus*)

5.1 Preface

The development of new therapeutic approaches, including gene therapy provide an exciting new modality which holds great promise for a novel treatment for CF airway disease in the future. However, prior to embarking on clinical trials the safety and efficacy of gene therapy must be explored in pre clinical animal models. To this end the CF ferret provides an animal model which far better recapitulates the respiratory phenotype than that of the transgenic CF knockout mouse models widely used in CF studies to date. Additionally, the common marmoset provides a primate animal model which is evolutionarily close to humans, allowing for a transitional step between mouse models and human clinical trials. This chapter is presented in two parts: Part A details a peer reviewed published study [129] on LV transduction in the airway of normal ferrets in preparation for future CF ferret trials and Part B presents findings from a peer reviewed published study [130] demonstrating the success of LV transduction in the airways of the common marmoset.

5.2 PART A: The Ferret (*Mustela putorius furo*)

The CF mouse has provided an animal model which has been useful in establishing proof of principle and a solid foundation for gene therapy development for CF. However, the absence of CF disease pathophysiology in the tracheobronchial region and distal parts of the lung in mice has restricted the value of this animal model. In recent years animal models have been developed that more accurately reproduce the CF disease phenotype in the respiratory airways observed in humans.

Amongst the new generation of CF animal models is the CFTR knockout ferret which exhibits many characteristics homologous to the human CF disease phenotype, including pancreatic, liver, and vas deferens disease; variably-penetrant meconium ileus; defective chloride transport, submucosal gland fluid secretion, and a propensity towards lung infection in the early post natal period [131]. The similarities between CF humans and CF ferrets in their respiratory pathophysiology provides a new animal model to build upon the foundation work achieved to date in the nasal conductive airways of CF mice. At present there is no CF ferret colony in Australia or the Southern Hemisphere and prior to embarking on the lengthy process of gaining permission to import the CF ferrets and establishing a colony, a pilot study was performed to assess delivery parameters and the effectiveness of an LPC pre-treatment and HIV-1 VSV-G pseudotyped lentiviral vector gene transfer protocol in the airways of normal ferrets.

Part A of this chapter presents the results of a pilot study in which normal ferrets were pre-treatmed with LPC followed by dosing of the HIV-1 VSV-G pseudotyped lentiviral vector using the LacZ marker gene to reveal the resulting gene expression.

This study is presented as published in BMC Pulmonary Medicine:

Cmielewski, P*., Farrow, N*., et al., *Transduction of ferret airway epithelia using a pre-treatment and lentiviral gene vector.* BMC Pulm Med, 2014. **14**(1): p. 183. [129]

* Cmielewski, P. and Farrow, N. Were equal first author contributors.

Patricia Cmielewski (patricia.cmielewski@health.sa.gov.au)
Nigel Farrow (nigel.farrow@adelaide.edu.au)
Martin Donnelley (martin.donnelley@adelaide.edu.au)
Chantelle McIntyre (chantelle.mcintyre@adelaide.edu.au)
Jahan Penny-Dimri (jahan.penny-dimri@student.adelaide.edu.au)
Tim Kuchel (tim.kuchel@sahmri.com)
David Parsons (david.parsons@health.sa.gov.au)

Statement of Authorship

Title of Paper	Transduction of ferret airway epithelia using a pre-treatment and lentiviral gene vector.
Publication Status	⊙ Published, ○ Accepted for Publication, ○ Submitted for Publication, ○ Publication style
Publication Details	Cmielewski, P., Farrow, N., Donnelley, M., McIntyre, C., Peny-Dimri, J., Kuchel, T., Parsons, D., Transduction of ferret airway epithelia using a pre-treatment and lentiviral gene vector. BMC Pulm Med, 2014. 14(1): p. 183. * Cmielewski, P. and Farrow, N. Were equal principal authors.

Author Contributions

By signing the Statement of Authorship, each author certifies that their stated contribution to the publication is accurate and that permission is granted for the publication to be included in the candidate's thesis.

Name of Principal Author (Candidate)	Nigel Farrow		
Contribution to the Paper	Performed animal experiments Performed molecular and histological analysis Interpreted data Wrote the initial manuscript, helped evaluate and edit manuscript		
Signature		Date	27/1/15

Name of Co-Author	equal principal author Patricia Cmielewski		
Contribution to the Paper	Designed study Performed animal experiments Helped evaluate and edit manuscript		
Signature		Date	27/1/15

Name of Co-Author	Martin Donnelley		
Contribution to the Paper	Designed study Helped evaluate and edit manuscript		
Signature		Date	27/1/15

Name of Co-Author	Chantelle McIntyre		
Contribution to the Paper	Performed molecular and histological analysis		
Signature		Date	27/1/15

Statement of Authorship

Title of Paper	Transduction of ferret airway epithelia using a pre-treatment and lentiviral gene vector.
Publication Status	⊙ Published, ○ Accepted for Publication, ○ Submitted for Publication, ○ Publication style
Publication Details	Cmielewski, P., Farrow, N., Donnelley, M., McIntyre, C., Peny-Dimri, J., Kuchel, T., Parsons, D., Transduction of ferret airway epithelia using a pre-treatment and lentiviral gene vector. BMC Pulm Med, 2014. 14(1): p. 183. * Cmielewski, P. and Farrow, N. Were equal principal authors.

Author Contributions

By signing the Statement of Authorship, each author certifies that their stated contribution to the publication is accurate and that permission is granted for the publication to be included in the candidate's thesis.

Name of Principal Author (Candidate)	
Contribution to the Paper	
Signature		Date	

Name of Co-Author	Jahan Peny-Dimri
Contribution to the Paper	Performed initial experiment planning including setup of animal procurement.
Signature		Date	27/1/15

Name of Co-Author	Tim Kuchel
Contribution to the Paper	TK provided ferret-specific veterinary advice and support.
Signature		Date	27/1/15

Name of Co-Author	David Parsons
Contribution to the Paper	Designed the study Helped evaluate and edit manuscript
Signature		Date	27/1/15

Transduction of ferret airway epithelia using a pre-treatment and lentiviral gene vector

Patricia Cmielewski[1,2,*,†]
Email: patricia.cmielewski@health.sa.gov.au

Nigel Farrow[1,2,3,†]
Email: nigel.farrow@adelaide.edu.au

Martin Donnelley[1,2,3]
Email: martin.donnelley@adelaide.edu.au

Chantelle McIntyre[1,3]
Email: chantelle.mcintyre@adelaide.edu.au

Jahan Penny-Dimri[3]
Email: jahan.penny-dimri@student.adelaide.edu.au

Tim Kuchel[4]
Email: tim.kuchel@sahmri.com

David Parsons[1,2,3]
Email: david.parsons@health.sa.gov.au

[1] Respiratory and Sleep Medicine, Women's and Children's Hospital, 72 King William Road, North Adelaide, SA 5006, Australia

[2] Centre for Stem Cell Research, University of Adelaide, Adelaide, SA 5001, Australia

[3] School of Paediatrics and Reproductive Health, University of Adelaide, Adelaide, SA 5001, Australia

[4] South Australian Health and Medical Research Institute, Gilles Plains, SA 5086, Australia

[*] Corresponding author.

[†] Equal contributors.

5.3 **Abstract**

5.3.1 Background

The safety and efficiency of gene therapies for CF need to be assessed in pre-clinical models. Using the normal ferret, this study sought to determine whether ferret airway epithelia could be transduced with a lysophosphatidylcholine (LPC) pre-treatment followed by a VSV-G pseudotyped HIV-1 based lentiviral (LV) vector, in preparation for future studies in CF ferrets.

5.3.2 Methods

Six normal ferrets (7 -8 weeks old) were treated with a 150 μL LPC pre-treatment, followed one hour later by a 500 μL LV vector dose containing the LacZ transgene. LacZ gene expression in the conducting airways and lung was assessed by X-gal staining after 7 days. The presence of transduction in the lung, as well as off-target transduction in the liver, spleen and gonads, were assessed by qPCR. The levels of LV vector p24 protein bio-distribution in blood sera were assessed by ELISA at 0, 1, 3, 5 and 7 days.

5.3.3 Results

The dosing protocol was well tolerated. LacZ gene expression was observed *en face* in the trachea of all animals. Histology showed that ciliated and airway stem cells were transduced in the trachea, with rare LacZ transduced single cells noted in lung. p24 levels was not detectable in the sera of 5 of the 6 animals. The LacZ gene was not detected in the lung tissue and no off-target transduction was detected by qPCR.

5.3.4 Conclusions

This study shows that ferret airway epithelia are transducible using our unique two-step pre-treatment and LV vector dosing protocol. We have identified a number of unusual anatomical factors that are likely to influence the level of transduction that can be achieved in ferret airways. The ability to transduce ferret airway epithelium is a promising step towards therapeutic LV-CFTR testing in a CF ferret model.

5.3.5 Keywords

Ferret, Lung, Lentivirus, Cystic fibrosis, Gene therapy

5.4 Background

Cystic Fibrosis (CF) is an autosomal recessive disorder caused by a mutational error in the Cystic Fibrosis Transmembrane Conductance Regulator (CFTR) gene and its associated protein [132]. The CFTR channel is used in multiple body systems that utilise epithelial ion gradients, including but not limited to the pancreas, sweat glands, gastrointestinal tract and most crucially the lungs [132]. The resultant dehydration of the airway surface, loss of cilia movement, and accumulation of highly viscous mucous obstructs the airways and hinders clearance, thereby promoting bacterial infection [133]. CF airway disease currently limits the life expectancy of a CF patient to a predicted median survival estimate of approximately 37 years [134]. Therefore, the successful treatment of CF airway disease, especially from the earliest stages of life, is imperative in improving short term and long term survival of those afflicted with CF.

Gene therapy for a loss-of-function disease like CF involves delivering the appropriate corrective DNA into the cells of an organism to produce adequate functional protein to ameliorate the symptoms of that disease. Lentiviral gene vectors have a number of potential benefits, including the ability to transduce both

dividing and non-dividing cells, be pseudotyped with an envelope glycoprotein to allow for broad tissue tropism [135] and have the ability to carry large genes such as CFTR [136].

Amongst the new generation of CF animal models, the CFTR knockout ferret exhibits many characteristics homologous to human CF, including disease of the pancreas, liver, vas deferens; and variably-penetrant meconium ileus . The similarities between CF humans and CF ferrets in their respiratory pathophysiology include defective chloride transport, submucosal gland fluid secretion, and a propensity towards lung infection in the early post natal period [131].

The aim of this study was to expand work done in the mouse, sheep and marmoset [99, 130, 137] and test the ability of our two-step LPC pre-treatment and lentiviral vector delivery system to transduce airway cells of the adolescent normal ferret. The rationale for this work was to prepare for the use of CF ferrets, by establishing dosing, technical, and analytical procedures to be applicable for future use in these expensive and husbandry-intensive disease-specific CF animals.

5.5 Methods

This study was approved by the Animal Ethics committees of the Women's and Children's Health Network, South Australia; SA Pathology, South Australia; and the University of Adelaide, South Australia. Six 7-8 week old adolescent ferrets *Mustela spp* (2 male and 4 female, weight 335 to 460 g) were sourced from a commercial ferret supplier. Experiments and subsequent monitoring were performed under specialist veterinarian supervision at the Gilles Plains South Australian Medical Research Facility.

5.5.1 Gene vector

The nuclear-localised LacZ (LacZnlsco) VSV-G pseudotyped HIV-1 based LV vector was produced by transient transfection of 293T cells using a five plasmid system according to previously published protocols [99, 138]. The ratio of plasmids used for all virus preparation (per 245 mm square plate) was 170 µg of the transgene 1SDmMPSV LacZnlsco, 3.16 µg of pcDNA3 Tat, 3.16 µg of pHCMVRev, 1 µg pHCMVgagpol, 7.9 µg pHCMV-G.

For purification approximately 1 L of vector supernatant was collected, and passed through a 0.45 µm filter (Whatman Polydisc AS, GE Healthcare, PA, USA) and then two MustangQ Acrodiscs (Pall Corporation, NY, USA) connected in series, at a flow rate of 10 ml/min. After loading, the Acrodiscs were immediately flushed with 30 ml of PBS. The viral particles were then eluted with 4 ml of 1.5 M NaCl into a sterile tube containing an equal volume of 2% (v/v) mouse serum in H_2O. The virus was concentrated by ultracentrifugation at 20,000 rpm (53,750 x g) for 90 minutes at 4°C and then resuspended in 6×100 µl aliquots of 0.9% (w/v) NaCl /0.1% (w/v) mouse serum albumin and stored at -80 °C. A second batch was made in the same manner and added to the first without thawing.

Virus titre was $4.7×10^8$ TU/ml as assayed by qPCR [97]. The LV vector volume (500 µl) was established based on body weight linear scale-up from vector deliveries in mice [137] and comparable dosage protocols in other animal models, including marmoset and sheep[130, 137].

5.5.2 *In vitro* assessment of vector delivery methods

Pre-treatment and vector were delivered using an ~15 cm PE delivery cannula (Sterihealth, VIC, Australia) attached to a syringe, to reach the distal portion of the very long ferret trachea (~9 cm with 60-70 cartilage rings [139]). To minimise delivery losses using the long cannula we tested several vector delivery methods in cell culture. Vector delivery was tested in a 10:1 scale system on CHO cells: (a) as a bolus delivered using a standard 200 μl lab pipette (control); (b) using the cannula and syringe setup; (c) via the cannula setup with a 20 μl air chaser [140]; (d) via the cannula with a 20 μl primer of 0.3% Bovine Serum Albumin (BSA, Sigma Aldrich, Cat # A7906), a known LV vector stabiliser. Note that only the 50 μl LV vector was delivered to the cells, leaving the 20 μl BSA in the syringe.

CHO cells were seeded at 0.5×10^6 cells/ml in 12 well plates and incubated at 37°C, 5% CO_2 for 3 hours in F12 Hams Media (SAFC Biosciences (USA) Cat # 51655) / 10% (v/v) Fetal Calf Serum (FCS, JRH Biosciences (USA) Cat # 12103)/ 2 mM glutamine (SAFC Biosciences (USA) Cat # 59202C) and 1:1000 penicillin / streptomycin (pen-strep, Sigma Aldrich (USA) Cat # P4458). Media was aspirated, replaced with F12/10% FCS/glutamine/pen-strep supplemented with 4 μg/ml polybrene and 2 μg/ml gentamycin and cells were transduced with the LV-LacZ vector diluted 1:200. A 50 μl aliquot of the LV vector was added to wells in triplicate, using the four groups described above. Plates were incubated at 37°C and media was changed at 24 hours and replaced with F12 / 10% FCS / glutamine for a further 48 hours. Media was aspirated and cells were rinsed with PBS and fixed with 0.1% glutaraldehyde in PBS for 15 minutes on a rocking platform at room temperature. Cells were washed 3 times in 1 mM $MgCl_2$ / PBS for 10 minutes each

and were incubated overnight with 1:40 dilution of Pre-Xgal (35 mM $K_3Fe(CN)_6$, 35 mM $K_4Fe(CN)_6$ 1 M $MgCl_2$: Xgal (40 mg/ml in dimethylformamamide)) solution at 37°C. The Xgal solution was aspirated, rinsed with PBS twice, and cells were stored in 80% glycerol. LacZ gene expression was quantified as the number of blue stained cells averaged from 3 fields of 3.83 cm^2/well using light microscopy.

5.5.3 Ferret *in vivo* pre-treatment and LV dosing

Anaesthesia was induced in each of the ferrets with a s.c. injection of medetomidine (Domitor, 0.15 mg/kg, Orion Corporation, Finland) and ketamine (12 mg/kg, Parnell Laboratories, Australia). Animals were intubated with an endotracheal tube (14 Ga. BD Insyte i.v. cannula, extended to 15 cm in length with polyethylene tubing) placed so that the tip was midway between the epiglottis and the carina. All dosing events were performed with the ferret held in a prone position, with the head raised at a 20 degree angle. The pre-treatment was a 150 μl of LPC (0.1% in PBS, Sigma Aldrich L4129). The concentration was derived from studies in mouse models [98, 137] and the volume was scaled up in the same manner as for the gene vector. The airway pre-treatment was administered through the PE cannula placed to project ~2 mm past the end of the endotracheal tube proximal to the carina, via a single bolus delivery over 10 seconds. Anaesthesia was maintained with a second s.c. injection of medetomidine (0.07 mg/kg) and ketamine (6 mg/kg) 30 minutes after pre-treatment. Lentiviral dosing was performed 1 hour after pre-treatment. Ferrets were kept intubated and maintained in a supine position for the hour after pre-treatment. A single priming dose of 200 μl BSA was drawn into the cannula, followed by the 500 μl LV-LacZ (200 μl diluted with 300 μl PBS) vector to be delivered. The 500 μl gene vector dose was administered through a cannula inserted through the

endotracheal tube using a single 500 µl bolus delivery over 15 seconds. Animals were kept anaesthetised and prone for a further 20 minutes following dosing. Anaesthetic was reversed using an s.c. injection of atipamezole (Antisedan, 1.5 mg/kg, Orion Corporation, Finland). Vital signs were monitored during pre-treatment and dosing as well as in the post-operative period.

5.5.4 Monitoring and tissue harvesting

Body weight and general behaviour were monitored daily, and blood samples were taken at baseline, 1, 3, 5 and 7 days after LV dosing. Samples were centrifuged at 13,000 rpm, with sera stored at -80°C. Animals were humanely killed one week after dosing by i.p. nembutal overdose (Lethabarb, >100mg/kg). The right-most rostral lobe of the lungs was ligated and the remainder of the lungs was inflation-fixed *in situ* for 15 minutes in 2% paraformaldehyde / 0.5% glutaraldehyde (PFA / Glut) in PBS at 4 °C and a pressure of 30 cmH$_2$O. The right-most rostral lobe of the lung was snap-frozen (dry ice), along with samples of liver, spleen and gonads.

5.5.5 LacZ gene expression: histology

The inflation fixed lung was then excised and submerged in fresh chilled PFA/Glut overnight, and were processed for LacZ expression by X-gal staining [137]. The extent of LacZ gene expression throughout the airways of the lung was assessed *prima facie* though examination of gross transversely-sectioned portions of trachea and lung. Portions that had indications of blue LacZ cell staining were prepared for routine histological sectioning and stained with a light eosin counterstain using standard methods.

5.5.6 LV vector presence: p24 ELISA analysis of sera

Blood sera was analysed using an HIV-1 p24 ELISA kit (Perkin Elmer Life Sciences USA) performed as per manufacturer instructions.

5.5.7 LacZ gene presence: qPCR

Tissue samples were processed to extract DNA via the Wizard SV Genomic DNA Purification System (Promega, USA, Cat. # A2361) as per manufacturer instructions. Qualitative PCR (CFX Connect Real-Time PCR, Bio-Rad) was used to identify the presence of integrated NLS-LacZ gene, compared to the ferret GAPDH housekeeping gene [141]. PCR was performed in 8 well strips and specific amplification was detected using a TaqMan probe master mix according to the manufacturer's standard protocol. All samples were performed in triplicate including a non-template control under the following cycles: 50°C for 2 min, 95°C for 10 min, 40 cycles of 95°C for 15 sec and 60°C for 1 min. Cycle thresholds (C_t) for the LacZ gene were normalised with respect to the housekeeping gene (ΔC_t) and copy numbers per cell of the gene were determined from ΔCt [8]. The following primers were used: NLS-LacZ forward GCC ACT TCT TGA TGG ACC ACT T, NLS-LacZ reverse CCG CCA CCG ACA TCA TCT, NLS-LacZ probe FAM-CAC GCG GGC GTA CAT-NFQ, GAPDH forward CAT CCG GTG TAC CTT TCC TT, GAPDH reverse CCA GGA AGA CAG GGA GAG TG, and GAPDH probe GCA CTG CTG CCA TGC (GeneWorks, Australia).

5.5.8 Statistical analysis

Results are represented as a mean and standard error of the mean. Statistical analyses were performed using GraphPad Prism 6. Statistical significance was set at $p = 0.05$.

Multiple treatment groups were analyzed by one way analysis of variance (ANOVA) with Dunnett's multiple comparisons.

5.6 Results

5.6.1 *In vitro* assessment of vector delivery methods

Figure 1 shows that direct bolus delivery through the 15 cm cannula produced significant loss of vector titre compared to a bolus control (p <0.01, ANOVA). Furthermore, using an air chaser to maximise volume delivery also resulted in a significantly reduced titre. However, using a liquid BSA primer was not significantly different to the bolus delivery, so this method was used for all subsequent animal studies.
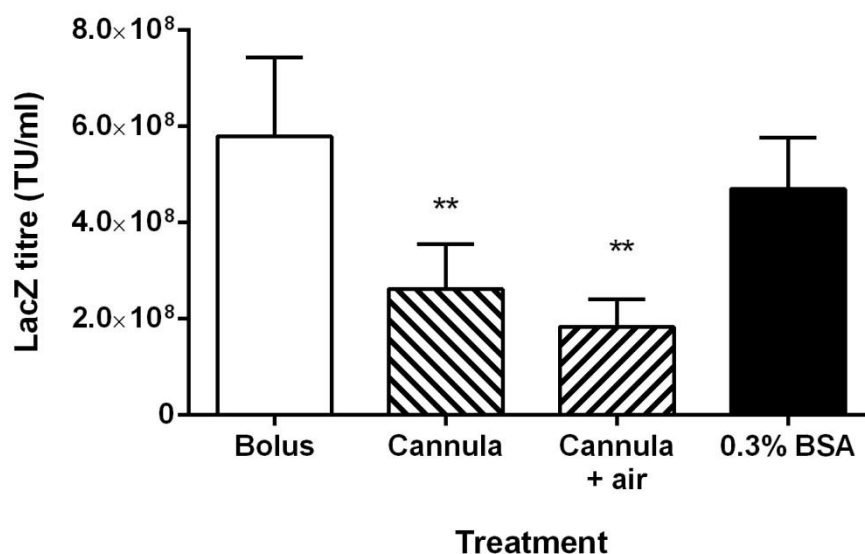
Figure 5-1: *In vitro* assessment of vector delivery methods.

In vitro testing showed significant reductions in titre when the vector was delivered via the 15 cm PE cannula, with or without an air chaser (**p <0.01, ANOVA compared to bolus, mean ± SE, n = 3). The addition of a BSA primer maintained a titre that was not significantly different to the bolus delivery, so this delivery method was chosen for all *in vivo* experiments.

5.6.2 Animal health

Based on vital signs monitoring and behavioural observations throughout the study the airway gene delivery procedure was well tolerated in all animals.

5.6.3 LacZ gene expression: Histology

The level of LacZ gene transfer was assessed *en face* and in cross-sections of ferret trachea and lung. All six ferrets showed small amounts of LacZ gene expression in the trachea, evident as blue-stained cells, with some stained cells present in the lobular regions of some animals. Figures 2, 3, 4 show typical examples of the patterns and extent of gene expression in the trachea, including both ciliated cells and stem cells. Areas of irregular lines or intense patches of blue-stained cell clusters were apparent. The majority of the LacZ expression was found in the trachea with very little extending into the lower lung airways and alveolar regions. Rare scattered LacZ transduced cells were observed in the lung (see Figure 5), but these were localised within the upper lobes rather than spread evenly across all lobes.
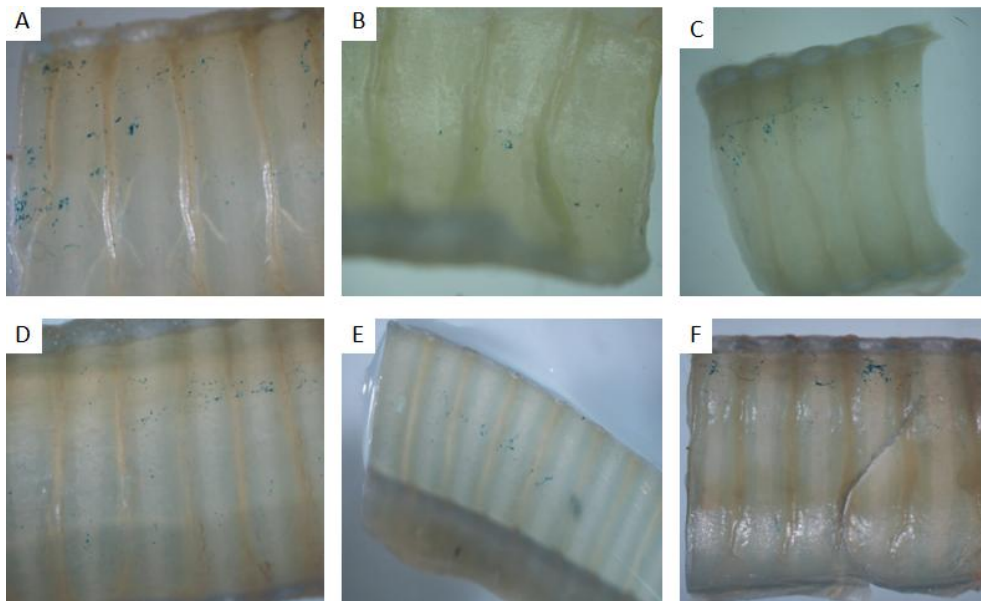
Figure 5-2: *En face* tracheal sections.

X-Gal stained *en face* sections of trachea (distal to the cannula tip) from all six ferrets (A-F), following intra-tracheal delivery of 150 μl of 0.1% LPC followed one hour later by 500 μl LV-LacZ, demonstrate low levels of

patchy LacZ gene transduction at 1 week (20× magnification).
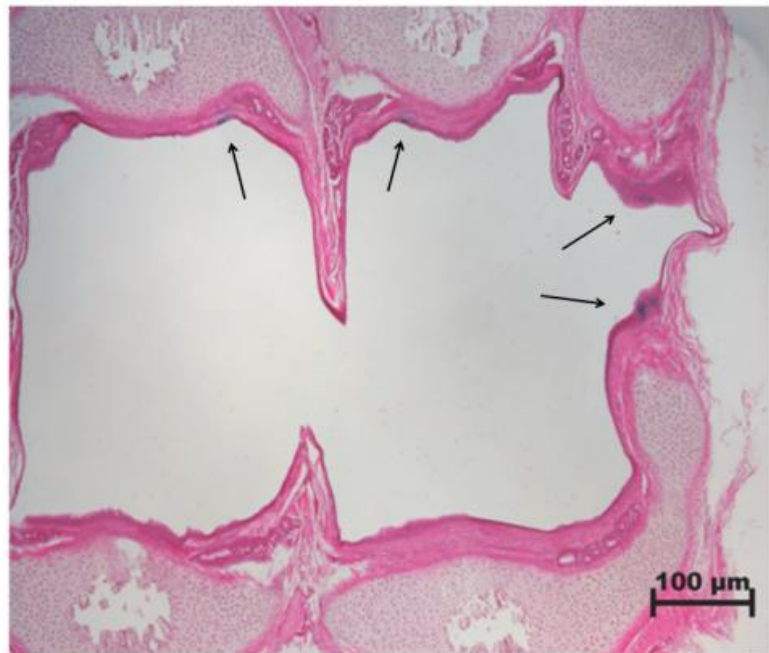
Figure 5-3: Tracheal histology.

Light eosin-stained tracheal cross section of trachea shows patchy LacZ transduction. Scale bar 100 μm. Arrows mark LacZ transduced tracheal cells.
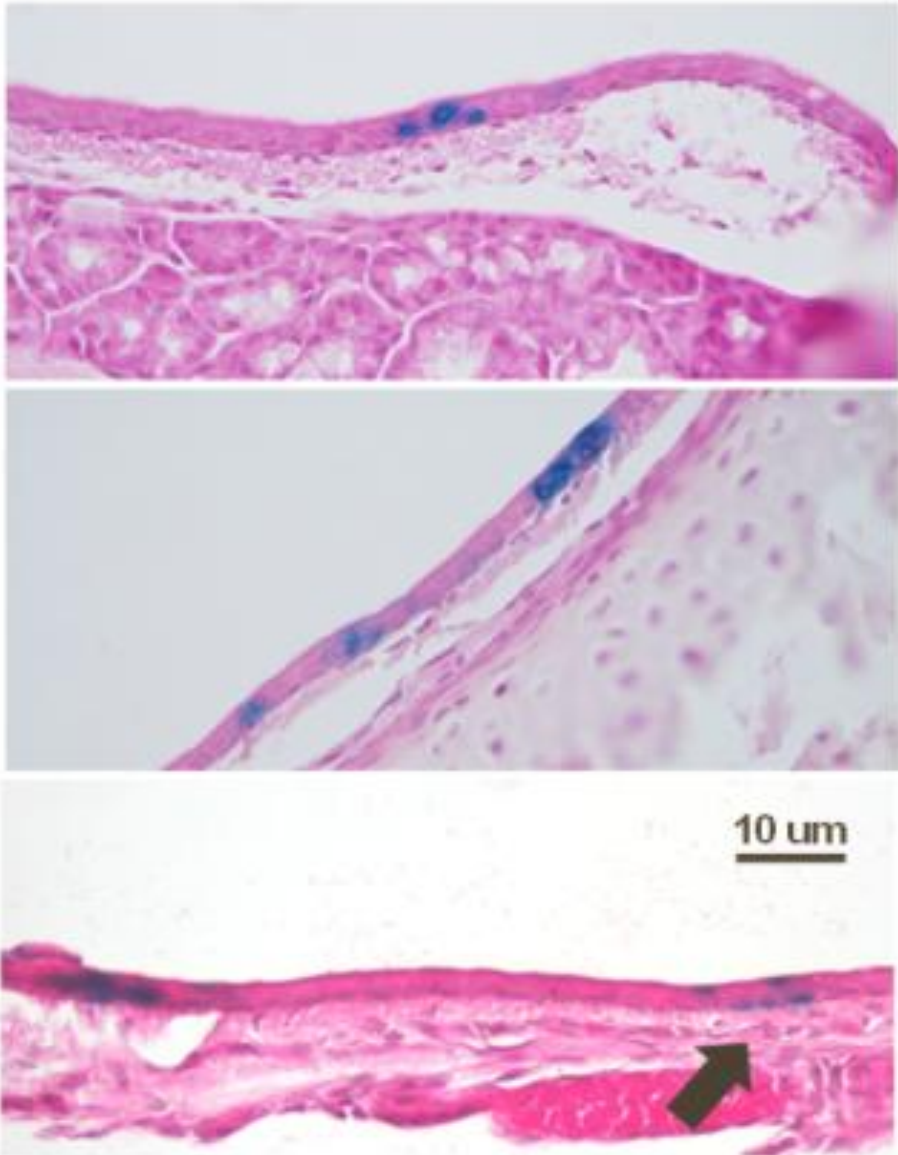
Figure 5-4: High-power tracheal histology.

Light eosin-stained high-power sections of trachea show LacZ transduction of ciliated and airway stem cells (A-C). Arrow in C points to an example of a transduced airway stem cell. Scale bar 10 μm.
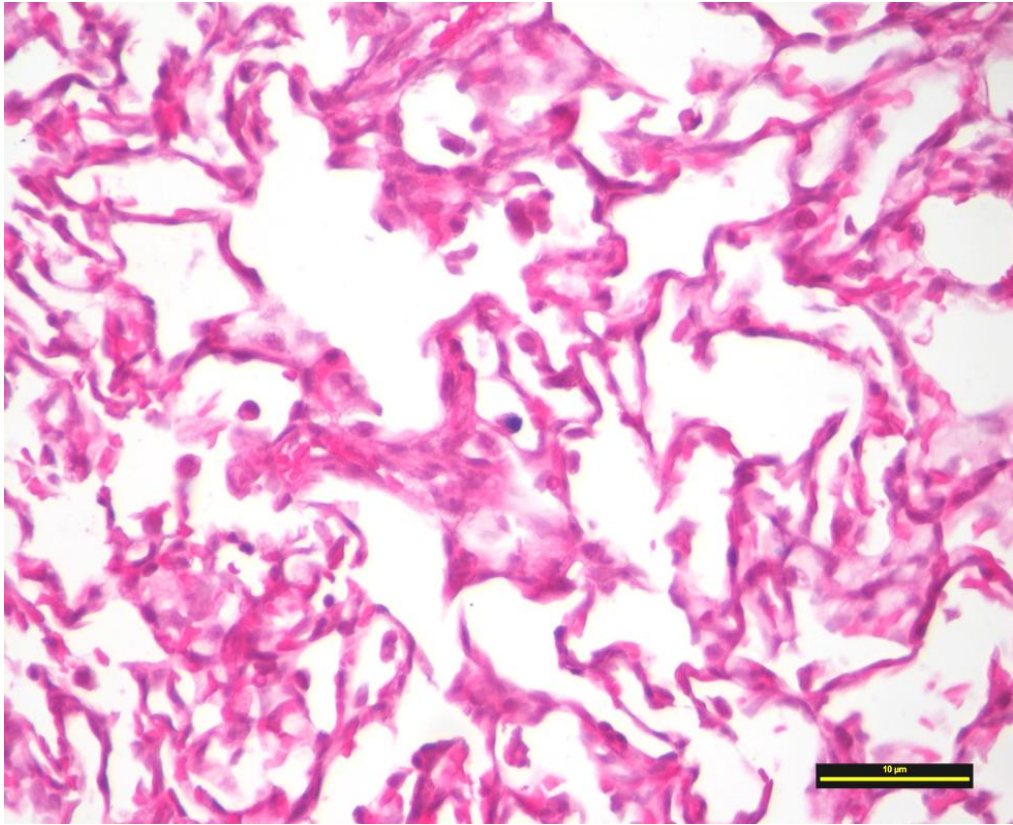
Figure 5-5: Lung histology.

In the lung only rare LacZ-stained alveolar macrophages (arrow) were detected in one or two lobes, in some animals (right). Scale bar 10 μm.

5.6.4 LV vector presence: p24 ELISA analysis of sera

The presence of the p24 protein in the blood is an indication of vector or vector constituents that have passed from the airway into the vascular space after dosing. p24 protein in serum was above the threshold of detection in one animal at day 1. This animal also had the highest level of LacZ transduction, as assessed subjectively during *en face* examination.

5.6.5 LacZ gene presence: qPCR

The presence of the LacZ gene in the lung, liver, spleen and gonads was assessed with qualitative PCR (qPCR). The LacZ gene was not detected in any of the animal tissues assayed.

5.7 Discussion

Our *in vitro* findings were surprising, firstly due to the magnitude of the losses when using the long cannula, and secondly that the losses could be prevented using a BSA primer. Use of an air chaser – as used by other lung gene vector dosing studies to ensure complete volume delivery and wide distribution [140] may not be an appropriate delivery strategy for use with LV vectors.

This study was designed to determine if the established LPC and gene vector delivery system we have developed in mice [96-98, 129, 137] and has been utilised by others in normal pigs [142] and rabbits [143] would also transduce the conducting airway tissues of the normal ferret. The results show that the tracheal airway in normal ferrets is transducible using our lentiviral gene transfer system employing an LPC pre-treatment. While total LacZ gene expression was low (but greater than that achieved in sheep [137]) the patchy pattern of LacZ marker gene expression is similar to that observed in other animal models [98, 130, 137].

Importantly, histological examination showed transduction of both ciliated cells and airway stem cells. Transduction of these cell types is important, firstly because airway ciliated cells are a primary target for a CF gene therapy, with the aim to restore the ASL depth and allow normal mucocilliary clearance to be driven by properly functioning ciliated cells. Secondly, the ability to transduce respiratory

airway stem cells enables the corrected CF gene to be passed on to all of its progeny during normal epithelial cell turnover, resulting in sustained gene expression.

There are a number of possible reasons why lower than expected levels of transgene expression were observed in this study: (1) the viral titre was a approximately 10-fold lower than previously used; (2) the lung volume of the ferret is not proportional to body size and exceeds the predicted value by 297% [144], so a linear volume scale up by weight from mouse may not be appropriate; (3) the trachea is longer than other similarly-sized animals (9 cm with 60-70 C-shaped tracheal rings [139]).

The upscaling required to produce the large vector volumes used in this study resulted in a vector titre that was 10-fold lower than previously used in mouse studies. Furthermore, the long tracheal length and the considerably larger than expected ratio between lung volume and body weight/size meant that animals did not receive sufficient gene vector. Overall, this suggests that a linear scale up by weight from previous mouse studies was insufficient. Results from the analysis of p24 presence in the blood serum also support the notion that the vector dose was insufficient.

The intubation tube was placed with the opening mid-way between the epiglottis and the carina so that the bulk of the pre-treatment and vector dose would be delivered to the distal portion of the trachea and lung. However, histological examination showed that there was LacZ expression along the length of the trachea, indicating significant retrograde transduction had occurred (as observed in mouse fluid-dosing studies [145]). Moreover, this would affect the volume reaching the distal trachea, lower conducting airways, and lung parenchyma.

Since the ferret trachea is very long (9 cm) and the lung volume is approximately three-fold larger than predicted allometrically [139, 144], it is likely that the delivered pre-treatment and vector doses were not sufficient to produce robust gene expression in the airways. The pre-treatment and vector volumes may not have acted on the same regions of airway epithelium, further reducing the effectiveness of the vector.

Although the bulk of the delivered doses may have been retained in the trachea, the level of tracheal transduction was still lower than expected. It is conceivable that the prone positioning resulted in retention of LPC within the trachea that may have subsequently reduced the viability of the LV vector. Furthermore, in this orientation vector dose could be more readily lost via fluid clearance and swallowing.

5.8 Conclusion

Despite the low levels of gene expression the outcomes confirm that the airways of the ferret can be transduced utilizing our gene delivery protocol employing LPC pre-treatment and a HIV-1 VSV-G pseudotyped lentiviral vector. Ciliated and airway stem cells types can be transduced, potentially providing a basis for both immediate and sustained transgene expression, respectively. This study has also revealed unique aspects of ferret conducting airways and alveolar space anatomy that may have affected the level of gene expression achieved. Ensuring adequate pre-treatment and vector volume, maximising the vector titre, attention to animal orientation during dosing, and determining the influence of LPC are specific factors to be addressed when embarking on future studies in normal and CF ferrets. With optimal dose volumes and vector titre for the ferret lung anatomy the levels of gene transfer are

likely to approach those in previous mouse studies and provide effective protocols for future use of lentiviral CFTR gene transfer studies in CF ferrets.

Abbreviations

CF, Cystic fibrosis; CFTR, Cystic fibrosis transmembrane conductance regulator; LPC, Lysophosphatidylcholine; LV, Lentiviral; PBS, Phosphate buffered saline

5.9 Competing interests

The authors declare they have no competing interests.

5.9.1 Authors' contributions

PC, MD and DP designed the study. PC and NF performed the animal experiments. NF and CM performed the molecular and histological analyses. TK provided ferret-specific veterinary advice and support, and JPD performed initial experiment planning including setup of animal procurement. NF, MD, PC, and DP drafted the manuscript. All authors read and approved the final manuscript.

5.9.2 Acknowledgements

5.10 PART B: The common Marmoset (*Callithrix jacchus*)

5.11 Introduction

The study outlined in this chapter was designed to test the efficacy of gene transduction and expression in the lung of a non-human primate, the marmoset (*Callithrix jacchus*).

Prior to clinical application of gene therapy for CF utilizing the HIV-1 VSV-G pseudotyped lentiviral vector the safety and efficacy of the vector must be assessed in valid and practical animal models. Non human primates (NHP) are animals which are evolutionarily far closer to humans than the inbred mouse animal models initially used for establishing proof of principle evidence for an effective gene therapy. Focusing on the aim to establish a safe and effective gene therapy preventative treatment for CF-associated lung disease, the marmoset (*Callithrix jacchus*), a small new world monkey, provides a suitable model. The marmoset shares a close homology to humans, which has already allowed it to be used in preclinical and safety toxicology studies [146]. Additionally, the marmoset has already been used for the purpose of testing a variety of gene therapy treatments and preclinical gene vector safety studies for a variety of diseases [147-149]. Furthermore, the marmoset has been used to assess gene therapy aimed at hematopoietic stem cells providing valuable insight into potential hurdles when moving from mouse models to human clinical application[150]. Importantly, Hanazono *et al* [150] reported that in initial human studies following transplantation of gene corrected stem cells there were lower levels of gene modified cells detected compared to mouse studies. This finding again confirms that findings from mouse studies are not always directly translatable to human clinical use, and that the use of a NHP can provide a substantially stronger

understanding of the efficacy and safety of a gene therapy treatment prior to human clinical trials beginning.

The use of a NHP will also potentially provide valuable safety information, regardless of the transducibility of cell types in a required anatomical region. When utilizing a lentiviral vector such as the HIV-1 VSV-G pseudotyped vector used in this study, it is important to consider the effect of the vector on the overall health of the recipient. Through the monitoring of body weight, general behaviour, post mortem organ examination and histological analysis this health effect can be assessed. Additionally, through the collection of pre and post treatment serum, samples can be used to monitor the dissemination and dynamics of the vector both intact and as non viable viral particles.

This study is presented as published in Scientific Reports:

Farrow, N., et al., *Airway gene transfer in a non-human primate: lentiviral gene expression in marmoset lungs.* Sci Rep, 2013. **3**: p. 1287. [130]

SCIENTIFIC
REP❂RTS

OPEN

Airway gene transfer in a non-human primate: Lentiviral gene expression in marmoset lungs

SUBJECT AREAS:
GENETIC VECTORS
PRE-CLINICAL STUDIES
TRANSFECTION
STEM-CELL RESEARCH

N. Farrow[1,2,3*], D. Miller[1,4*], P. Cmielewski[1,2,3], M. Donnelley[1,2,3], R. Bright[1,4] & D. W. Parsons[1,2,3,4]

Statement of Authorship

Title of Paper	Airway gene transfer in a non-human primate: Lentiviral gene expression in marmoset lungs
Publication Status	⊙ Published, ○ Accepted for Publication, ○ Submitted for Publication, ○ Publication style
Publication Details	Farrow, N., Miller, D., Cmielewski, P., Donnelley, M., Bright, R. and Parsons, D., Airway gene transfer in a non-human primate: lentiviral gene expression in marmoset lungs. Sci Rep, 2013. 3: p. 1287

Author Contributions

By signing the Statement of Authorship, each author certifies that their stated contribution to the publication is accurate and that permission is granted for the publication to be included in the candidate's thesis.

Name of Principal Author (Candidate)	Nigel Farrow		
Contribution to the Paper	Performed tissue harvesting Performed molecular and histological analysis contributed to the initial manuscript, helped evaluate and edit manuscript		
Signature		Date	27/1/15

Name of Co-Author	Darren Miller		
Contribution to the Paper	performed gene transfer protocol Performed animal experiments Conducted laboratory studies		
Signature		Date	27/1/15

Name of Co-Author	Patricia Cmielewski		
Contribution to the Paper	Conducted Laboratory studies		
Signature		Date	27/1/15

Name of Co-Author	Martin Donnelley		
Contribution to the Paper	contributed to the initial manuscript, helped evaluate and edit manuscript		
Signature		Date	27/1/15

Statement of Authorship

Title of Paper	Airway gene transfer in a non-human primate: Lentiviral gene expression in marmoset lungs
Publication Status	⦿ Published, ◯ Accepted for Publication, ◯ Submitted for Publication, ◯ Publication style
Publication Details	Farrow, N., Miller, D., Cmielewski, P., Donnelley, M., Bright, R. and Parsons, D., Airway gene transfer in a non-human primate: lentiviral gene expression in marmoset lungs. Sci Rep, 2013. 3: p. 1287

Author Contributions

By signing the Statement of Authorship, each author certifies that their stated contribution to the publication is accurate and that permission is granted for the publication to be included in the candidate's thesis.

Name of Principal Author (Candidate)	
Contribution to the Paper	
Signature		Date	

Name of Co-Author	Richard Bright
Contribution to the Paper	Performed initial gene transfer protocol Performed tissue harvesting
Signature		Date	27/1/15

Name of Co-Author	David Parsons
Contribution to the Paper	Conceived and designed the study Performed initial gene transfer protocol Conducted laboratory studies Contributed to the initial manuscript, helped evaluate and edit manuscript
Signature		Date	27/1/15

Name of Co-Author	
Contribution to the Paper	
Signature		Date	

Airway gene transfer in a non-human primate: Lentiviral gene expression in marmoset lungs

N. Farrow[1,2,3] *, D. Miller[1,4] *, P. Cmielewski[1,2,3], M. Donnelley[1,2,3], R. Bright[1,4], D.W. *Parsons[1,2,3,4]

[1]*Respiratory and Sleep Medicine, Women's and Children's Health Network, 72 King William Rd., North Adelaide, South Australia, 5006,*

[2]*Centre for Stem Cell Research, University of Adelaide, South Australia, 5000*

[3]*Department of Paediatrics and Reproductive Health, University of Adelaide, South Australia, 5000*

[4]*Women's and Children's Health Research Institute, 72 King William Rd., North Adelaide, South Australia, 5006*

* Denotes equal first author contributions

*Correspondence to: david.parsons@health.sa.gov.au

Keywords:

Lung; Airway; Gene Transfer; Cystic Fibrosis; Lentivirus; Marmoset; Non-Human Primate

5.12 **Abstract**

Genetic therapies for cystic fibrosis (CF) must be assessed for safety and efficacy, so testing in a non-human primate (NHP) model is invaluable. In this pilot study we determined if the conducting airways of marmosets (n=2) could be transduced using an airway pre-treatment followed by an intratracheal bolus dose of a VSV-G pseudotyped HIV-1 based lentiviral (LV) vector (LacZ reporter).

LacZ gene expression (X-gal) was assessed after 7 days and found primarily in conducting airway epithelia as well as in alveolar regions. The LacZ gene was not detected in liver or spleen via qPCR. Vector p24 protein bio-distribution into blood was transient. Dosing was well tolerated.

This preliminary study confirmed the transducibility of CF-relevant airway cell types. The marmoset is a promising NHP model for testing and translating genetic treatments for CF airway disease towards clinical trials.

5.13 **Introduction**

The relentless progression of cystic fibrosis (CF) airway disease remains an unresolved problem although the rate of decline has been slowed by the range of treatments now available. The majority of morbidity and mortality relates to the chronic airway infection and inflammation that commences in early infancy and leads to premature death from lung failure.

Gene-based correction of defective airway epithelial cell function, by introduction of the functional CF transmembrane conductance regulator (CFTR) gene, is a rational approach designed to produce lasting therapeutic benefit and could be the basis for a cure. Practical success would restore CFTR ion-channel function, producing a

physiologically-balanced treatment for CF airway disease. Additionally, CFTR gene transduction of airway stem / progenitor cells should produce extended correction because the daughter cells that re-populate the airway epithelium contain the corrected CFTR gene [151]. Early correction, when CF lungs are considered to be functionally unaffected, has the potential to prevent the initiation of CF lung disease [152].

In mice our single-dose lentiviral (LV) airway gene transfer technique produces immediate as well as long-term airway reporter gene transfer [96], extending up to a mouse lifetime. Use of a lysophosphatidylcholine (LPC) airway pre-treatment improves gene transfer and may enable access to airway stem/progenitor cells able to support long term gene expression [99]. Importantly, this method has already shown its utility with the therapeutic CFTR gene; we have reported more than 12 months of functional CFTR gene expression in CF mouse airways [153]. Furthermore, we have demonstrated robust reporter gene transfer in mouse lung and produced low-level proof-of-principle expression in sheep lung [137].

The aim of this pilot study was to test the potential of this method in the lungs of a non-human primate (NHP), the marmoset (*Callithrix jacchus*). The marmoset has a number of advantages as a NHP animal model for studying lung gene transfer. In particular, due to its small size, similar in body size to a very large rat, the modest LV volumes required are within the capabilities of current vector production methods

5.14 **Results**

This preliminary study was designed to establish if our LV vector delivery system could transduce NHP conducting airway tissue prior to proposing and designing

more extensive NHP gene transfer studies. For that reason in this short-term study only two animals (one male and one female) were used. No experimental controls were employed since published [96, 97, 137, 153] data and our previous studies in mice and sheep strongly indicate that none of these controls would elicit gene expression.

LPC and LV dose deliveries were uneventful. General behaviour (demeanour, feeding, and respiration) and auscultation findings were within normal limits over the post-treatment study period. In both animals the gross appearance of the lungs was unremarkable when the chest was opened. Histological examination of lung tissue by a veterinary pathologist showed no abnormalities (including cellular infiltration) of consequence.

5.14.1 LacZ gene expression: Histology

One week post-dosing LacZ gene expression was visible in excised lung tissue from both marmosets, although the female showed a higher level of transduction. Figure 5-6 shows an *en face* example of LacZ gene expression in lung tissue. LacZ gene expression was present primarily in surface and basal epithelial cells in the conducting airways. The patchy blue cell staining had a generally peribronchiolar distribution along conducting airways in several lobes (Figure 5-6). In cross-sections of the trachea (Figure 5-7) patchy transduction was observed across the full thickness of the epithelium.

In the alveolar tissue (Figure 5-8) there was substantially less cell transduction present compared to the conducting airways. The transduced cells in the distal lung airways included alveolar Type 1 and Type II cells (Figure 5-8 b-c) and inflammatory cells such as alveolar macrophages (Figure 5-8 d-e), and these were

distributed across the lobes, again in a patchy pattern. The macrophages displayed blue LacZ staining indicating that both direct transduction and phagocytic capture of transduced cells could occur.

Histological analysis of the liver and spleen samples showed no LacZ gene expression.
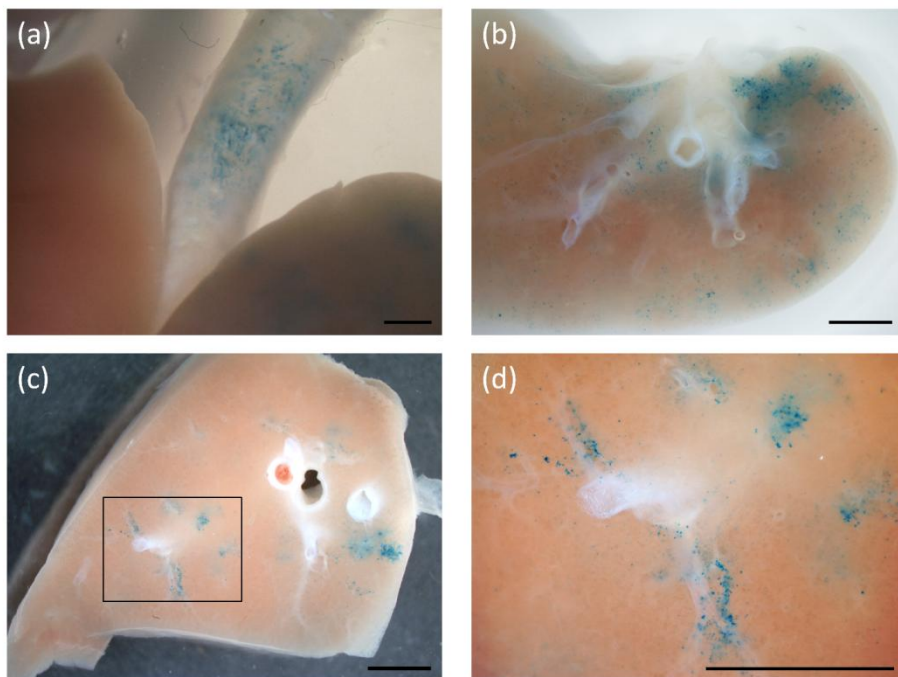
Figure 5-6: LacZ gene expression (blue stained cells) in marmoset lung one week after gene transfer.

Transduction across several lobes occurred in an airway-associated and a patchy-diffuse pattern. (a) Gene expression is apparent in the intact trachea above the carina and adjacent to the upper lobes seen here in the un-dissected lung after X-gal processing. (b) shows an *en face* gross lobe section with blue stained cell patches distributed around the lobe periphery. (c) In another thick *en face* section the patchy peri-bronchioar distribution is evident, with the boxed region enlarged for clarity in (d). Scale bars 2.5 mm.
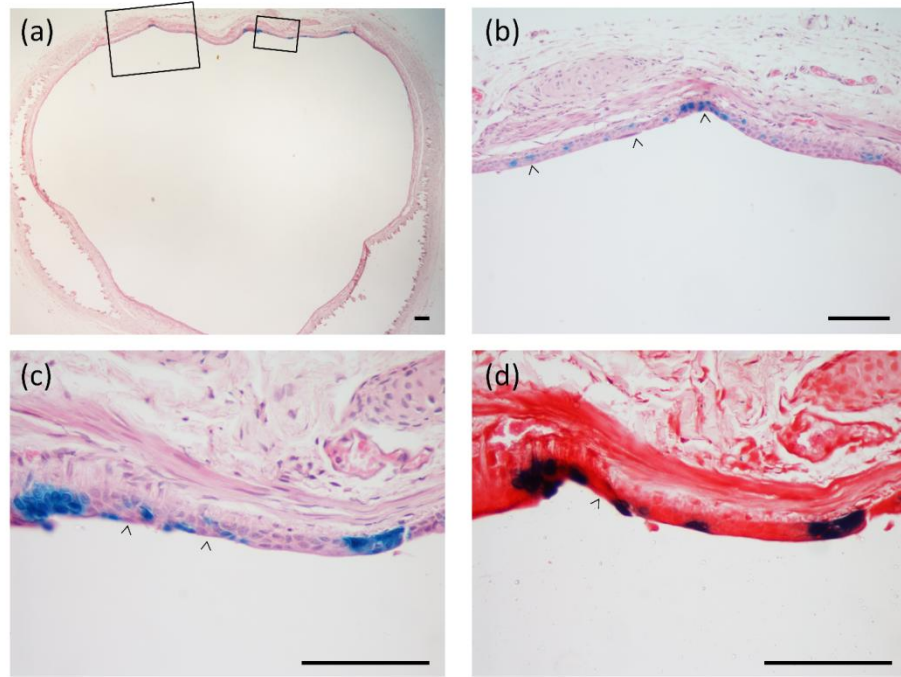
Figure 5-7: LacZ histology:

(a) Cross-sections show regions of patchy LacZ gene expression along the trachea. The boxed areas in (a) are magnified in (b) and (c) to show the nature of transduction of the conducting airway epithelium. Examples of full thickness staining that includes airway stem cells (arrow heads), surface and individual-cell gene expression are shown. In (d) the next serial section adjacent to that shown in (c) is counterstained with Safranin-O and more clearly displays the epithelial layer staining. H&E stain in (a), (b), and (c). Scale bars 100 μm.
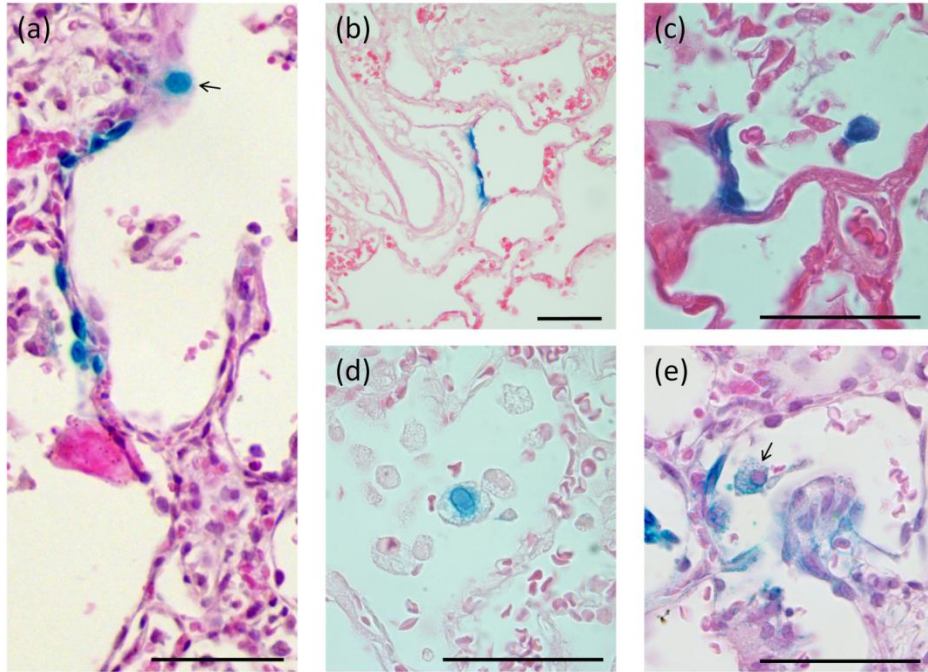
Figure 5-8: 7-day LacZ gene expression in the alveolar region.

(a) A grouping of LacZ-expressing alveolar cells are present together with an alveolar macrophage (arrow). Examples of (b) Type I pneumocyte transduction, and (c) Type II pneumocyte transduction of several adjacent cells with strong nuclear LacZ staining that has bled into the cytoplasm; (d) and (e) show examples of alveolar macrophage staining showing evidence of phagocytic LacZ staining (blue granules within the cytoplasm) and direct cellular transduction (blue nuclear staining; arrow), respectively. Scale bar 50 μm.

5.14.2 LacZ gene presence: PCR

LacZ gene presence in the lung, liver and spleen was assessed by quantitative PCR (qPCR). The LacZ gene was detected in the lung tissue from the female marmoset (the ΔC_t values for the three tissue samples, performed in triplicate, were 11.91, 6.57 and 5.89), but not in the sampled lung tissue from the male. The LacZ gene was not detected in the liver or spleen tissue from either marmoset, nor in scavenged (untreated colony cull) marmoset control tissue.

5.14.3 Vector particle dissemination

The protein p24 is a component of the HIV-based LV vector virion, and its presence in blood was used to determine the extent of non-target distribution of vector or vector constituents after vector delivery into the airway. The levels of serum p24 in both animals (Figure 5-9) show that although the protein is found in serum one day after dosing the levels declined therafter and returned to baseline by day six.
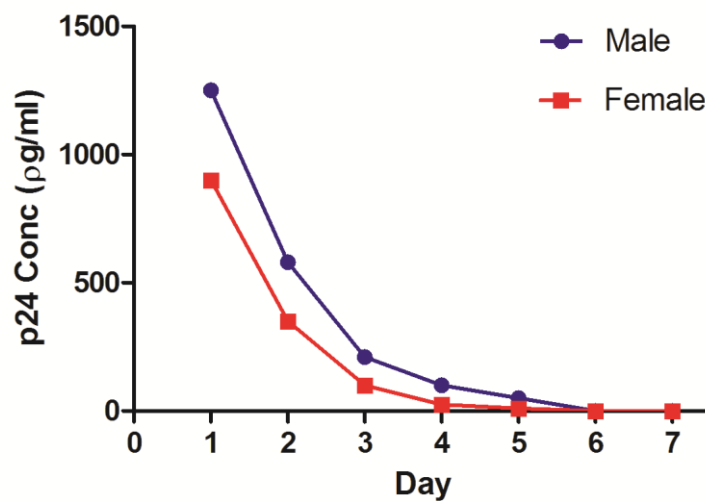
Figure 5-9: p24 assay on marmoset serum demonstrates that the vector components are present in the blood shortly after dosing, but are cleared prior to day 7.

5.15 Discussion

To our knowledge these are the first studies to test and show that airway gene transfer can be achieved *in vivo* using a VSV-G pseudotyped HIV-based LV vector in an adult NHP model. Our findings extend earlier work in human airway cell cultures and tracheal explants showing efficient transduction with an Ebola-pseudotyped HIV vector [154], and airway transduction in infant macaques after *in utero* parenchymal lung injection of a VSV-G pseudotyped HIV-based vector [155].

The primary finding was that the marmoset lung can be transduced using our LV vector delivery system. Based on our behavioural assessments, gross post mortem organ examination, and histological analysis, no adverse effects of either LPC or the LV vector were apparent. As this was a limited observational pilot-study design there were insufficient numbers of animals to provide detailed quantitative comparisons.

The patchy gene expression observed in both marmosets has also been observed in mice and sheep [137] when fluid-based gene vector dosing was used. This may be caused by multiple factors including, but not limited to, incomplete coverage of the large surface area of the lung airways by the relatively small dose volume, specificity of the vector for particular cell types, and a mismatch in the areas treated by the LPC and LV vector doses. Importantly, the patchiness that would accompany LV-CFTR vector dosed in the same way does not prevent physiologically functional CFTR gene expression occurring in our CF mouse nasal airway studies [96, 153].

Ciliated airway surface epithelial cells are a primary target of CF gene therapies, but are terminally-differentiated [156]. Gene expression will be lost when those cells undergo apoptosis as part of normal lung cell turnover processes. The lifespan of these epithelial cells in the marmoset is unknown, but transduction of stem/progenitor cells may be important for producing long-term gene expression. Studies in mice suggest that the epithelial stem/progenitor cells responsible for regular regeneration of the conducting airway epithelium reside, in part, in the epithelial basal-cell compartment [110]. The transient permeabilisation that LPC imposes on epithelial cell tight junctions [99] can provide access to those deep lying airway stem cells. Importantly, we detected LacZ gene expression in these deep

114

lying epithelial cells at 7 days, suggesting our LV vector can reach regions where some niches of adult stem/progenitor cells are expected to reside in mammalian airways [157]. Similarly, alveolar epithelial cells and macrophages [158] were also transduced, with the latter finding extending the results in rodents to a NHP model.

LacZ gene expression was not detected via X-gal staining or qPCR in any sub-epithelial tissues or in the liver or spleen. Although LacZ positive cells were visible in the lungs of both animals, the negative qPCR finding in the male may have been the result of the randomly selected tissue samples not containing any LacZ transduced cells. The finding of a transient presence of the vector protein component p24 in serum (Figure 5-9) confirms that although LV vector or vector components can reach the circulation they are rapidly removed. Although even conventional lipid-based lung gene transfer events can deliver vector DNA to non-target organs [159], further studies are required to elucidate the mechanisms and implications of any off-target organ transduction.

While the finding of gene transfer and expression in airway epithelial cells is clear, there are obvious limitations. The very small group size and absence of control animals (other than scavenged tissue for qPCR analyses) were deliberately chosen to prevent unwarranted use of additional NHPs should reporter gene transfer had not proven effective. With the success of this pilot study, future studies now warrant the use of larger group sizes including control animals. Studies should be designed to assess the longevity of gene expression, and should include a LV-only treatment group to directly determine the requirement for LPC in the production of both short and long-term lung gene expression. Additional detailed biosafety assays and physiological, behavioural, immunological and histological monitoring must also be

included.

In summary, this pilot study demonstrated the successful extension of our LV delivery technique into a NHP lung. In the translation of basic and preclinical science into useful human therapies this initial success validates the use of LV gene delivery into a NHP lung and suggests marmosets could serve as a valuable pre-clinical model for translational studies in respiratory medicine.

5.16 **Materials and Methods**

This multi-institutional study was approved by the Animal Ethics committees of the Women's and Children's Health Network, South Australia; and Monash University, Victoria. Two marmosets, one female (F: ~275 g) and one male (M: ~300 g) were sourced from the marmoset colony of the NH&MRC National Primate Colony, Monash University. Animal husbandry, experiments and subsequent monitoring were performed under specialist NHP veterinarian supervision and care provided by Monash Animal Services, Victoria, Australia.

5.16.1 Airway pre-treatment

Airway pre-treatment with LPC (Sigma Aldrich L4129, prepared w/v in PBS) was given prior to a single airway gene transfer event. The LPC concentration (0.1% w/v) was derived from mouse studies [137, 153] where effectiveness and tolerability were previously established. LPC dose volumes (F: 200 μl and M: 350 μl) were calculated by scaling-up our successful mouse lung gene transfer doses [137].

5.16.2 Gene vector

The nuclear-localised LacZ (NLS-LacZ) VSV-G pseudotyped HIV-1 based LV

vector was a 5-plasmid non-replicating SIN vector produced according to previously published methods [73, 153]. Virus titre was 1.2 x 10^9 viral genome equivalents per ml as assayed by quantitative PCR [97]. The LV vector volumes (F: 350 µl and M: 500 µl) were also estimated by scale-up from our mouse deliveries.

5.16.3 Pre-treatment and LV dosing

Anaesthetic induction was with 10mg/ml alfaxalone (Jurox Rutherford, NSW, Australia) and animals were intubated with an endotracheal tube (Sheridan Uncuffed 2.0, Hudson RCI, USA) placed with the tip midway between the epiglottis and the carina. Anaesthesia was maintained using 1.25% - 1.5% isofluorane. Dosing was performed in a Class II biosafety cabinet with animals held supine throughout. The LV vector was delivered as a single fluid bolus to the trachea via the endotracheal tube over ten seconds, one hour after the LPC pre-treatment. Animals were held anaesthetised and supine in the cabinet for an additional hour after LV dosing before being extubated and placed in PC-2 caging facilities.

5.16.4 Monitoring

Vital signs were monitored throughout dosing and in the post-operative period. Body weight and general behaviour were monitored daily along with blood sampling (centrifuged at 13,000 rpm, with sera stored at -80°C until required).

5.16.5 Tissue harvesting

Animals were humanely killed at 7 days using an Alfaxalone induction followed by pentobarbital overdose. The lungs were inflation-fixed *in situ* in 2% paraformaldehyde / 0.5% glutaraldehyde (PFA/Glut) in PBS at 4°C and a pressure of 30 cmH$_2$O for 15 mins. Samples of liver and spleen were also harvested and fixed in

PFA/Glut at 4°C.

5.16.6 LacZ gene expression: Histology

The lungs were then excised and submerged in fresh chilled PFA/Glut overnight, and were subsequently processed for LacZ expression by our standard X-gal staining method [137]. The extent of LacZ gene expression in airway cells was first assessed *en face* in gross transversely-sectioned portions of lung. Blocks that showed blue LacZ staining were then prepared for routine histological sectioning with haematoxylin/eosin (H&E) or a Safranin-O counterstain.

5.16.7 LacZ gene presence: qPCR

Triplicate tissue samples (20 mg) were selected from random locations in the lungs, liver and spleen. Scavenged tissue from untreated animals was used as a negative control. All lung samples were then incubated at 55°C overnight in tail lysis buffer (Viagen Biotech, USA, Cat. # AB102-T) and 20 mg/ml Proteinase K (Promega, USA, Cat. # V3021) at a 1:50 ratio then heated to 80°C for one hour and crude lysates were stored at -20°C until analysis. All other samples were processed via the Wizard SV Genomic DNA Purification System (Promega, USA, Cat. # A2361) according to manufacturers specifications.

qPCR for the NLS-LacZ gene and marmoset GAPDH housekeeping gene [160] was performed in a 96 well plate format (CFX Connect Real-Time PCR, Bio-Rad) according to the manufacturers standard protocol. Specific amplification was detected using SYBR Green (Fast SYBR Green Master Mix, Applied Biosystems USA, Cat. # 4381562). Cycle thresholds (C_t) for the LacZ gene were normalised with respect to the housekeeping gene and presented as ΔC_t. The following primers

were used: NLS-LacZ forward GCC ACT TCT TGA TGG ACC ACT T, NLS-LacZ reverse CCG CCA CCG ACA TCA TCT, GAPDH forward AAA GTG GAT GTC GTC GCC ATC AAT GAT and GAPDH reverse CTG GAA GAT GGT GAT GGG ATT TCC ATT (GeneWorks, Australia).

5.16.8 Vector particle dissemination

Sera were analysed using a HIV-1 p24 ELISA Kit (Perkin Elmer Life Sciences USA Ca# NEK050) performed as per manufacturer instructions.

5.17 Acknowledgements

5.18 Author Contribution Statement

DWP conceived and designed the study. DWP, DM and RB performed the gene transfer protocols; NF, DM, RB and DWP completed tissue harvesting; NF, DM, PC, RB, and DWP conducted laboratory studies and data analyses; DWP, NF and MD wrote the manuscript.

All authors reviewed the manuscript.

5.19 **Conflict of Interest**

All authors declare there are no competing financial interests in relation to the work described.

5.20 **Additional discussion**

This additional discussion has been included to consider information from literature published after the publication of the paper presented in this section of the Chapter.

The distribution of ciliated cells in the conductive airways of the marmoset has now been shown to be restricted to portions around the circumference of the tracheal airway. In a study published after the study presented here was published, an important finding which has an impact on the observations of this study was reported. Hoffmann *et al* [161] used light and scanning electron microscopy to evaluate the morphology of the tracheal epithelium of the common marmoset, after an inhomogeneous distribution of ciliated cells in the marmoset trachea was observed in a previous ultrastructural investigation [161, 162]. Hoffmann's findings showed that in the marmoset trachea; ciliated cells were virtually absent in the epithelium over cartilage rings, and that these cells decreased in number in the short transitional zone; and were concentrated in cartilage-free areas of the respiratory airway [161] (Figure 5-10). In light of this recent finding the patchy distribution of LacZ positive cells in the trachea (Figure 5-6 a) and (Figure 5-7 a & b) coincide with the diminished number and location of ciliated cells in the marmoset trachea. At present it is unknown if the distribution pattern of cilia in the marmoset trachea, which is uncommon to other mammals [161] is recapitulated in the more distal parts of the marmoset conductive airways.
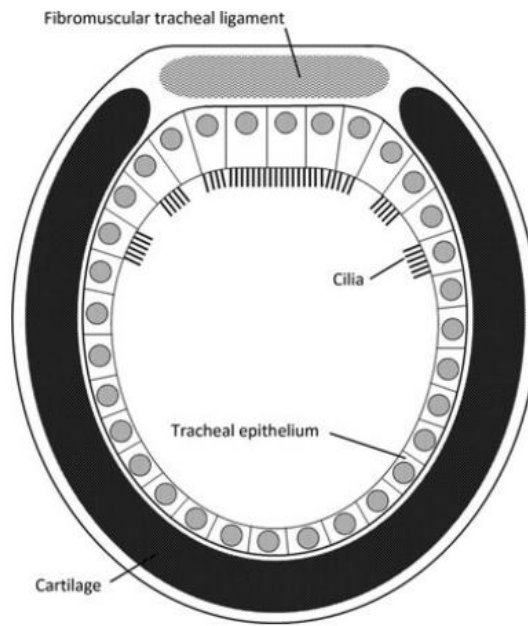
Figure 5-10: Schematic drawing of a tracheal ring cross section showing the pattern and distribution of ciliated cells in the common marmoset. Adapted from Hoffman *et al* 2014 [161].

6 Discussion

Gene therapy aimed at correcting the underlying cause of CF associated lung disease is no longer in its infancy. Since the isolation and discovery of the CFTR gene in 1989 there have been numerous attempts to use the gene therapy approach utilizing both non viral and viral vectors. To date, non viral vectors have proven to be unsatisfactory in providing an efficient method of gene delivery to the airways. While the progress of AdV and AAV vectors have been limited by problems encountered during clinical trials, LV vectors have shown the potential to provide successful transgene delivery and sustained transgene expression. Recently, LV vectors have successfully been used to treat inherited genetic disorders such as chronic granulomatous disease and ADA-SCID providing a proof of principle for this vector class and for its potential use as a gene therapy vector for other monogenetic diseases such as CF.

An effective gene therapy for CF airway disease requires that lifelong correction is achieved. LV vectors have shown potential at being less immunogenic [95] than previous vectors also raising the possibility that repeat administration could be possible, something that cannot be achieved with other viral vectors.

Despite the possibility that repeated dosing may achieve lifelong correction, a single effective treatment that achieves stable lifelong correction may be more beneficial for a number of reasons. Firstly, it would remove the need for a patient to be continually treated at intervals for the remainder of their life. Secondly, it would be more feasible economically to administer a single treatment than to burden the health system with a treatment that needs to be repeatedly readministered over the lifetime of the patient. Thirdly, as a personal belief I feel medicine is morally and ethically

obliged to explore potential treatments that provide maximum health benefits to the patient with minimal disruption to their day to day lives. In short, a single gene therapy treatment providing lifelong correction to the airways of CF patients is practically, economically and morally a therapeutic paradigm that requires further consideration.

The aims of the studies presented in this thesis were: (1) Establish if long term transgene expression following treatment with the HIV-1 viral vector and LPC pre treatment is a consequence of transducing airway stem cells. (2) Isolation and quantification of stem cells and mucin secretory cells in the airways of CF mice to assess if remodeling of the CF epithelium in terms of cell hyperplasia is present. (3) Determine if the HIV-1 vector can transduce the relevant cells types including stem cells in the airways of the normal ferret. (4) Determine if the HIV-1 vector can transduce the relevant cell types including stem cells in the airways of a non human primate.

In the first section of this thesis, Aim 1 investigated whether the transduction of airway stem cells with a HIV-1 VSV-G LV vector following pre-treatment with LPC would explain the basis behind long term transgene expression. The premise of the study was that by transducing the airway stem cells the transgene would be passed on to their progeny during mitosis following the natural turnover process of terminally differentiated cells of the airway epithelium. To evaluate the premise, the conductive airways of mice were pre-treated with LPC then followed by delivery of the LV vector. A forced injury model was subsequently employed to transiently ablate the airway epithelium to force epithelial regeneration and determine if the transgene was passed from transduced airway stem cells to the differentiated cells of

the new epithelium. At the conclusion of this study, the airway epithelium contained clusters of LacZ positive cells only in the forced injury model groups.

The presence of LacZ positive cells following ablation and regeneration suggest that the transgene had been passed on to the progeny of transduced airway stem cells during the repair process. Furthermore, the clustered patterns of LacZ positive cells observed in the forced injury model groups upon epithelial regeneration compared to the speckled pattern in the terminally differentiated cells of the short term controls is supportive of transduced airway stem cells.

The clusters of LacZ positive cells present following regeneration occurred in two distinct patterns: a rounded symmetrical shape and a linear shape (Figure 3-7). The first pattern of a rounded symmetrical shape was as predicted [95], as the progeny grow out uniformly from a central transduced airway stem cell. The linear pattern however, is suggestive of a subset of transduced airway stem cells that have renewed and /or differentiated spreading along an axis to cover the wide area that the injury model has ablated. However, the two different patterns of clonal regrowth may be a consequence of the experimental design, i.e. specifically a result of the forced injury method, and may not reflect the usual nature of clonal expansion patterns during the normal cellular turnover process. It is also possible the forced injury model has changed the natural expression of cytokines and/or other cellular factors influencing the expansion of clonal colonies in the manner observed. Further work is required to properly understand these factors.

The evidence of airway stem cell transduction and subsequent dissemination of the transgene to its differentiated progeny in both nasal and tracheal airways provides proof of principle to the proposition of transducing airway stem cells to obtain

sustained transgene expression. With this foundation future studies can be proposed to help explore methods to enhance the targeting of airway stem cells and subsequently improve overall differentiated cell transgene expression to the therapeutic level required for the correction of the CF airway phenotype. As discussed in Chapter 3, one avenue to explore is the addition of the RGD motif on the viral vector envelope in conjunction with the VSV-G pseudotype to target specific integrins on the surface of airway stem cells.

While effective targeting of airway stem cells for sustained transgene expression has been demonstrated in this thesis, the theoretical possibility of neutral drift of airway stem cells needs to be clarified to ascertain if it is a limiting factor. As explained in the discussion section of Chapter 3, there are currently two proposed models of tissue self-renewal: the division asymmetry model, and the population asymmetry model. The division symmetry model proposes that each airway stem cell will self-renew as well as differentiate; hence a transduced stem cell would potentially be present for life. The population asymmetry model proposes that a proportion of the airway stem cells will differentiate without self-renewal, leading to the gradual potential loss of transduced stem cells through neutral drift. A long term study quantifying the percentage of transduced airway stem cells at different time point throughout the life span of mice would potentially clarify if neutral drift is a limiting factor

The second aim of this research was to investigate and clarify epithelia remodelling of airway stem cells and airway goblet cells in CF mice. Airway stem cell hyperplasia was detected in the CF mouse airway epithelium; however the data quantifying airway stem cells in the CF mouse airways revealed other potential

influences that were not considered in the original study design. The data presented in Chapter 4 showed a hyperplasia of airway stem cells in both CF mouse models in three of the four assays. However, further analysis of the data showed that although airway stem cell hyperplasia was present in both CF mouse models approximately 7 months of age, there was a substantially lower level of hyperplasia in CF UNC mice and it was absent in CF FABP mice at an average age of 4.5 months. These findings suggest the possibility that the degree of hyperplasia maybe age/development dependent. These observations of a potential age or development influence on airway stem cell hyperplasia warrants further investigation.

While goblet cell hyperplasia in CF airways has been previously reported [32] [111] it was important to confirm its presence in the airways of CF mice used in the investigation of CF related airway stem cell hyperplasia.

Both goblet cell hyperplasia and hypertrophy were present, and when taken together there was an overall 4.4 fold increase in the mucin load for release into the airway. Such an increase in available mucins would exacerbate the effects of a reduced ASL present in CF as the airway may be inundated with a heavy mucin load from the hyperplasic and hypertrophic goblet cells. It is acknowledged that while there is a significant increase in available mucins for secretion, whether these mucins are actually released into the airway, as well as the mechanisms governing mucin release are poorly understood and need to be addressed in future studies.

The presence of hyperplastic airway stem cells and goblet cells existing together in the CF airway epithelium as shown here may be the result of activity in the Notch signalling pathway. This pathway plays a role in determining cell fate in both the developing and regenerating airway epithelium [127], and may provide one

mechanism to produce the dual hyperplasic cell types in the CF airway. That is the raised pro inflammatory cytokines such as IL-8 in the CF airways up regulate the Notch signalling pathway and direct cell fate towards the production of goblet cells and potentially airway stem cells [110].

The third and fourth aims explored the potential of the LPC pre-treatment, HIV-1 VSV-G pseudotyped LV vector delivery and its potential to transduce the desired ciliated cells and airway stem cells in additional animal models. Such studies can ensure that observed gene transfer affects are not restricted to a particular species and can provide supportive evidence of likely applications in humans.

To bridge the gap between proof of principle studies in mice and potential use in humans, additional animal models including non-human primates that have closer relevance to humans were trialled. The same established protocol and LV vector used in the airway stem cell transduction studies with relevant changes in vector volume to accommodate animal size were utilised to test transducion in the ferret and in a non-human primate, the common marmoset. In both studies LV vector mediated transgene expression was observed in both ciliated cells and airway stem cells. These observations of successful transduction of airway stem cells in these very different animal models provides further support for the premise of effective airway gene transfer and for the ability to access and transduce airway stem cells for sustained gene correction in CF.

Additionally, the transduction of desired cell types in the ferret airway provides a foundation from which to explore testing of the therapeutic CFTR gene in the emerging CF ferret model which displays a human like CF airway phenotype that is not present in any of the CF mouse models.

A limiting factor for a CFTR gene therapy aimed at targeting airway stem cells in the upper airways of CF animal models such as the CF ferret and CF pig is the lack of functional *in vivo* assays or means to quantify the desired changes such as a restored ASL depth and MCT. In Appendix B, evidence is presented in 3 published papers I co-investigated/authored during my candidature which demonstrate a new means to assess and quantify changes in the ASL and MCT potentially providing a direction that could be developed to assess the effects of instilling a therapeutic CFTR gene into a CF airway.

7 Conclusion

The work presented in this thesis has shown that transduction of airway stem cells, and their subsequent dissemination of the transgene into the differentiated cell progeny can be successfully achieved in both the nasal and tracheal regions of the airways. Airway epithelial goblet cell hyperplasia and hypertrophy in the CF mouse compared to normal mice was also described. The hyperplasia in airway stem cells found here in CF mice may be age or development dependent; and this finding warrants follow up studies. The transduction of relevant airway cell types, including airway stem cells, was demonstrated in two further animal models, the ferret and the marmoset. This indicates a general ability of the LPC/LV vector gene delivery protocol to transduce the airway epithelium, *in situ*, in mammals.

The evidence presented in this thesis provides support for the continued investigation of targeting airway stem cells for long term transgene expression in an effort to provide an effective protocol to correct the CF airway disease phenotype over an extended period.

8 Appendix

8.1 Appendix A

8.1.1 Tracheal ring remodelling in CF mice

There have been reports of tracheal cartilage ring remodelling in CF knockout mice, however while there is a consensus in some research areas of cartilage ring remodelling there is also a discrepancy. The discrepancy reported is that Bonvin *et al* observed no change in cartilage ring numbers between CF knockout mice and controls while in contrast Wallace *et al* observed there was a statistical difference [36, 37].

8.1.2 Methods

Trachea cartilage rings, 5 µm sections of trachea, mounted on glass microscope slides were stained with H&E, inspected microscopically and scored as distance between first five cartilage rings immediately following the cricoid cartilage and number of cartilage rings over a distance of 2mm in the same area.

8.1.3 Results

8.1.3.1 Tracheal cartilage ring remodelling

Tracheal remodelling of the cartilage rings was confirmed in CF FABP mice (6.2 ± 0.2 cartilage rings) (n=5) compared to controls (7.2 ± 0.3 cartilage rings) (n=5) with a 1.16 fold decrease over a distance of 2 mm (Figure 8-1 a). The CF mice also showed on average a 310 µm increase in distance over five tracheal rings (1627 ± 69.1 µm) compared to the control (1317 ± 73.7 µm) (Figure 8-1 b)
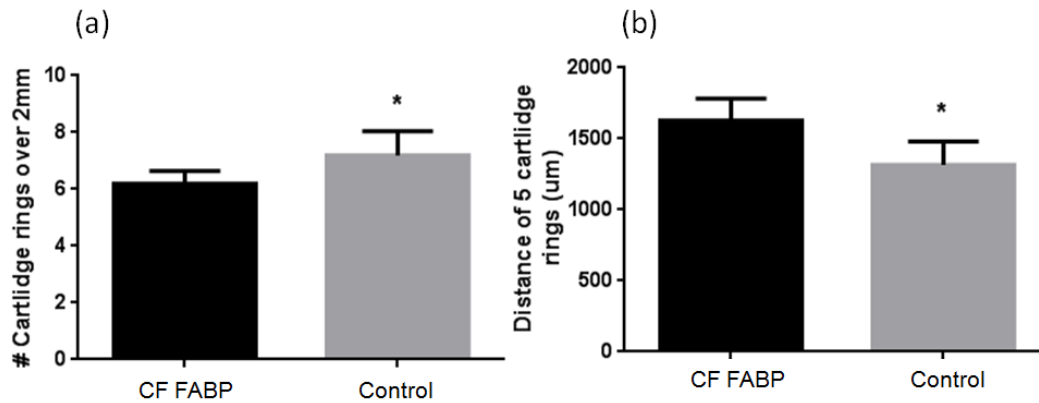
Figure 8-1: Remodelling of the tracheal cartilage in CF mice.

Analysis of cartilage rings in CF FABP mice showed a statistically significant reduction of the number of rings over 2mm (a) and an increase in the distance of 5 cartilage rings (b).* p = < 0.05 unpaired t test, n=5.

8.1.4 Discussion

Given the disparity in reporting of potential trachea cartilage ring remodelling [36, 37] it was important to assess and clarify this discrepancy. Tracheal ring remodelling observed in this study (Figure 8-1) is not consistent with that reported by Bonvin *et al* [36], however in another study tracheal cartilage rings were found to be diminished in number in CF knockout mice compared to controls [37] which is consistent with the finding in this study. The proximal location was chosen as it is this area that a narrowing of the trachea in CF knockout mice has been reported [36, 37]. The observation that there is evidence to support tracheal cartilage ring remodelling with fewer rings in CF mice compared to controls provides independent supportive data potentially clearing up the discrepancy between the two previous findings by Bonvin *et al* and Wallace *et al*.

8.2 **Appendix B**

8.2.1 **Synchrotron based studies: development of new methods for assessing CF disease and treatment**

The primary goal of gene therapy for CF airway disease is to correct the ion channel defect, thereby restoring the ASL depth and MCT to that observed in the normal airways, eradicating an environment susceptible to bacterial colonisation. A limiting factor in assessing the potential for gene therapy (and indeed other pharmaceutical therapies) in the airways is the inability to accurately measure the ASL depth and MCT changes *in vivo*. CF drug development studies in animal models and humans are currently restricted to choices such as lung function testing, structural lung imaging and quality of life assessments, which are all indirect and delayed measures of airway hydration. The synchrotron X-ray based studies presented in this Appendix use the recently developed techniques of phase contrast X-ray imaging (PCXI) [163] and single-grid-based phased contrast x-ray imaging (SGB-PCXI) [164, 165] to rapidly and non-invasively visualise and measure MCT and ASL depth respectively *in vivo*.

A synchrotron is a large particle accelerator that is specifically designed to produce extremely bright light by deflecting a beam of electrons through a magnetic field. The synchrotron light can range from visible to hard x-ray wavelengths, and is highly coherent. When x-rays pass through an object some are absorbed (this is how normal x-ray images are formed) and some are refracted at the interfaces between materials of different x-ray index (more correctly, the x-rays change phase). Using a highly coherent x-ray source and introducing a spacing between the object and detector allows this phase information to be recorded, and this is the basis of PCXI.

The boundaries between tissue and air produce large phase differences, making PCXI ideal for imaging the respiratory system. The high flux and collimation available at long beamlines, such as the BL20XU biomedical imaging beamline at the SPring-8 synchrotron in Japan are ideal for imaging small regions of interest (typically ~2 x 1 mm) at high resolution and high frame rates. We have been developing PCXI techniques that utilise synchrotron x-rays to visualise the airway surfaces at high magnification to assess changes in ASL and MCT.

8.2.2 Airway surface liquid depth assessment, non-invasively

The first paper in this appendix "*In Vivo* X-Ray Imaging Improves Airway Surface Hydration after Therapy Designed for Cystic Fibrosis" utilised the SGB-PCXI technique to non-invasively assess the effects of a two-agent rehydrating treatment on the ASL. Briefly, SGB-PCXI uses a uniform absorption or phase grid in front of the sample to produce a high contrast reference pattern. Subtle changes in the x-ray phase at the tissue to ASL interface alter this pattern, allowing the tissue to ASL interface to be detected, and the depth measurement to be made. In this experiment a long-acting sodium channel blocker (P308; Parion Sciences, Durham, NC) (1mM) in 7% hypertonic saline (the latter an established beneficial treatment in CF children and adults) was aerosolized onto the trachea of live anaesthetised mice. The airway was imaged at high magnification and the ASL depth was measured, showing that the average ASL depth increased by 10-15µm. The development and demonstration of this new non-invasive technique allows repeated measures to be performed on the same animal at multiple time points which may have an application in assessing CFTR gene therapy and its effects on ASL in CFTR animal models.

8.2.3 Non-invasive measurement of mucociliary transit activity on live and intact airway surfaces

The last two papers in the Appendix "Non-invasive airway health assessment: Synchrotron imaging reveals effects of rehydrating treatments on mucociliary transit in-vivo" and "Tracking extended mucociliary transport activity of individual deposited particles: longitudinal synchrotron X-ray imaging in live mice" utilised the same PCXI technique to track the effect of ASL rehydration on MCT. Briefly, the same two-agent rehydrating treatment used in the SGB-PCXI studies was applied after micron-sized marker particles were delivered to the airways. The micron-sized particles were then tracked via the PCXI X-ray images obtained at regular intervals over time allowing for the change in MCT that was produced by ASL rehydration to be quantified. As the final paper demonstrates, these measurements were successfully performed over staggered repeat time points allowing for greater insight to be gained on the effects of ASL rehydrating agents on the airways.

Statement of Authorship

Title of Paper	In vivo X-ray Imaging Reveals Improved Airway Surface Hydration after a Therapy Designed for Cystic Fibrosis
Publication Status	⊗ Published, ○ Accepted for Publication, ○ Submitted for Publication, ○ Publication style
Publication Details	K. Morgan, M. Donnelley, N. Farrow, A. Fouras, R. Boucher, N. Yagi, Y. Suzuki, A. Takeuchi, K. Uesugi, K. Siu, D. Parsons, In vivo X-ray Imaging Reveals Improved Airway Surface Hydration after a Therapy Designed for Cystic Fibrosis, American Journal of Respiratory and Critical Care Medicine, vol. 190, pp 469-472, 2014.

Author Contributions

By signing the Statement of Authorship, each author certifies that their stated contribution to the publication is accurate and that permission is granted for the publication to be included in the candidate's thesis.

Name of Principal Author (Candidate)	Kaye Morgan		
Contribution to the Paper	Designed the grid imaging method Image analysis Paper writing		
Signature		Date	23/1/15

Name of Co-Author	Martin Donnelley		
Contribution to the Paper	Performed experiments Paper writing		
Signature		Date	23/1/15

Name of Co-Author	Nigel Farrow		
Contribution to the Paper	Performed all animal work, including intubation, animal preparation, etc in Japan Contributed to paper writing		
Signature		Date	23/1/15

Name of Co-Author	Andreas Fouras		
Contribution to the Paper	Provided technical expertise		
Signature		Date	23/1/15

Statement of Authorship

Title of Paper	In vivo X-ray Imaging Reveals Improved Airway Surface Hydration after a Therapy Designed for Cystic Fibrosis
Publication Status	⊗ Published, ○ Accepted for Publication, ○ Submitted for Publication, ○ Publication style
Publication Details	K. Morgan, M. Donnelley, N. Farrow, A. Fouras, R. Boucher, N. Yagi, Y. Suzuki, A. Takeuchi, K. Uesugi, K. Siu, D. Parsons, In vivo X-ray Imaging Reveals Improved Airway Surface Hydration after a Therapy Designed for Cystic Fibrosis, American Journal of Respiratory and Critical Care Medicine, vol. 190, pp 469-472, 2014.

Author Contributions

By signing the Statement of Authorship, each author certifies that their stated contribution to the publication is accurate and that permission is granted for the publication to be included in the candidate's thesis.

Name of Principal Author (Candidate)	Richard Boucher		
Contribution to the Paper	Provided CF related biological expertise		
Signature		Date	23/1/15

Name of Co-Author	Naoto Yagi		
Contribution to the Paper	Chief beamline scientist at SPring-8, Japan		
Signature	N/A	Date	

Name of Co-Author	Yoshio Suzuki		
Contribution to the Paper	Beamline scientist at SPring-8, Japan		
Signature	N/A	Date	

Name of Co-Author	Akahisa Takeuchi		
Contribution to the Paper	Beamline scientist at SPring-8, Japan		
Signature	N/A	Date	

Statement of Authorship

Title of Paper	In vivo X-ray Imaging Reveals Improved Airway Surface Hydration after a Therapy Designed for Cystic Fibrosis
Publication Status	⊗ Published, ◯ Accepted for Publication, ◯ Submitted for Publication, ◯ Publication style
Publication Details	K. Morgan, M. Donnelley, N. Farrow, A. Fouras, R. Boucher, N. Yagi, Y. Suzuki, A. Takeuchi, K. Uesugi, K. Siu, D. Parsons, In vivo X-ray Imaging Reveals Improved Airway Surface Hydration after a Therapy Designed for Cystic Fibrosis, American Journal of Respiratory and Critical Care Medicine, vol. 190, pp 469-472, 2014.

Author Contributions

By signing the Statement of Authorship, each author certifies that their stated contribution to the publication is accurate and that permission is granted for the publication to be included in the candidate's thesis.

Name of Principal Author (Candidate)	Kentaro Uesugi
Contribution to the Paper	Beamline scientist at SPring-8, Japan
Signature	N/A	Date	

Name of Co-Author	Karen Siu
Contribution to the Paper	Experimental design Assisted with development of grid-based imaging method
Signature		Date	23/1/15

Name of Co-Author	David Parsons
Contribution to the Paper	Experimental design "MacGyver'ed" bits and pieces together Paper writing
Signature		Date	23/1/15

Name of Co-Author	
Contribution to the Paper	
Signature		Date	

8.2.4 In Vivo X-Ray Imaging Reveals Improved Airway Surface Hydration after a Therapy Designed for Cystic Fibrosis.

CORRESPONDENCE

In Vivo X-Ray Imaging Reveals Improved Airway Surface Hydration after a Therapy Designed for Cystic Fibrosis

To the Editor:

Sufficient airway surface liquid (ASL) depth is critical to ensure that the mucociliary transport system can effectively clear inhaled pathogens from the lungs. In those with cystic fibrosis (CF), the CF transmembrane conductance regulator gene defect decreases airway surface hydration (1, 2), compromising lung defense mechanisms, resulting in progressive lung infection and early death (3). An effective CF respiratory therapy should increase the ASL depth, restoring clearance mechanisms, but it is difficult to measure this depth *in vivo*. Current clinical health measures used for CF drug development studies include lung function testing and structural lung imaging (i.e., computed tomography), both indirect and delayed measures of airway hydration. Although the ASL depth has been measured by confocal microscopy in epithelial cultures (1, 4) and histologically in fragments of trachea (5), these technologies are not feasible *in vivo*.

We have realized a technique called single-grid–based phase–contrast X-ray imaging (SGB-PCXI) (Figure 1A) (6–9), which is capable of non-invasive ASL imaging, and we previously demonstrated its ability to measure the ASL rehydrating effects of aerosolized hypertonic saline (HS) in the excised trachea of a mouse (10). In this letter, we report the first *in vivo* measures of ASL using this technique.

PCXI methods capture information on how the sample refracts the X-ray wavefield to provide exquisite soft tissue images. This differs from conventional X-ray imaging, where absorption of the X-ray wavefield provides very little soft tissue contrast (11). ASL measurements were not feasible with previous PCXI methods, which lacked either the speed to capture these high-magnification images without motion blur, or the sensitivity to differentiate ASL from surrounding tissue. Our SGB-PCXI method provides the necessary speed and sensitivity by illuminating the airways with a grid pattern. At the image detector, the grid will appear distorted according to the refractive properties of the airway tissue, in the same way the tile pattern on the bottom of a swimming pool will appear distorted according to the refractive properties of the water

(10). By analyzing these distortions, we can quickly and sensitively produce an image of the ASL (6–8).

Using SGB-PCXI, we measured the effects of a two-agent rehydrating treatment—an aerosol containing a long-acting epithelial sodium channel blocker (P308; Parion Sciences, Durham, NC), at a concentration of 1 mM in 7% HS—on ASL depth in live, anesthetized mice. C57Bl/6 mice ($n = 14$) were prepared for ventilation and imaging, as previously detailed (12), and placed in a supine position so that the ventral surface could be imaged to avoid multiple overlaid tracheal edges and ensure that any bulk fluid formed during aerosol delivery did not pool in the field of view. Treatments were delivered using an Aeroneb Pro nebulizer (Aerogen, Galway, Ireland), designed to produce 3.5-μm volume median diameter aerosol, integrated in the ventilator system, for a period of 90 seconds, 50% duty cycle. For each mouse, images of the ventral tracheal surface were captured at 3-minute intervals, before and for 15 minutes after delivery of the control (isotonic saline) treatment; after a break of 5 minutes, the 15-minute imaging sequence was repeated in the same mouse then being delivered the HS-P308 treatment (Figure 1D).

Before any image analysis was performed, six mice were rejected from the study (leaving $n = 8$). One mouse shifted position such that the airway moved out of the field of view; for two mice, the custom-built nebulizer control system malfunctioned; and in three mice, the intubation was placed too deeply into the airway for tracheal aerosol delivery (with the position observed immediately when X-ray imaging began). This failure rate illustrates the initial technical difficulty involved with these complex experiments, but sufficient sample size remained. We anticipate that these problems will decrease with experience, as in our previous imaging development work.

Measurements were made (observer blinded to treatment) by manually tracing the tissue–cartilage, tissue–ASL, and ASL–airway interfaces. Manual traces showed an acceptably high intraclass correlation of 0.992 between five different scorers in our previous study (10). The distance between marked interface lines was measured computationally, taking the average distance over the length of airway traced in that image. Measures taken at all time points were then analyzed by repeated-measures ANOVA (Prism 5; GraphPad, San Diego, CA).

Although the presence of overlying tissue and skin *in vivo* reduces the visibility of the subtle ASL–tissue interface compared with our previous *ex vivo* studies (10), ASL depth measurements were still possible, as seen by the *left bracket* in Figure 1B. The HS-P308 sequences showed lumen movement and increased ASL depth after treatment delivery (Figure 1C). The control (isotonic saline) sequences showed very little movement throughout, and this low, stationary ASL made it difficult to reliably identify the ASL–tissue interface, particularly given the obscuring influence of overlying skin/tissue. Therefore, to quantify biological changes in response to isotonic saline versus HS-P308, we measured the distance between the outer edge of a reference cartilage ring and the ASL–airway lumen interface, as indicated by the *bracket* in the *right* of Figure 1B.

A statistically significant increase in the position of the ASL surface (relative to the cartilage) was observed in the airways treated with HS-P308 compared with the earlier isotonic saline treatment for all time points after and including 6 minutes after aerosol delivery, as seen in Figure 1D. In the direct measures of ASL depth (Figure 1C) there was a significant increase in depth compared with baseline at 9 and 12 minutes after delivery of

141

Figure 1. (A) Experimental setup using 25-keV X-rays at beamline BL20XU at the SPring-8 synchrotron in Japan, using the setup described in Reference 10, with a gold absorption grid of 25.4-μm period (Gilder grids, G1000HS-G3), and distances of 0.1 m grid-to-sample and 1 m sample-to-detector. The lens-coupled charge-coupled device detector captures a 721 × 497-μm field of view with 0.18-μm pixels using a 100-ms exposure. Airway images are reconstructed using a correlation-based analysis detailed in References 6–8. (B) Single-grid–based phase–contrast X-ray imaging (SGB-PCXI) differential contrast image of the *in vivo* trachea surface. *Scale bar* = 100 μm. (C) Airway surface liquid (ASL) depth measurements, where each data point represents a measurement, and the *darker bars* indicate the mean (±SD) of measurements at that time point. Hypertonic saline (HS)–P308 was delivered after the t = 0 time point, analyzed by one-way repeated-measures (RM)-ANOVA to detect differences compared to baseline (t = 0). Statistical significance was set at a *P* value of 0.05 and a power of 0.8 for all analyses. (D) Changes in the cartilage-to-surface distance over time, analyzed by two-way RM-ANOVA with Bonferroni multiple comparisons to detect significant differences between treatments at matching time points. In the 5-minute break between sequences, researchers entered the imaging hutch to change the treatment solution.

HS-P308. Although some mice showed a large increase within 3 minutes of treatment delivery, others had a more delayed effect, resulting in a large spread of values at 3 minutes. A similarly large spread of values was seen at 15 minutes, when the treatment effect may have waned for some of the mice, increasing the variability of the dataset at that final time point.

The relative increase in the ASL depth was of similar magnitude to that seen in our *ex vivo* study (10), with the average depth increasing by a maximum of 10–15 μm. This effect is consistent

in magnitude and duration with tissue culture studies (13). It is interesting to note that the increase in the cartilage-to-airway measure (Figure 1D) was greater than the increase in ASL depth measure (Figure 1C, subtracting baseline), peaking at around 30 μm compared with 10 μm. This finding suggests that there may be additional liquid drawn from surrounding tissue into the submucosal compartment, causing that region to swell and raise the surface of the liquid further from the cartilage. In contrast, our *ex vivo* studies observed a decrease in airway tissue volume from 3 minutes

142

after treatment, when there was no surrounding tissue present (10). This difference illustrates the importance of conducting studies *in vivo* when assessing a physiological response to treatment. We also noted that the treatment effect lasted longer *in vivo* with HS-P308 treatment compared with *ex vivo* with HS treatment. Because both the treatment agent and the nature of the measurements (*in/ex vivo*) were different between this and previous studies, we cannot determine which factor produced this extended effect.

We believe that these are the first reported noninvasive *in vivo* measurements of changes in ASL volume (depth) in response to an airway-rehydrating treatment. Our transition from *ex vivo* to *in vivo* imaging is significant, enabling biologically relevant results, longitudinal studies, and treatment delivery technique studies. The research and clinical utilities of a rapid, noninvasive ASL depth measurement technique are significant. Although clinical implementation presents some challenges, continuing developments in image detectors and compact X-ray sources suitable for PCXI mean that this is still a possibility, although some compromises in image quality may be necessary to reduce radiation dose. In addition, these kinds of technical developments will certainly improve the accessibility, speed, and spatial resolution of our technique for research (note the use of light at X-ray wavelengths means that our images are several orders of magnitude from the fundamental spatial resolution limits). Direct observations of *in vivo* changes in the ASL depth immediately after application of known or potential therapies can lead to a better understanding of how CF transmembrane conductance regulator gene, protein, and channel activity alterations influence fundamental airway surface ion–water balance processes. Furthermore, rapid and accurate *in vivo* physiological outcome assessments of drugs emerging from the CF pharmaceutical development pipeline can be made at the site of action, and reveal biophysical mechanisms that precede more global measurements of airway function (e.g., FEV_1). Studies can also examine a range of disease models, and the noninvasive nature of this new measure means that repeat measures can be captured on the same animals across a range of time scales (14). ∎

Kaye S. Morgan, Ph.D.
Monash University
Clayton, Victoria, Australia

Martin Donnelley, Ph.D.
Nigel Farrow
Women's and Children's Hospital
North Adelaide, South Australia, Australia
and
Robinson Institute, University of Adelaide
Adelaide, South Australia, Australia

Andreas Fouras, Ph.D.
Monash University
Clayton, Victoria, Australia

Naoto Yagi, Ph.D.
Yoshio Suzuki, Ph.D.
Akihisa Takeuchi, Ph.D.

Kentaro Uesugi, Ph.D.
SPring-8/Japan Synchrotron Radiation Research Institute
Kouto, Hyogo, Japan

Richard C. Boucher, M.D.
University of North Carolina
Chapel Hill, North Carolina

Karen K. W. Siu, Ph.D.*
Monash University
Clayton, Victoria, Australia

David W. Parsons, Ph.D.*
Women's and Children's Hospital
North Adelaide, South Australia, Australia
and
Robinson Institute, University of Adelaide
Adelaide, South Australia, Australia

*K.K.W.S. and D.W.P. contributed equally as senior authors.

References

1. Matsui H, Grubb BR, Tarran R, Randell SH, Gatzy JT, Davis CW, Boucher RC. Evidence for periciliary liquid layer depletion, not abnormal ion composition, in the pathogenesis of cystic fibrosis airways disease. *Cell* 1998;95:1005–1015.
2. Boucher RC. Evidence for airway surface dehydration as the initiating event in CF airway disease. *J Intern Med* 2007;261:5–16.
3. Daviskas E, Anderson SD. Hyperosmolar agents and clearance of mucus in the diseased airway. *J Aerosol Med* 2006;19:100–109.
4. Donaldson SH, Bennett WD, Zeman KL, Knowles MR, Tarran R, Boucher RC. Mucus clearance and lung function in cystic fibrosis with hypertonic saline. *N Engl J Med* 2006;354:241–250.
5. Song Y, Namkung W, Nielson DW, Lee JW, Finkbeiner WE, Verkman AS. Airway surface liquid depth measured in *ex vivo* fragments of pig and human trachea: dependence on Na^+ and Cl^- channel function. *Am J Physiol Lung Cell Mol Physiol* 2009;297:L1131–L1140.
6. Morgan KS, Paganin DM, Siu KKW. Quantitative X-ray phase–contrast imaging using a single grating of comparable pitch to sample feature size. *Opt Lett* 2011;36:55–57.
7. Morgan KS, Paganin DM, Siu KKW. Quantitative single-exposure X-ray phase contrast imaging using a single attenuation grid. *Opt Express* 2011;19:19781–19789.
8. Morgan KS, Modregger P, Irvine SC, Rutishauser S, Guzenko VA, Stampanoni M, David C. A sensitive X-ray phase contrast technique for rapid imaging using a single phase grid analyzer. *Opt Lett* 2013;38: 4605–4608.
9. Morgan KS, Paganin DM, Parsons DW, Donnelley M, Yagi N, Uesugi K, Suzuki Y, Takeuchi A, Siu KKW. Single grating X-ray imaging for dynamic biological systems. *AIP Conf Proc* 2012;1466:124–129.
10. Morgan KS, Donnelley M, Paganin DM, Fouras A, Yagi N, Suzuki Y, Takeuchi A, Uesugi K, Boucher RC, Parsons DW, *et al*. Measuring airway surface liquid depth in *ex vivo* mouse airways by X-ray imaging for the assessment of cystic fibrosis airway therapies. *PLoS One* 2013;8:e55822.
11. Bravin A, Coan P, Suortti P. X-ray phase–contrast imaging: from pre-clinical applications towards clinics. *Phys Med Biol* 2013;58:R1–R35.
12. Donnelley M, Parsons D, Morgan K, Siu K. Animals in synchrotrons: overcoming challenges for high-resolution, live, small-animal imaging. *AIP Conf Proc* 2010;1266:30–34.
13. Tarran R, Grubb BR, Parsons D, Picher M, Hirsh AJ, Davis CW, Boucher RC. The CF salt controversy: *in vivo* observations and therapeutic approaches. *Mol Cell* 2001;8:149–158.
14. Donnelley M, Morgan KS, Siu KKW, Fouras A, Farrow NR, Carnibella RP, Parsons DW. Tracking extended mucociliary transport activity of individual deposited particles: longitudinal synchrotron imaging in live mice. *J Synchrotron Radiat* 2014;21:768–773.

Statement of Authorship

Title of Paper	Tracking extended mucociliary transport activity of individual deposited particles: Longitudinal synchrotron imaging in live mice
Publication Status	⊗ Published, ○ Accepted for Publication, ○ Submitted for Publication, ○ Publication style
Publication Details	M. Donnelley, K. Morgan, K. Siu, A. Fouras, N. Farrow, R. Carnibella, D. Parsons, Tracking extended mucociliary transport activity of individual deposited particles: Longitudinal synchrotron imaging in live mice, Journal of Synchrotron Radiation, vol. 21, 2014

Author Contributions

By signing the Statement of Authorship, each author certifies that their stated contribution to the publication is accurate and that permission is granted for the publication to be included in the candidate's thesis.

Name of Principal Author (Candidate)	Martin Donnelley		
Contribution to the Paper	Experimental design Performed experiments Paper writing		
Signature		Date	23/1/15

Name of Co-Author	Kaye Morgan		
Contribution to the Paper	Performed experiments Paper writing		
Signature		Date	23/1/15

Name of Co-Author	Karen Siu		
Contribution to the Paper	Performed experiments Provided synchrotron related technical advice		
Signature		Date	23/1/15

Name of Co-Author	Andreas Fouras		
Contribution to the Paper	Provided technical advice		
Signature		Date	23/1/15

Statement of Authorship

Title of Paper	Tracking extended mucociliary transport activity of individual deposited particles: Longitudinal synchrotron imaging in live mice
Publication Status	◯ Published, ◯ Accepted for Publication, ◯ Submitted for Publication, ◯ Publication style
Publication Details	M. Donnelley, K. Morgan, K. Siu, A. Fouras, N. Farrow, R. Carnibella, D. Parsons, Tracking extended mucociliary transport activity of individual deposited particles: Longitudinal synchrotron imaging in live mice, Journal of Synchrotron Radiation, vol. 21, 2014

Author Contributions

By signing the Statement of Authorship, each author certifies that their stated contribution to the publication is accurate and that permission is granted for the publication to be included in the candidate's thesis.

Name of Principal Author (Candidate)	Nigel Farrow		
Contribution to the Paper	Performed all animal preparation at SPring-8 in Japan Paper writing		
Signature		Date	23/1/15

Name of Co-Author	Richard Carnibella		
Contribution to the Paper	Assisted with experiments		
Signature		Date	23/1/15

Name of Co-Author	David Parsons		
Contribution to the Paper	Experiment design Assisted with experiments Paper writing		
Signature		Date	23/1/15

Name of Co-Author			
Contribution to the Paper			
Signature		Date	

8.2.5 Tracking extended mucociliary transport activity of individual particles: longitudinal synchrotron X-ray imaging in live mice.

Tracking extended mucociliary transport activity of individual deposited particles: longitudinal synchrotron X-ray imaging in live mice

Martin Donnelley,[a,b,c]* Kaye S. Morgan,[d] Karen K. W. Siu,[d] Andreas Fouras,[e] Nigel R. Farrow,[a,b,c] Richard P. Carnibella[e] and David W. Parsons[a,b,c]

[a]Respiratory and Sleep Medicine, Women's and Children's Hospital, 72 King William Road, North Adelaide, SA 5006, Australia, [b]Robinson Research Institute, University of Adelaide, SA 5001, Australia, [c]School of Paediatrics and Reproductive Health, University of Adelaide, SA 5001, Australia, [d]School of Physics, Monash University, Clayton, Vic 3800, Australia, and [e]Mechanical and Aerospace Engineering, Monash University, Clayton, Vic 3800, Australia.
*E-mail: martin.donnelley@adelaide.edu.au

To assess potential therapies for respiratory diseases in which mucociliary transit (MCT) is impaired, such as cystic fibrosis and primary ciliary dyskinesia, a novel and non-invasive MCT quantification method has been developed in which the transit rate and behaviour of individual micrometre-sized deposited particles are measured in live mice using synchrotron phase-contrast X-ray imaging. Particle clearance by MCT is known to be a two-phase process that occurs over a period of minutes to days. Previous studies have assessed MCT in the fast-clearance phase, $\sim$20 min after marker particle dosing. The aim of this study was to non-invasively image changes in particle presence and MCT during the slow-clearance phase, and simultaneously determine whether repeat synchrotron X-ray imaging of mice was feasible over periods of 3, 9 and 25 h. All mice tolerated the repeat imaging procedure with no adverse effects. Quantitative image analysis revealed that the particle MCT rate and the number of particles present in the airway both decreased with time. This study successfully demonstrated for the first time that longitudinal synchrotron X-ray imaging studies are possible in live small animals, provided appropriate animal handling techniques are used and care is taken to reduce the delivered radiation dose.

Keywords: particles; airway surface; lung; trachea; mucociliary transit; non-invasive; X-ray imaging; phase contrast; mouse; longitudinal; repeat; dose.

1. Introduction and objectives

Mucociliary transport (MCT) is the coordinated beating of cilia, *i.e.* the microscopic hair-like structures that project into the airway surface liquid (ASL) from the surfaces of epithelial cells, that removes deposited pathogens, particulates and mucus from the airways. In cystic fibrosis (CF) airways disease an improperly functioning CF transmembrane conductance regulator (CFTR) ion channel in airway epithelial cells results in ASL dehydration and impaired MCT. Over time this causes retention of pathogens and particulates, increasing mucus obstructions, chronic infection and inflammation, and eventually results in lung failure (Boucher, 2004). In another inherited condition, primary ciliary dyskinesia (PCD), the cilia are immotile or ineffective, resulting in poor MCT, persistent respiratory infections and deteriorating lung function (Chodhari *et al.*, 2004).

A logical method to assess native MCT behaviour, as well as the effectiveness of CF and PCD therapies on that airway surface behaviour, is to directly measure MCT activity by tracking the movement of deposited marker particles. We have developed a novel MCT monitoring method for use *in vivo* in live anaesthetized mice that is based on quantifying the transit rate and behaviour of individual deposited particles using synchrotron phase-contrast X-ray imaging (PCXI) (Donnelley *et al.*, 2009, 2010, 2012). In contrast, conventional *in vivo* MCT measurement methods, such as inhaled radio-tracers, typically measure bulk particle clearance from the airways (Grubb *et al.*, 2004; Donaldson *et al.*, 2007; Livraghi & Randell, 2007; Hua *et al.*, 2010) but are unable to track the motion of *individual* micrometre-sized deposited particles with high spatial or temporal resolution, and therefore cannot assess localized changes in MCT behaviour. The ability to do this should allow identification of early regions of disease, char-

146

acterization of the heterogeneity underlying bulk MCT and potential assessment of the regionality of drugs designed to alter MCT.

PCXI is ideally suited to non-invasive airway surface imaging in small-animal models. Provided the incident X-ray beam is spatially coherent, increasing the sample-to-detector distance (Snigirev *et al.*, 1995; Cloetens *et al.*, 1996; Wilkins *et al.*, 1996) enhances air-to-tissue interfaces due to the phase changes that are induced by differences in the tissue X-ray refractive indices. Our previous studies have assessed the MCT behaviour of a range of inhaled pollutant particles (Donnelley *et al.*, 2012) as well as the effects of inhaled clinical CF therapeutics on MCT (Donnelley *et al.*, 2014). These studies have also revealed that deposited lead dust, predominantly ranging in size from 5 µm up to 12 µm diameter, with a small number of larger particles present (see Fig. 3 of Donnelley *et al.*, 2010), is a suitable marker for analysing tracheal MCT behaviour *via* PCXI.

In previous experiments we examined the post-deposition behaviour of particles in the ∼20 min after delivery. Although we have visualized and described particle clearance within this short period, the particulates are by no means cleared from the airways. Clearance is known to be a two-phase process, with a fast-clearance phase that removes the bulk of the particles within hours, and a slow-clearance phase that removes additional particles over a period of multiple days (Falk *et al.*, 1999; Hofmann & Asgharian, 2003; Moller *et al.*, 2004). Reductions in radiation dose resulting from recent improvements in detector technology and experimental methodologies now allow the use of repeated-measures study designs to monitor MCT changes in individual animals. Although other researchers seek to perform longitudinal synchrotron X-ray imaging studies (Coan *et al.*, 2010), we are unaware of any reports of repeat-imaging experiments in living animals.

The primary aim of this study was to confirm for the first time the feasibility of performing repeat synchrotron phase-contrast imaging of the same mice over time. The secondary aim was to non-invasively observe and describe the surface activity of live mouse airways at micrometre resolution and to image and quantify changes in individual particle MCT during the slow-clearance phase, for up to 25 h.

2. Methods

The BL20XU undulator beamline at the SPring-8 synchrotron radiation facility in Japan was used for all imaging experiments, under approvals from the Animal Ethics Committees of SPring-8, the Women's and Children's Health Network, and the University of Adelaide.

2.1. Imaging set-up

The imaging set-up was as previously described (Donnelley *et al.*, 2012). Briefly, imaging was performed in the downstream experimental hutch located in the Biomedical Imaging Centre, at a distance of 245 m from the storage ring. Monochromatic 25 keV X-rays and a sample-to-detector distance of ∼1 m were used. Images were captured using a high-resolution X-ray converter (SPring-8 BM3 with a 10 µm-thick scintillator) coupled to a sCMOS detector (pco.edge; PCO Imaging, Michigan, USA) *via* a ×10 microscope objective lens (numerical aperture 0.45). This set-up produced images with an effective isotropic pixel size of 0.56 µm and a field of view of 1.43 mm × 1.2 mm (2560 × 2160 pixels). The incident beam was also limited to this size using slits to reduce the radiation dose to the animals. An ion chamber (S-1329A; Oken, Tokyo, Japan) was placed immediately after the slits to measure the photon flux. Image capture was synchronized with a fast shutter (Uniblitz XRS6 with VMM-T1 timer unit; Vincent Associates, NY, USA) to minimize the dose between exposures. Exposure lengths of 50 ms were used to produce a high signal-to-noise ratio without movement blur.

2.2. Animal preparation

All mice (*n* = 24 female C57Bl/6, weight ∼18–20 g) were prepared as for previous experiments (Donnelley *et al.*, 2012). Each mouse was anaesthetized with pentobarbital (Somnopentil; Pitman-Moore, Washington Crossing, USA; 100 mg kg^{-1} i.p.) with top-up doses delivered as required to maintain adequate depth of anaesthesia. The fur around the imaging area was removed using surgical clippers (Neuro blade; CareFusion, San Diego, USA) followed by depilatory cream (Nair, Church & Dwight, Australia) to minimize imaging interference. The mice were then intubated using a fibre-optic illuminated guide wire and a 20 Ga i.v. catheter (Insyte; Becton Dickinson, Utah, USA) as an endotracheal (ET) tube. The ET tube was inserted into the trachea such that the tip was approximately half way between the epiglottis and the carina to avoid physically perturbing the more distal imaging region. A small quantity (less than 0.001 g) of lead dust was delivered to the trachea and lungs *via* the ET tube using a Dry Powder Insufflator® Model DP-4M (Penn-Century; Wyndmoor, PA, USA). Owing to high variability in the particle mass delivered on the first actuation of the air pump, this first output was discarded and the second actuation was used to deliver the sample to the airways (Donnelley *et al.*, 2012). The particle size distribution was as described previously (Donnelley *et al.*, 2012).

Each mouse was then tethered in a custom-designed imaging holder designed to minimize body movements that interfere with high-resolution imaging. The mouse holder was mounted on the hutch sample stage so that the mouse was oriented supine and the X-ray beam passed laterally through the trachea distal to the ET tube tip. The ET tube was attached to a flexiVent small-animal ventilator (SCIREQ; Montreal, Canada), and ventilation was set at 120 breaths min^{-1}, a tidal volume of 15 ml kg^{-1} and ∼3 cm H$_2$O of PEEP. The flexiVent provided a trigger within each end-expiratory pause. Body temperature was maintained using an infrared heat lamp and monitored *via* a rectal probe. The imaging region was located using as few exposures as possible to minimize the radiation dose delivered.

Mice were randomly assigned to one of three groups; 3 h imaging, 9 h imaging or 25 h imaging ($n = 8$ per group). These times were chosen to represent a short, moderate and day-long period, and were designed to fit the entire experiment within two days of allocated synchrotron beam time. All groups were imaged after particle delivery (0 h) to determine the baseline particle distribution and MCT behaviour. At baseline, one image was captured every ten breaths (5.5 s) for 1 min and after a 4 min delay this imaging sequence was repeated, producing a total baseline set of 24 images. Mice were then removed from the hutch, extubated, allowed to recover from anaesthesia in a 310 K incubator, and provided food and water *ad libitum*. Animal recovery, external signs of skin or tissue damage, and general behaviour were monitored.

At the appropriate time ($\sim$20 min before the 3, 9 or 25 h time elapsed, depending on the group) each mouse was re-anaesthetized, re-intubated, tethered in the imaging holder and re-mounted on the sample stage. After the imaging region was re-located (by matching as closely as possible to the corresponding baseline images, using a bony landmark for registration), one image was captured every ten breaths until a set of 110 images was collected ($\sim$10 min). After the repeat-imaging, the mice were humanely killed *via* Nembutal overdose without waking from anaesthesia, thus we did not attempt to limit the radiation dose at the second timepoint.

The tracheal tissue was excised and fixed in 10% neutral buffered formalin, and processed for wax histology and staining with haematoxylin and eosin. Tissue from the un-irradiated proximal trachea adjacent to the epiglottis was used as control tissue for the irradiated region.

2.3. Post-experimental analyses

All images were flat-field and dark-current corrected (Matlab R2012b; The Mathworks, Natick, MA, USA). Individual particle MCT rates were quantified using a Matlab program that presented an observer with 12 image frames (the first minute of either the baseline or repeat-imaging data, as appropriate) over which particle MCT was to be tracked. Images from the second baseline imaging period and the remaining 9 min of later repeat-imaging data were not used for this particular analysis. The observer was then prompted to manually track the location of a chosen particle *moving* through each of those 12 frames. The 12-frame sequence was then presented again, this time with the location of the previously tracked particle(s) shown, and the observer was prompted to track another particle. This process was repeated until a maximum of 50 particles were tracked, or until no additional moving particles could be identified in the sequence. This cycle was repeated for each animal (both baseline and repeat imaging), with the observer blinded to any information that would identify the group to which the animal belonged. The location of each of the selected points was stored in a spreadsheet. Separately, the location of every *stationary* particle (up to a maximum of 250 particles) in the first frame of each sequence was also recorded in a similar manner.

The pixel distance that each particle moved between each of the 12 frames was calculated and converted to millimetres based on the size of the field of view. The particle MCT rate was then calculated based on the time between analysis frames. A mean MCT rate and the total number of particles (either moving or stationary) were calculated for each time-point in every animal.

Statistical analyses were performed using *GraphPad Prism5*. Data were tested for normality, statistical significance was set at $p = 0.05$ and power = 0.80, and MCT rates were analysed by RM-ANOVA with Sidak's multiple comparisons or Kruskal-Wallis One-way ANOVA with Dunn's multiple comparisons, as appropriate. MCT rates are presented as mean and standard deviation [$\bar{X} \pm$ standard deviation (SD)].

3. Results

For the 24 animals studied here the mean time between dry particle insufflation and initiation of the imaging run was 5 min (SD 4 min), and involved setting up the mouse in the hutch and closing the hutch radiation door. The mean times between the baseline and repeat imaging were 3 h 4 min (SD 14 min), 9 h 36 min (SD 13 min) and 25 h 28 min (SD 11 min). The ion chamber output was used to estimate the photon flux and absorbed dose. For the baseline imaging a mean of 5.9 images (SD 4.5) was used to locate the imaging area. Combined with the 24 baseline image acquisitions this resulted in a mean dose of 1.35 Gy (SD 0.2). For the repeat imaging (after which the animals were humanely killed) a mean dose of 5.57 Gy (SD 0.74) was used. All mice survived the repeat-imaging protocol with no discernible adverse effects attributable to the baseline radiation exposure, regardless of the recovery period or dose delivered. Blinded histological analysis by an experienced research veterinarian also indicated that there was no difference in gross histo-morphology to untreated animals.

Lead particles were immediately visible in the trachea of all animals when baseline imaging began, but the majority were stationary. An example of the identified particles is shown in Fig. 1; the top row shows the baseline and the bottom row shows the repeat-imaging. The number of particles delivered by the Dry Powder Insufflator™ was sufficient for distribution across the trachea, and for visualizing and quantifying MCT. For all rate analyses the limit of detection for MCT movement was $\sim$0.02 mm min^{-1}. Fig. 2(a) shows the recorded MCT rate of every moving particle. A total of 48 moving particles were tracked at baseline, 25 at 3 h, 0 at 9 h and 2 at 25 h. The reduction in MCT rate at 3 and 25 h was statistically significant compared with baseline. Fig. 2(b) shows the same data but presented as an average MCT rate for each animal. This analysis did not show any statistically significant differences between the rates at each timepoint. As previously reported (Donnelley *et al.*, 2009, 2010, 2012), the *moving* particles followed unpredictable and non-linear paths along the airway. It was not possible to accurately identify the size, shape or surface properties of individual moving or stationary particles,

148
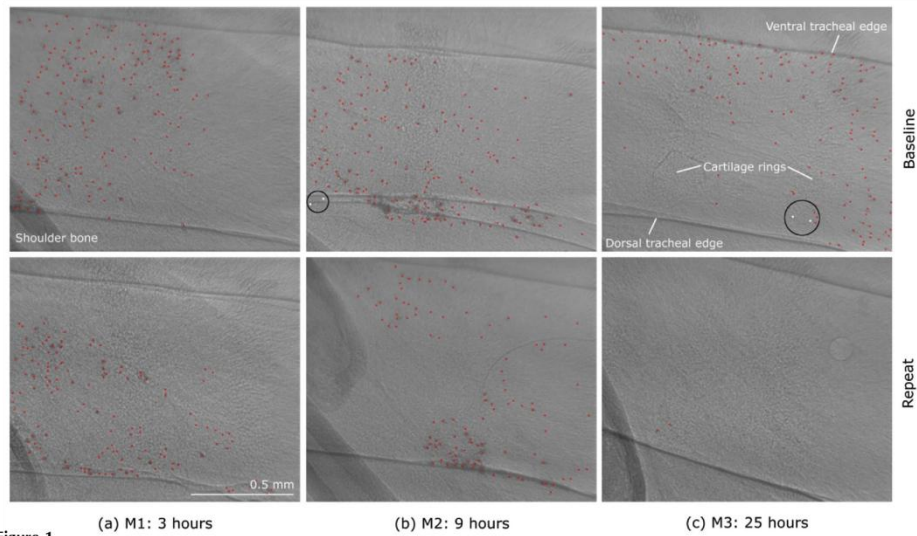
Figure 1
High-magnification images of lead dust in the trachea of three live mice (M1–M3) after particle insufflation, assessed using a repeat-imaging study design. The head is to the right and the spine is toward the bottom. The top row of images was taken at baseline, shortly after lead dust was delivered to the airway surface. The bottom row shows approximately the same locations (*a*) 3 h, (*b*) 9 h and (*c*) 25 h later. Imaging typically included the same bone edge (bottom left-hand corner) to help ensure that the same airway region was examined each time. Imaging location is just above the carina and the image dimensions are 1.45 mm × 1.2 mm. Stationary particles are marked in red and (the few) moving particles in white (black circles).

so we did not perform a quantitative analysis of these properties. However, subjectively it did not appear that particle size directly correlated with the rate at which the particles were cleared.

The total number of *moving* and *stationary* particles in every animal was also determined at each timepoint and is shown in Fig. 3. Although only a small number of *moving* particles were detected, many *stationary* particles were located in the first frame from each timepoint (these particles are marked red in Fig. 1). Notably, the number had halved after 3 h and were absent or very low at the later timepoints. Fig. 3 shows that while there was substantial variability in the number of particles detected at baseline, the mean number of particles in each group was similar. There were statistically significant reductions in the number of particles present at 9 and 25 h, but there was no difference at 3 h.

The ratio of the total particle count (*moving* and *stationary*) compared with baseline in each animal at each of the repeat-imaging timepoints is shown in Fig. 4. Each value was calculated by dividing the total number of particles in each animal at the repeat timepoint by the number present at baseline. Some mice contained more particles in the imaging region at the 3 h (*n* = 4 mice) and 9 h (*n* = 1 mouse) timepoints (*i.e.* proportion of baseline > 1). Significantly fewer particles remained at the 9 and 25 h timepoints compared with the 3 h timepoint.

4. Discussion

This study is the first report demonstrating the feasibility of repeat synchrotron X-ray imaging of MCT in live anaesthetized mice. Studies of this type will now allow changes in individual particle clearance to be visualized and quantified over extended periods of time after particle delivery. Minimizing the radiation dose delivered by reducing the number of exposures and the length of each exposure (while retaining a sufficient signal-to-noise ratio) is key to the success of repeat-imaging experiments of this type. Furthermore, the ability to reliably perform rapid and minimally invasive endotracheal intubations, a detailed knowledge of anatomical landmarks to facilitate rapid region of interest location, validation of appropriate marker particles, as well as stable and predictable anaesthesia within a remote delivery and physiological monitoring setting, are also essential.

High-resolution X-ray imaging requires large radiation doses to produce high-quality images. Although the radiation dose used in this study was high, it was localized to a very small area of the trachea ($\sim$1.7 mm^2), and did not pass through any other major anatomical structures or organs other than the skin and tissue surrounding the trachea. We did not observe any untoward physiological or histological effects in the mice over the study period, suggesting that this technique is appropriate for future studies of this type.
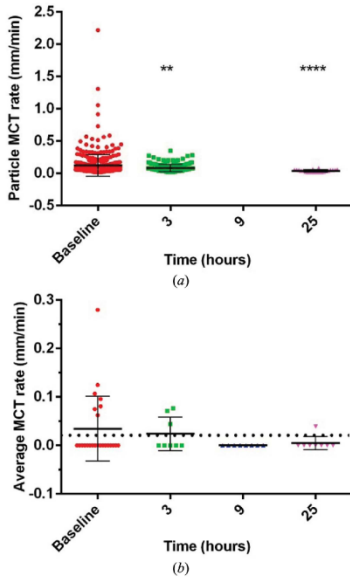
Figure 2

Characteristics of moving particles. (*a*) MCT rate of all detected moving particles at each timepoint. Note that no moving particles were detected at 9 h. The MCT rate at 3 and 25 h was significantly reduced compared with baseline. **p < 0.01, ****p < 0.0001, Kruskal-Wallis One-way ANOVA with Dunn's multiple comparisons. (*b*) Average MCT rate for each animal across the study period. The limit of detection is marked with a dotted line.

Our results showed that the particle MCT rate decreases over time and that the number of particles present in the imaging region also decreases with time. Together this suggests that particle clearance continues to occur throughout the study period, but the particles remaining at the later timepoints take longer to clear because they are moving more slowly. This is consistent with the two-phase clearance process previously described (Falk *et al.*, 1999; Hofmann & Asgharian, 2003; Moller *et al.*, 2004). The lead dust used in this experiment had heterogeneous shape and surface characteristics, so it is possible that the particles that remained at the later timepoints may have been more tightly bound to surface mucus or trapped within the epithelial cell layer (Donnelley *et al.*, 2010).

The number of particles present at baseline also varied substantially between animals, suggesting that the Dry Powder Insufflator™ does not deliver a uniform quantity of dry particles despite being loaded in a similar manner prior to each actuation. The ability to accurately deliver small quantities of particles to the airways is desirable for this type of experiment; however, to account for this variability we calculated the proportion of particles present at the repeat timepoints compared with baseline (Fig. 4). This analysis
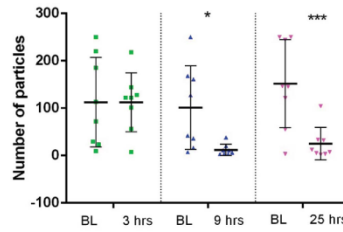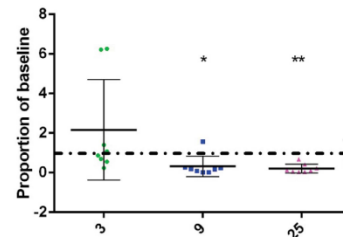

Figure 3

Total number of particles at each timepoint (moving and stationary). The total number of particles present at 9 and 25 h was significantly reduced compared with baseline (BL). There was no significant difference at 3 h. *p < 0.05, ***p < 0.001 RM-ANOVA with Sidak's multiple comparisons.

showed that in some animals there were larger numbers of particles present in the trachea at the 3 and 9 h timepoints than at baseline, suggesting that clearance from the more distal conducting airways and alveoli was occurring. This was not the case at 25 h, and may suggest that the most mobile particles are all cleared within this time.

This study had a number of limitations. Firstly, although the radiation produced no detectable physiological effects, it may have been sufficient to produce transient radiation damage to the trachea and surrounding tissue, altering the MCT behaviour that we sought to measure. More complex studies should be performed in the future to elucidate this effect. Secondly, the number of particles delivered was both small and inconsistent, and the particles themselves varied in size, shape and surface properties. These factors would all influence the MCT rate of every recorded particle. We have already initiated studies using more uniformly sized and shaped particles to minimize this effect. Thirdly, during imaging the animals breathed dry imaging hutch air provided by the ventilator and this may have reduced the baseline MCT rate and subsequent clearance behaviour compared with air that is normally humidified by transit through the mouse nasal airways.

The timepoints chosen were limited by the two days of available beam time at the SPring-8 synchrotron. In future

Figure 4

Proportion of particles (moving and stationary) at each repeat imaging point, compared with baseline. Significantly less particles remained at 9 (*p < 0.05) and 25 h (**p < 0.01) compared with at 3 h. Kruskal-Wallis One-way ANOVA with Dunn's multiple comparisons.

150

research papers

studies we plan to use larger groups of mice with more time-points extending for longer periods to more thoroughly examine how MCT occurs over time. Furthermore, we plan to also test common clinical rehydrating treatments for CF, such as hypertonic saline and mannitol, to determine how they affect the long-term clearance of particulates.

In summary, these studies have shown that it is now possible to perform repeat synchrotron X-ray imaging studies. The ability to perform repeat-imaging experiments may have applications in further understanding the physiological and physical basis of inhaled particle clearance and testing the efficacy of pharmaceuticals designed to improve MCT.

References

Boucher, R. C. (2004). *Eur. Respir. J.* **23**, 146–158.
Chodhari, R., Mitchison, H. M. & Meeks, M. (2004). *Paediatr. Respir. Rev.* **5**, 69–76.
Cloetens, P., Barrett, R., Baruchel, J., Guigay, J. P. & Schlenker, M. (1996). *J. Phys. D*, **29**, 133–146.
Coan, P., Wagner, A., Bravin, A., Diemoz, P. C., Keyriläinen, J. & Mollenhauer, J. (2010). *Phys. Med. Biol.* **55**, 7649–7662.
Donaldson, S. H., Corcoran, T. E., Laube, B. L. & Bennett, W. D. (2007). *Proc. Am. Thorac. Soc.* **4**, 399–405.
Donnelley, M., Morgan, K. S., Fouras, A., Skinner, W., Uesugi, K., Yagi, N., Siu, K. K. W. & Parsons, D. W. (2009). *J. Synchrotron Rad.* **16**, 553–561.
Donnelley, M., Morgan, K. S., Siu, K. K., Farrow, N. R., Stahr, C. S., Boucher, R. C., Fouras, A. & Parsons, D. W. (2014). *Sci. Rep.* **4**, 3689.
Donnelley, M., Morgan, K. S., Siu, K. K. W. & Parsons, D. W. (2012). *J. Synchrotron Rad.* **19**, 551–558.
Donnelley, M., Siu, K. K. W., Morgan, K. S., Skinner, W., Suzuki, Y., Takeuchi, A., Uesugi, K., Yagi, N. & Parsons, D. W. (2010). *J. Synchrotron Rad.* **17**, 719–729.
Falk, R., Philipson, K., Svartengren, M., Bergmann, R., Hofmann, W., Jarvis, N., Bailey, M. & Camner, P. (1999). *Exp. Lung Res.* **25**, 495–516.
Grubb, B. R., Jones, J. H. & Boucher, R. C. (2004). *Am. J. Physiol. Lung Cell. Mol. Physiol.* **286**, L588–L595.
Hofmann, W. & Asgharian, B. (2003). *Toxicol. Sci.* **73**, 448–456.
Hua, X. Y., Zeman, K. L., Zhou, B. Q., Hua, Q. Q., Senior, B. A., Tilley, S. L. & Bennett, W. D. (2010). *J. Appl. Physiol.* **108**, 189–196.
Livraghi, A. & Randell, S. H. (2007). *Toxicol. Pathol.* **35**, 116–129.
Moller, W., Haussinger, K., Winkler-Heil, R., Stahlhofen, W., Meyer, T., Hofmann, W. & Heyder, J. (2004). *J. Appl. Physiol.* **97**, 2200–2206.
Snigirev, A., Snigireva, I., Kohn, V., Kuznetsov, S. & Schelokov, I. (1995). *Rev. Sci. Instrum.* **66**, 5486.
Wilkins, S. W., Gureyev, T. E., Gao, D., Pogany, A. & Stevenson, A. W. (1996). *Nature (London)*, **384**, 335–338.

Statement of Authorship

Title of Paper	Non-invasive airway health assessment: Synchrotron imaging reveals effects of rehydrating treatments on mucociliary transit in-vivo
Publication Status	⊗ Published, ○ Accepted for Publication, ○ Submitted for Publication, ○ Publication style
Publication Details	M. Donnelley, K. Morgan, K. Siu, N. Farrow, C. Stahr, R. Boucher, A. Fouras, D. Parsons, Non-invasive airway health assessment: Synchrotron imaging reveals effects of rehydrating treatments on mucociliary transit in-vivo, Scientific Reports, vol. 4 (3689), 2014

Author Contributions

By signing the Statement of Authorship, each author certifies that their stated contribution to the publication is accurate and that permission is granted for the publication to be included in the candidate's thesis.

Name of Principal Author (Candidate)	Martin Donnelley		
Contribution to the Paper	Experiment design Performed experiments Data analysis Paper writing		
Signature		Date	23/1/15

Name of Co-Author	Kaye Morgan		
Contribution to the Paper	Performed experiments Paper writing		
Signature		Date	23/1/15

Name of Co-Author	Karen Siu		
Contribution to the Paper	Assisted with experiments Provided synchrotron related advice		
Signature		Date	23/1/15

Name of Co-Author	Nigel Farrow		
Contribution to the Paper	Performed all animal work at SPring-8 in Japan Paper writing		
Signature		Date	23/1/15

Statement of Authorship

Title of Paper	Non-invasive airway health assessment: Synchrotron imaging reveals effects of rehydrating treatments on mucociliary transit in-vivo
Publication Status	⊗ Published, ○ Accepted for Publication, ○ Submitted for Publication, ○ Publication style
Publication Details	M. Donnelley, K. Morgan, K. Siu, N. Farrow, C. Stahr, R. Boucher, A. Fouras, D. Parsons, Non-invasive airway health assessment: Synchrotron imaging reveals effects of rehydrating treatments on mucociliary transit in-vivo, Scientific Reports, vol. 4 (3689), 2014

Author Contributions

By signing the Statement of Authorship, each author certifies that their stated contribution to the publication is accurate and that permission is granted for the publication to be included in the candidate's thesis.

Name of Principal Author (Candidate)	Charlene Stahr		
Contribution to the Paper	Assisted with animal experiments		
Signature		Date	23/1/15

Name of Co-Author	Richard Boucher		
Contribution to the Paper	Provided expert CF-related biological advice Paper writing		
Signature		Date	23/1/15

Name of Co-Author	Andreas Fouras		
Contribution to the Paper	Provided technical advice		
Signature		Date	23/1/15

Name of Co-Author	David Parsons		
Contribution to the Paper	Experiment design Assisted with experiments Paper writing		
Signature		Date	23/1/15

8.2.6 Non-invasive health assessment: Synchrotron imaging reveals effects of rehydrating treatments on mucociliary transit in-vivo.

SCIENTIFIC REPORTS

Non-invasive airway health assessment: Synchrotron imaging reveals effects of rehydrating treatments on mucociliary transit in-vivo

Martin Donnelley[1,2,3], Kaye S. Morgan[4], Karen K. W. Siu[4,5,6], Nigel R. Farrow[1,2,3], Charlene S. Stahr[7], Richard C. Boucher[8], Andreas Fouras[7] & David W. Parsons[1,2,3]

[1]Respiratory and Sleep Medicine, Women's and Children's Hospital, 72 King William Road, North Adelaide, SA, 5006, Australia, [2]Centre for Stem Cell Research, University of Adelaide, SA, 5001, Australia, [3]School of Paediatrics and Reproductive Health, University of Adelaide, SA, 5001, Australia, [4]School of Physics, Monash University, Clayton, Vic, 3800, Australia, [5]Monash Biomedical Imaging, Monash University, Clayton, Vic, 3800, Australia, [6]Imaging and Medical Beamline, Australian Synchrotron, Clayton, Vic, 3800, Australia, [7]Mechanical and Aerospace Engineering, Monash University, Clayton, Vic, 3800, Australia, [8]CF/Pulmonary Research & Treatment Center, The University of North Carolina at Chapel Hill, Chapel Hill, North Carolina, USA.

To determine the efficacy of potential cystic fibrosis (CF) therapies we have developed a novel mucociliary transit (MCT) measurement that uses synchrotron phase contrast X-ray imaging (PCXI) to non-invasively measure the transit rate of individual micron-sized particles deposited into the airways of live mice. The aim of this study was to image changes in MCT produced by a rehydrating treatment based on hypertonic saline (HS), a current CF clinical treatment. Live mice received HS containing a long acting epithelial sodium channel blocker (P308); isotonic saline; or no treatment, using a nebuliser integrated within a small-animal ventilator circuit. Marker particle motion was tracked for 20 minutes using PCXI. There were statistically significant increases in MCT in the isotonic and HS-P308 groups. The ability to quantify *in vivo* changes in MCT may have utility in pre-clinical research studies designed to bring new genetic and pharmaceutical treatments for respiratory diseases into clinical trials.

Mucociliary transport (MCT) requires the coordinated beating of cilia, microscopic hair-like structures, to propel the airway surface liquid (ASL) across the surfaces of epithelial cells. This integrated activity provides the primary method for removing deposited pathogens and particulates from airway surfaces. In cystic fibrosis (CF), a dysfunctional CF transmembrane conductance regulator (CFTR) ion channel in airway epithelial cells results in dehydration of the ASL and impaired MCT. The MCT failure produces retention of inhaled pathogens and particulates, mucus obstruction, chronic infection, and eventually lung failure[1]. Current clinical assessments of CF airway disease and its treatment are indirect. A logical method to assess the effect of CF treatments on airway surfaces is to directly measure restoration of MCT activity by tracking the movement of deposited marker particles along the airways. The ability to directly visualise deposited particle MCT behaviour in live animal model airways could provide spatio-temporal information pertaining to the initiation and maintenance of CF pathophysiology and potentially reveal novel directions for the development of preventative therapies for CF airway disease.

To determine the efficacy of genetic[2,3] and other potential therapies for CF airway disease in animal models, with a view to ultimate use in humans, we have developed a novel MCT monitoring method based on measuring the transit rate and behaviour of individual particles deposited in the lungs using synchrotron phase contrast X-ray imaging (PCXI). This technique can be used *in vivo* in live anaesthetised mice[4-6]. By comparison, conventional *in vivo* MCT measurement methods rely on measuring bulk particle clearance from the airways[7-10], are unable to track the motion of *individual* micron sized deposited particles with high spatial or temporal resolution, and cannot be used to assess spatial or temporal variations in MCT homogeneity within the airways.

An alternative method to accurately track individual particle MCT involves the use of an *ex vivo* system. A recent study examined the transit of individual deposited particles of dried ink in an *ex vivo* porcine system, and determined that MCT on untreated airways was ~4 mm/min and varied with treatment[11]. Similarly, Ballard et al.[12]

154

showed that treatment with hypertonic saline restored MCT in only half of the *ex vivo* porcine tracheas they tested, but that surface active substances provided additional benefits in restoration of MCT. However, the obvious limitation of these systems is the requirement for tissue excision and support in an artificial environment. We propose that direct, non-invasive visualisation of individual deposited particle MCT in live intact animal-model airways should: (1) improve our understanding of airway health and disease and (2) allow the effects of therapeutic agents on MCT to be rapidly and accurately quantified.

PCXI can produce enhanced soft tissue contrast even when the absorption differences are small by utilising X-ray refraction in addition to conventional absorption. Provided the X-ray beam is spatially coherent, increasing the sample to detector distance[13–15] enhances tissue boundaries due to the phase changes that are induced by differences in the tissue X-ray refractive indices. We have reported on the benefits of PCXI for non-invasive airspace imaging in small animals[16], for non-invasive particulate detection in live mouse airways[4–6,17], and for the visualisation and assessment of surrogate fluid dosing regimes for airway gene therapy treatments in live mice[18,19]. Our previous studies also examined the MCT behaviour of a range of common pollutant particles delivered to the airways in either a saline carrier fluid[5,6] or as a dry powder[4]. These studies revealed that deposited lead dust, typically ranging from 5 μm up to 12 μm diameter and with a small number of larger particles present (see Figure 3 in Donnelley, Siu, et al.[5]), was a suitable marker for analysing tracheal MCT behaviour via PCXI. Furthermore, this technique also permits long-term repeated-measure study designs to assess treatments without animal sacrifice.

The aims of this study were to non-invasively observe the basal surface mucus transport activity of live mouse airways, at micron resolution, and to image and quantify changes in particle MCT produced by a rehydrating treatment for CF airways disease, i.e. inhaled hypertonic saline (HS) combined with a long acting epithelial sodium channel (ENaC) blocker (P308). HS acutely increases MCT in both CF and normal patients by directly increasing the osmotic load on the airway surface and triggering a water flux onto the airway surface. In CF this response can help rehydrate the airway surface and improve airway clearance[20]. The ENaC channel is upregulated in CF and further increases the ASL dehydration produced by the CFTR dysfunction, so any compound that inhibits the action of the ENaC channel should increase epithelial hydration. In this study the combined HS-P308 treatment was used to maximise this rehydration effect, thereby producing a large change in MCT. Although the effects of rehydrating treatments such as HS on MCT have previously been observed in excised sections of airway epithelium[12], they have never been examined or quantified in intact airways *in vivo*.

Results

Experiments were performed at the SPring-8 synchrotron radiation facility in Japan. Lead marker particles were delivered to the airways of live anaesthetized and intubated mice, prior to PCXI. Mice (n = 5 per group) were randomly assigned to a no treatment control group, an isotonic saline aerosol control group, or the HS-P308 aerosol treatment group. Images were captured prior to, during and after aerosol delivery, and all particle movement was tracked to determine the MCT rate.

Assessment of the MCT rate of a large number of particles was chosen as a reliable indicator of the immediate effectiveness of isotonic saline or HS-P308 to alter airway MCT rates. For the 12 animals successfully studied (aerosol delivery failed in one animal from the isotonic group, and two from the HS-P308 group), the mean time between dry particle insufflation and initiation of the imaging run was 5 minutes. Deposited lead particles were immediately visible in the trachea of all animals when imaging began, but the majority were stationary for the first two imaging periods (i.e. during baseline, prior to aerosol delivery). The MCT rate rapidly increased within the aerosol delivery period. However, the particle transit was heterogeneous: that is, some particles did not move while others transited the field of view rapidly. In addition, as previously reported[4–6], many particles followed unpredictable and non-linear paths along the airway. An example of this motion is shown in Figure 3 and in the Supplementary Video.

A total of 11,743 individual particle MCT measurements were made for the 12 mice in the study. Figure 4 shows that the MCT rate was increased in the isotonic saline and HS-P308 treatment groups compared to the No Rx Control group at all post delivery time points. The MCT rate of the No Rx Control group was 0.27 ± 0.11 mm/min. Isotonic saline produced a more pronounced early (5.5 min) effect than HS-308, but the effect of HS-P308 was sustained and greater in magnitude at the later time points. Specifically, at the 5.5 min time-point the isotonic MCT rate was statistically higher than the HS-P308 group, whereas at the 13.5 min time-point the HS-P308 MCT
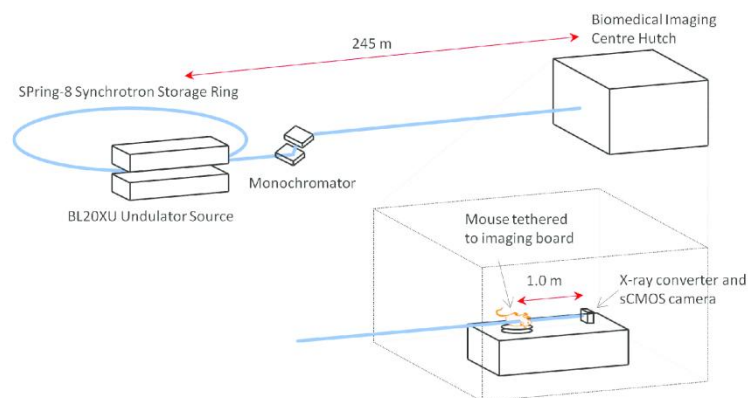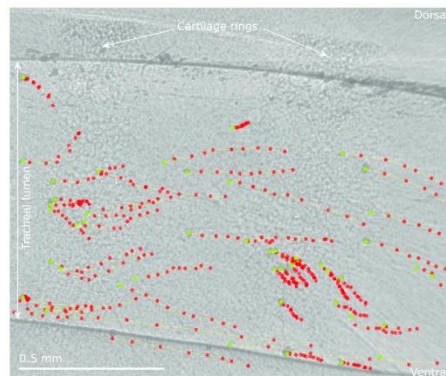

Figure 1 | The synchrotron *in vivo* PCXI setup. Mice are held supine on an x-y-rotation stage in the BL20XU imaging hutch, 245 m from the undulator X-ray source. A propagation distance of 1 m was used.
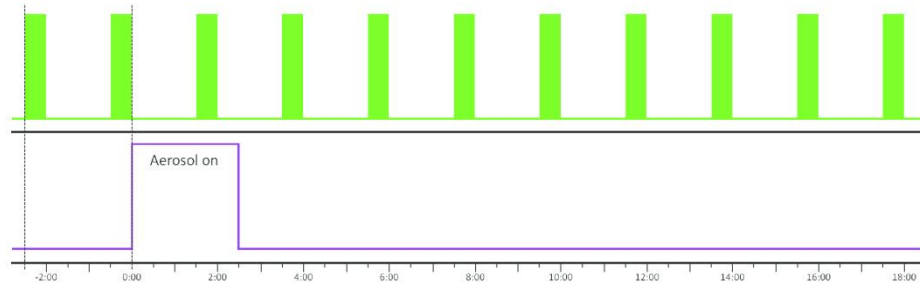
Figure 2 | The experimental imaging plan. Images were acquired in 30 second blocks (green bars, top panel) every two minutes at a rate of one image per breath (2 Hz). After two baseline imaging periods the aerosol (purple, lower panel) was delivered for 2.5 min. Imaging continued for a further ~18 minutes.

rate was significantly higher than the isotonic group. A total of 335 particles (i.e. <3% of the total number of particles tracked) were excluded from the analysis based on the chosen maximum-speed criteria, with a significantly greater number of particles excluded from the HS-P308 group than the isotonic group (P < 0.05, unpaired t-test). These results show that delivery of aerosolised fluid increased the MCT rate compared to control/baseline, regardless of the tonicity of the fluid. However, the initiation and duration of MCT effects after aerosol treatment differed with treatment.

The complex airway surface MCT particle movements are difficult to adequately describe and difficult to represent in static images (See Fig. 3), so the Supplementary Video should be viewed to reveal the nature of particle movements and to enable dynamic visual comparison of the effects of the isotonic saline and HS-P308 aerosols with the control group. The rapid onset of the effects of isotonic saline and the durable effect of HS-P308 are clearly visible in this comparison

video. Note that in these X-ray image sequences all particle activities on both (lateral) tracheal walls are superimposed, so it is not possible to determine which tracheal wall surface (i.e. the near or the far wall) the particulates are located on. In addition, some particulates and particulate motion appears to be located below the apparent tracheal edge. As previously reported[4], this phenomenon is due to the ω shaped dorsal wall of the trachea formed by an epithelial protrusion in the dorsal surface of the trachea into the lumen.

Discussion

This study has demonstrated that aerosolised fluid increased the mean MCT rate of individual particles deposited onto the tracheal airway surface compared to a control group, and that HS-P308, a CF airway-hydrating therapy, produced a more sustained increase in MCT rate compared to isotonic saline. Importantly, these findings show for the first time that it is possible to directly compare the effects of pharmaceutical treatments on individual particle MCT in mice *in vivo*.

The basal rates of transit measured in this study were lower than those reported by Grubb *et al.*[7] who used a dye-transit technique and reported that bulk mouse tracheal MCT was 2.2 ± 0.45 (SE) mm/min. Via comparisons to other studies, Grubb *et al.* also noted that the recorded MCT rate was heavily influenced by the marker size/type used. The lead particles used in the present study may be
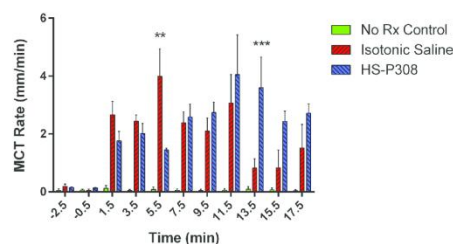

Figure 3 | Typical PCXI image showing the result from manual particle tracking at one imaging period. The mouse is supine with the lungs to the left and the mouth to the right; MCT is primarily in a left-to-right direction. The first frame (marked in green) from a sequence of 10 is shown with the location of tracked particles in the following frames marked with a red dot. Note that particle motion is not homogeneous; some particles move long distances, some short distances, and some (unmarked, primarily along the dorsal tracheal surface) remain stationary over those 10 frames.

Figure 4 | Effect of therapeutics on MCT. The MCT rate was calculated by manually tracking the movement of up to 50 particles across 10 frames at each time point in each mouse. MCT rates are presented as mean and standard error of the mean ($\overline{X} \pm SE$). Statistical significance was set at p = 0.05 and power = 0.80 and MCT rates were analysed by two way RM-ANOVA with Bonferroni multiple comparisons. The difference in MCT rate between the Isotonic and HS-P308 group at the 5.5 and 13.5 min time points was statistically significant (**p < 0.01 and *** p < 0.001).

156

handled by the MCT system in a different manner to either fluorescent dyes[7] or ink particles[11], both of which are much smaller and lighter. However, in a previous lead marker particle study we recorded a tracheal MCT rate of 1.82 ± 1.6 mm/min[4], a rate that was substantially higher than what we recorded in this study. We hypothesise that the absence of an inspiratory humidification system in this study may have resulted in dehydration of the airway surface by the dry imaging hutch air used to ventilate the animals, resulting in slower baseline and control MCT rates.

The effects of isotonic saline on accelerating MCT were rapid, i.e., peaked at 5.5 min, but were short-lived. We speculate that the initial, rapid effect was mediated by rehydrating the ventilator-induced dehydrated airway surface, with restoration of MCT. However, the effect of isotonic saline was relatively short lived because the added volume was rapidly absorbed by the epithelium by an ENaC mediated Na+ absorption mechanism[21,22]. In contrast, the effect of HS-P308 on MCT exhibited the opposite pattern, i.e., a moderate early effect (5.5 min) with a more robust delayed (15.5 min) response. Two possible explanations could account for the moderation of the early response. First, it has been reported that amiloride blocks aquaporin mediated transepithelial water flow in response to imposed osmotic gradients[23]. However, the newer and more highly potent ENaC blockers, such as P308, do not appear to exhibit an aquaporin block activity[24]. Second, it has been reported that rapid delivery of HS can overwhelm the ability of transepithelial water flow to buffer ASL hypertonicity following rapid aerosolization of HS[25]. The consequence is loss of water from epithelial cells into the lumen, cell shrinkage, reduction in cilial beat frequency, and slowed MCT. Although we favour the latter explanation, studies of HS vs. P308 alone will be required to rigorously test this possibility. With respect to the larger "delayed" increase in MCT following HS-P308 vs. isotonic saline, it is likely the extended duration reflects the block of ENaC mediated absorption of the salt deposited on aerosol surfaces via aerosolization. Thus, the liquid added to the tracheal surface added in response to aerosolized HS-P308 remained on the tracheal surface for prolonged periods.

Our study provides unique details into the mode of clearance of particles from the trachea. As seen in the Supplementary Movie, particles in the aerosol treated groups continually moved up from deeper in the lungs, into the trachea, suggesting that the insufflation technique dosed lung regions distal to the delivery site. Although we observed particle movement throughout the imaging period, the particulates were not expected to be completely cleared from the imaged airway region over this short imaging period. However, as noted above, the data shows that an aerosol treatment can increase the particle clearance rate when compared to baseline. In all animals, there were particles that remained immobile, likely due to their capture within the periciliary layer and/or persistent adherent mucus. This finding shows that changes in MCT activity produced by rehydration are heterogeneous and that rehydration of adherent mucus may not be rapid. The failure to mobilize all particles suggests that studies must be directed towards understanding this phenomena and how to address it therapeutically. Conversely, there were many particles that moved much more rapidly throughout the imaging period, with a maximum particle MCT rate of 140 mm/min recorded. These high rates typically resulted from cough-like respiratory movements (as suggested by transient spikes in airway pressure; data not shown), or rapid bulk fluid movements, and so were excluded from the statistical analyses.

This study had several limitations. The primary limitation was the small number of mice in the aerosol treatment groups, a direct result of the limited beam-time allocation (a total of 48 hours including experimental setup) available at the SPring-8 synchrotron. In future studies, the effects of MCT altering therapeutics in larger groups of mice, including distinguishing the effects of HS alone (since HS is already used as a CF clinical treatment) from the P308 ENaC blocker

will be studied. Similarly, the effects of using a humidification chamber in the ventilator inspiratory line on the measured MCT will also be quantified. Tracking particles for extended periods (longer than 20 minutes) should also further distinguish the effects of HS and P308. Future studies may also use tracking particles with improved characteristics. The relatively large size of lead particles and the lack of particle surface uniformity likely affected the MCT rates observed. However, the marker particles must be of the appropriate size and X-ray density to be detectable *in vivo* by PCXI, and a dispersion of sizes may mimic real environmental exposures. Finally, it is also possible that the requirement for manual tracking of the deposited particles resulted in observer bias. We minimised this effect by blinding the observer to the treatments. However, we have begun to develop new visual analytical techniques to better address this particle tracking issue.

In summary, this study has shown that the effects of therapeutics thought to restore the MCT rate can be directly quantified using synchrotron PCXI. Moreover, this technique can be readily applied to assessing MCT at any appropriate time-point within lung clearance studies, to test the effects of a variety of pharmaceutical treatments in appropriate mouse model strains. We are continuing our efforts to improve our direct and non-invasive MCT imaging assessment methods to assist our understanding and treatment of respiratory diseases such as CF.

Methods

Ethics statement. Experiments were performed on the BL20XU undulator beamline at the SPring-8 synchrotron radiation facility in Japan, under approvals from the Animal Ethics Committees of SPring-8, the Women's and Children's Health Network, and the University of Adelaide.

Imaging setup. The experimental hutch was located in the Biomedical Imaging Centre, 245 metres from the storage ring (see Fig. 1). Monochromatic 25 keV ($\lambda = 0.5$Å) X-rays were selected using a standard double-crystal monochromator[26]. A propagation (sample to detector) distance of ~1 m was used as in previous experiments[4]. Images were captured using a high-resolution X-ray converter (SPring-8 BM3) with a sCMOS detector. The converter used a 10 µm thick scintillator (Lu_2SiO_5:Ce) to convert X-rays to visible light, which was then directed to the sCMOS sensor using a ×10 microscope objective lens (NA 0.45). The sCMOS detector was a pco.edge (PCO Imaging) with an array size of 2560 × 2160 pixels and a 6.5 × 6.5 µm native pixel size. This setup resulted in an effective isotropic pixel size of 0.56 µm and a field of view of 1.43 mm × 1.2 mm. The incident beam was limited to this size using slits to reduce the radiation dose to the animals. Image capture was synchronised with a fast shutter (Uniblitz XRS6 with VMM-T1 timer unit) and triggered by the ventilator (refer to animal preparation description below) to minimise the dose between exposures. An exposure length of 10 ms was optimal for producing a high SNR without movement blur.

Animal preparation. Mice (n = 15, C57Bl/6, weight ~18–20 grams) were prepared as for previous experiments[27]. Briefly, mice were anaesthetized with pentobarbital (Somnopentil, Pitman-Moore, Washington Crossing, USA; 100 mg/kg i.p.) and intubated using a fibre-optic illuminated guide wire and a 20 Ga i.v. catheter (Insyte, Becton Dickinson, Utah, USA) as an endotracheal (ET) tube[28]. The ET tube was inserted into the trachea to a fixed depth of 22.5 mm from the nose tip. This location placed the ET tube tip approximately half way between the epiglottis and the carina to avoid physically perturbing the more distal imaging region. The fur around the imaging area was removed using surgical clippers (CareFusion, San Diego, USA; Neuro blade) followed by depilatory cream (Nair, Church & Dwight, Australia). After intubation a small quantity (less than 0.001 g) of lead dust was delivered to the trachea and lungs using a Dry Powder Insufflator™ Model DP-4M (Penn-Century, Wyndmoor, PA, USA). The particle size distribution was as previously described[4]. Due to high variability in the output (particle mass) of the first actuation of the air pump, the first output was discarded and the second actuation was used to deliver the sample to the airways. The insufflator was thoroughly cleaned with compressed air between deliveries to remove any residual particles prior to reloading.

Mice were tethered to an imaging board with their dorsal incisors hooked over a stainless-steel wire loop and the limbs, and their shoulders and torso were taped to the board to minimise body movements that interfere with high-resolution imaging. The imaging board was mounted on the hutch sample stage so that the mouse was oriented supine and the X-ray beam passed laterally through the mouse trachea, approximately five cartilage rings distal to the tip of the ET tube. Anaesthesia was maintained throughout the experiment by constant pentobarbital infusion (0.1 mg/kg/sec) via an indwelling i.p. needle attached to a micro-syringe pump (UltraMicroPump III and Micro4 controller, World Precision Instruments, Florida, USA). The ET tube was attached to a flexiVent small animal ventilator (SCIREQ, Montreal, Canada), and ventilation was set at 120 breaths/min, a tidal volume of

15 ml/kg (minute ventilation of approximately 1.8 ml/g), and ~3 cmH$_2$O of PEEP. The flexiVent provided a trigger to capture a single image during each end-expiratory pause. Body temperature was maintained using an infrared heat lamp.

Aerosol treatment and imaging. Mice were randomly assigned to one of three groups; a no treatment control group (No Rx Control, n = 5); an isotonic saline control group (n = 4); or the treatment group (n = 3). Mice in the treatment group (HS-P308) received compound P308 (Parion Sciences, Durham, NC, USA), a potent and long acting epithelial sodium channel (ENaC) blocker, at a concentration of 1 mM, in 7% HS to produce the maximal rehydrating effect. One image was captured per breath (2 Hz) for a 30 second period every 2 min (see Fig. 2) to reduce radiation dose and maintain shutter performance. After two imaging periods were obtained to calculate the baseline MCT rate prior to treatment, the aerosol was delivered for 2.5 min using an Aeroneb nebuliser (Aerogen, Ireland) designed to produce a 4–6 µm volume median diameter aerosol. The Aeroneb was attached to the ventilator inspiratory line, and the flexiVent controlled aerosol delivery to occur at a 50% duty cycle during inspiration only. Imaging continued for a further ~20 minutes (a total of 11 time-points) before mice were humanely killed via Nembutal overdose without waking from anaesthesia.

Post experimental analyses. All images were flat-field and dark-current corrected (Matlab R2012b, The Mathworks, Natick, MA, USA). Changes in image brightness produced by the inherent instability of the X-ray beam (manifested primarily as flicker caused by rapid changes in the vertical position of the beam over time) were minimised using a flicker-reduction algorithm that normalised the intensity of each row of pixels in the image.

Individual particle MCT rates were quantified using a Matlab program that presented an observer with 10 frames (from one imaging period) over which particle motion was to be tracked. For the treatment groups the 10 frames were sequential (i.e. every breath). For the control group and all baseline measurements every fifth frame was used to improve tracking accuracy at slow particle MCT rates. The observer was then asked to manually track the location of a chosen particle in each of those 10 frames. The 10 frame sequence was then presented again, this time with the location of the previously tracked particle(s) shown, and the observer was asked to track another particle. This process was repeated until a maximum of 50 particles were tracked, or no further moving particles could be identified in the sequence. The analysis then proceeded to the next imaging period (see Fig. 2), until all 11 periods were analysed. This whole analysis was repeated for each animal, with the observer blinded to any information that would identify the treatment that an animal had received, thereby preventing observer bias.

The distance that each particle moved between each of the 10 frames was calculated in pixels and converted to millimetres based on the size of the field of view. The MCT rate was then calculated (in mm/min) based on the time between analysis frames. Particles moving faster than 15 mm/min (chosen based on previous studies[11,12]) were excluded from further analysis because these likely resulted from 'cough-like' movements or rapid bulk fluid movements. A mean MCT rate was calculated for each time-point in every animal. Statistical analyses were performed using GraphPad Prism 5. Data were tested for normality, statistical significance was set at p = 0.05 and power = 0.80 and MCT rates were analysed by two way RM-ANOVA with Bonferroni multiple comparisons. MCT rates are presented as mean and standard error of the mean ($\overline{X} \pm SE$).

Images were created to show the motion of tracked particles at each time-point. A supplementary movie file (.avi format) was also assembled from the processed post-deposition images to compare particulate behaviour on the tracheal airway surface in the three groups. The movie frame rate was set to 5× normal speed, was encoded using the Xvid codec and can be played using the free VLC Media Player (available at http://www.videolan.org/vlc/).

1. Boucher, R. C. New concepts of the pathogenesis of cystic fibrosis lung disease. *Eur Respir J* **23**, 146–158, doi:10.1183/09031936.03.00057003 (2004).
2. Stocker, A. *et al.* Single-dose lentiviral gene transfer for lifetime airway gene expression. *J Gene Med* **11**, 861–867, doi:10.1002/jgm.1368 (2009).
3. Limberis, M., Anson, D. S., Fuller, M. & Parsons, D. W. Recovery of airway cystic fibrosis transmembrane conductance regulator function in mice with cystic fibrosis after single-dose lentivirus-mediated gene transfer. *Hum Gene Ther* **13**, 2112–2112, doi:10.1089/10430340260355365 (2002).
4. Donnelley, M., Morgan, K., Siu, K. K. W. & Parsons, D. W. Dry deposition of pollutant and marker particles onto live mouse airway surfaces enhances monitoring of individual particle mucociliary transit behaviour. *J Synchrotron Radiat* **19**, 551–558, doi:10.1107/S0909049512018250 (2012).
5. Donnelley, M. *et al.* A new technique to examine individual particle and fibre deposition and transit on live mouse trachea. *J Synchrotron Radiat* **17**, 719–729, doi:10.1107/S0909049510028451 (2010).
6. Donnelley, M. *et al.* Real-time non-invasive detection of inhalable particulates delivered into live mouse airways. **16**, 553–561, doi:10.1107/S0909049509012618 (2009).
7. Grubb, B. R., Jones, J. H. & Boucher, R. C. Mucociliary transport determined by in vivo microdialysis in the airways of normal and CF mice. *Am J Physiol Lung Cell Mol Physiol* **286**, L588–595, doi:10.1152/ajplung.00302.2003 (2004).
8. Donaldson, S. H., Corcoran, T. E., Laube, B. L. & Bennett, W. D. Mucociliary clearance as an outcome measure for cystic fibrosis clinical research. *Proc Am Thorac Soc* **4**, 399–405, doi:10.1513/pats.200703-042BR (2007).
9. Livraghi, A. & Randell, S. H. Cystic fibrosis and other respiratory diseases of impaired mucus clearance. *Toxicologic pathology* **35**, 116–129, doi:10.1080/01926230601060025 (2007).
10. Hua, X. Y. *et al.* Noninvasive real-time measurement of nasal mucociliary clearance in mice by pinhole gamma scintigraphy. *J Appl Physiol* **108**, 189–196, doi:10.1152/japplphysiol.00669.2009 (2010).
11. Cooper, J. L., Quinton, P. M. & Ballard, S. T. Mucociliary transport in porcine trachea: differential effects of inhibiting chloride and bicarbonate secretion. *Am J Physiol Lung C* **304**, L184–L190, doi:10.1152/ajplung.00143.2012 (2013).
12. Ballard, S. T., Parker, J. C. & Hamm, C. R. Restoration of mucociliary transport in the fluid-depleted trachea by surface-active instillates. *Am J Resp Cell Mol* **34**, 500–504, doi:10.1165/rcmb.2005-0214OC (2006).
13. Snigirev, A., Snigireva, I., Kohn, V., Kuznetsov, S. & Schelokov, I. On the possibilities of x-ray phase contrast microimaging by coherent high-energy synchrotron radiation. *Rev Sci Instrum* **66**, 5486–5492, doi:10.1063/1.1146073 (1995).
14. Cloetens, P., Barrett, R., Baruchel, J., Guigay, J. P. & Schlenker, M. Phase objects in synchrotron radiation hard X-ray imaging. *J Phys D Appl Phys* **29**, 133–146, doi:10.1088/0022-3727/29/1/023 (1996).
15. Wilkins, S. W., Gureyev, T. E., Gao, D., Pogany, A. & Stevenson, A. W. Phase-contrast imaging using polychromatic hard X-rays. *Nature* **384**, 335–338, doi:10.1038/384335a0 (1996).
16. Parsons, D. W. *et al.* High-resolution visualization of airspace structures in intact mice via synchrotron phase-contrast X-ray imaging (PCXI). *J Anat* **213**, 217–227, doi:10.1111/j.1469-7580.2008.00950.x (2008).
17. Siu, K. K. W. *et al.* Phase contrast X-ray imaging for the non-invasive detection of airway surfaces and lumen characteristics in mouse models of airway disease. *Eur J Radiol* **68**, S22–S26, doi:10.1016/j.ejrad.2008.04.029 (2008).
18. Donnelley, M., Morgan, K., Siu, K. & Parsons, D. Variability of in vivo fluid dose distribution in mouse airways is visualized by high-speed synchrotron x-ray imaging. *J Aerosol Med Pulm D* **26**, 1–10, doi:10.1089/jamp.2012.1007 (2012).
19. Donnelley, M., Siu, K., Jamison, A. & Parsons, D. Synchrotron phase contrast X-ray imaging reveals fluid dosing dynamics in mouse airways. *Gene Ther* **19**, 8–14, doi:10.1038/gt.2011.80 (2012).
20. Robinson, M. *et al.* Effect of increasing doses of hypertonic saline on mucociliary clearance in patients with cystic fibrosis. *Thorax* **52**, 900–903, doi:10.1136/thx.52.10.900 (1997).
21. Button, B., Okada, S. F., Frederick, C. B., Thelin, W. R. & Boucher, R. C. Mechanosensitive ATP release maintains proper mucus hydration of airways. *Science signaling* **6**, ra46, doi:10.1126/scisignal.2003755 (2013).
22. Tarran, R., Trout, L., Donaldson, S. H. & Boucher, R. C. Soluble mediators, not cilia, determine airway surface liquid volume in normal and cystic fibrosis superficial airway epithelia. *The Journal of general physiology* **127**, 591–604, doi:10.1085/jgp.200509468 (2006).
23. Donaldson, S. H. *et al.* Mucus clearance and lung function in cystic fibrosis with hypertonic saline. *New Engl J Med* **354**, 241–250, doi:10.1056/Nejmoa043891 (2006).
24. Hirsh, A. J. *et al.* Pharmacological properties of N-(3,5-diamino-6-chloropyrazine-2-carbonyl)-N '-4-[4-(2,3-dihydroxypropoxy)phenyl]butyl-guanidine methanesulfonate (552-02), a novel epithelial sodium channel blocker with potential clinical efficacy for cystic fibrosis lung disease. *J Pharmacol Exp Ther* **325**, 77–88, doi:10.1124/jpet.107.130443 (2008).
25. JL, G. & B, B. An In Vitro Study of the Kinetics of Hypertonic Saline on ASL Height. *Pediatr Pulm* **45:S33**, 291.
26. Yabashi, M. *et al.* SPring-8 standard x-ray monochromators. *Proc. SPIE* **3773**, 2–13, doi:10.1117/12.370098 (1999).
27. Donnelley, M., Parsons, D., Morgan, K & Siu, K. Animals In Synchrotrons: Overcoming Challenges For High-Resolution, Live, Small-Animal Imaging. *AIP Conf Proc* **1266**, doi:10.1063/1.3478192 (2010).
28. Hamacher, J. *et al.* Microscopic wire guide-based orotracheal mouse intubation: description, evaluation and comparison with transillumination. *Lab Anim* **42**, 222–230, doi:10.1258/la.2007.006068 (2008).

158

Author contributions

M.D. and D.P. conceived and designed the experiments. M.D., K.M., K.S., N.F., C.S., A.F. and D.P. performed the experiments. M.D., R.B. and D.P. analysed the data and wrote the manuscript. All authors reviewed and edited the manuscript.

Additional information

Supplementary information accompanies this paper at http://www.nature.com/scientificreports

Competing financial interests: RCB is a co-founder and Chairman of the Board of Parion Sciences Inc. There are no other competing financial interests.

159

9 References

1. Amaral, M.D., *Processing of CFTR: traversing the cellular maze--how much CFTR needs to go through to avoid cystic fibrosis?* Pediatr Pulmonol, 2005. **39**(6): p. 479-91.
2. Fanconi G, U.E., Knauer C., *Das Coeliakie-syndrom bei angeborener zystischer Pankreasfibromatose und Bronchiektasien (Celiac syndrome with congenital cystic fibromatosis of the pancreas and bronchiectasis)* Wiener Medizinische Wochenschrift, 1936. **86**: p. 753-756.
3. Busch, R., *On the history of cystic fibrosis.* Acta Univ Carol Med (Praha), 1990. **36**(1-4): p. 13-5.
4. Schmidt, J.G., *Book of Folk Philosophy.* 1779.
5. Garrod, A.E.a.H., W. H, *Congenital familial steatorrhoea.* The Quarterly Journal of Medicine, 1912. **6**: p. 242-258.
6. Andersen, D.H., *Cystic fibrosis of the pancreas and its relation to celiac disease: a clinical and pathological study.* The American Journal of disease of children, 1938. **56**: p. 344-399.
7. Farber, S., *Some organic digestive disturbances in early life.* The Journal of the Michigan State medical Society., 1945. **44**(587-594).
8. Andersen, D.H.a.H., R. C, *Celiac syndrome V. Genetics of cystic fibrosis of the pancreas with consideration of the etiology.* The american Journal of Disease in Children, 1946. **72**: p. 62-80.
9. Kessler, W.R. and D.H. Andersen, *Heat prostration in fibrocystic disease of the pancreas and other conditions.* Pediatrics, 1951. **8**(5): p. 648-56.
10. Di Sant'Agnese, P.A., et al., *Abnormal electrolyte composition of sweat in cystic fibrosis of the pancreas; clinical significance and relationship to the disease.* Pediatrics, 1953. **12**(5): p. 549-63.
11. LeGrys, V.A. and R.W. Burnett, *Current status of sweat testing in North America. Results of the College of American Pathologists needs assessment survey.* Arch Pathol Lab Med, 1994. **118**(9): p. 865-7.
12. Zuelzer, W.W. and W.A. Newton, Jr., *The pathogenesis of fibrocystic disease of the pancreas; a study of 36 cases with special reference to the pulmonary lesions.* Pediatrics, 1949. **4**(1): p. 53-69.
13. Di, S.A.P.E. and D.H. Andersen, *Celiac syndrome; chemotherapy in infections of the respiratory tract associated with cystic fibrosis of the pancreas; observations with penicillin and drugs of the sulfonamide group, with special reference to penicillin aerosol.* Am J Dis Child, 1946. **72**: p. 17-61.
14. Stoppelman, M.R. and H. Shwachman, *Effect of antibiotic therapy on mucoviscidosis; a bacteriologic study.* N Engl J Med, 1954. **251**(19): p. 759-63.
15. West, J.R., S.M. Levin, and P.A. Di Sant'Agnese, *Pulmonary function in cystic fibrosis of the pancreas.* Pediatrics, 1954. **13**(2): p. 155-64.
16. Tsui, L.C., et al., *Cystic fibrosis locus defined by a genetically linked polymorphic DNA marker.* Science, 1985. **230**(4729): p. 1054-7.
17. Wainwright, B.J., et al., *Localization of cystic fibrosis locus to human chromosome 7cen-q22.* Nature, 1985. **318**(6044): p. 384-5.
18. Kerem, B., et al., *Identification of the cystic fibrosis gene: genetic analysis.* Science, 1989. **245**(4922): p. 1073-80.

19. Riordan, J.R., et al., *Identification of the cystic fibrosis gene: cloning and characterization of complementary DNA.* Science, 1989. **245**(4922): p. 1066-73.

20. Rommens, J.M., et al., *Identification of the cystic fibrosis gene: chromosome walking and jumping.* Science, 1989. **245**(4922): p. 1059-65.

21. Rowe, S.M., S. Miller, and E.J. Sorscher, *Cystic fibrosis.* N Engl J Med, 2005. **352**(19): p. 1992-2001.

22. Gregory, R.J., et al., *Expression and characterization of the cystic fibrosis transmembrane conductance regulator.* Nature, 1990. **347**(6291): p. 382-6.

23. Sheppard, D.N. and M.J. Welsh, *Structure and function of the CFTR chloride channel.* Physiol Rev, 1999. **79**(1 Suppl): p. S23-45.

24. Rosenstein, B.J. and P.L. Zeitlin, *Cystic fibrosis.* Lancet, 1998. **351**(9098): p. 277-82.

25. Boyle, M.P. and K. De Boeck, *A new era in the treatment of cystic fibrosis: correction of the underlying CFTR defect.* Lancet Respir Med, 2013. **1**(2): p. 158-63.

26. Dorwart, M., P. Thibodeau, and P. Thomas, *Cystic fibrosis: recent structural insights.* J Cyst Fibros, 2004. **3 Suppl 2**: p. 91-4.

27. Davies, J.C., D.M. Geddes, and E.W. Alton, *Gene therapy for cystic fibrosis.* J Gene Med, 2001. **3**(5): p. 409-17.

28. Orenstein, D., B. Rosenstein, and R. Stern, *Cystic Fibrosis Medical Care.* 2000, USA: Lippincott Williams & Wilkins.

29. De Braekeleer, M., et al., *Genotype-phenotype correlation in cystic fibrosis patients compound heterozygous for the A455E mutation.* Hum Genet, 1997. **101**(2): p. 208-11.

30. De Braekeleer, M., et al., *Genotype-phenotype correlation in five cystic fibrosis patients homozygous for the 621 + 1G-->T mutation.* J Med Genet, 1997. **34**(9): p. 788-9.

31. Quinton, P.M., *Too much salt, too little soda: cystic fibrosis.* Sheng Li Xue Bao, 2007. **59**(4): p. 397-415.

32. Tarran, R., et al., *The CF salt controversy: in vivo observations and therapeutic approaches.* Mol Cell, 2001. **8**(1): p. 149-58.

33. Hays, S.R. and J.V. Fahy, *Characterizing mucous cell remodeling in cystic fibrosis: relationship to neutrophils.* Am J Respir Crit Care Med, 2006. **174**(9): p. 1018-24.

34. Voynow, J.A., et al., *Neutrophil elastase increases MUC5AC mRNA and protein expression in respiratory epithelial cells.* Am J Physiol, 1999. **276**(5 Pt 1): p. L835-43.

35. Boucher, R.C., *An overview of the pathogenesis of cystic fibrosis lung disease.* Adv Drug Deliv Rev, 2002. **54**(11): p. 1359-71.

36. Bonvin, E., et al., *Congenital tracheal malformation in cystic fibrosis transmembrane conductance regulator-deficient mice.* J Physiol, 2008. **586**(13): p. 3231-43.

37. Wallace, H.L., et al., *Abnormal tracheal smooth muscle function in the CF mouse.* Physiological Reports, 2013. **1**(6): p. n/a-n/a.

38. Davies, J.C. and E.W. Alton, *Gene therapy for cystic fibrosis.* Proc Am Thorac Soc, 2010. **7**(6): p. 408-14.

39. Hansen, C.R., et al., *Long-term azitromycin treatment of cystic fibrosis patients with chronic Pseudomonas aeruginosa infection; an observational cohort study.* J Cyst Fibros, 2005. **4**(1): p. 35-40.

40. Eckford, P.D., et al., *Cystic fibrosis transmembrane conductance regulator (CFTR) potentiator VX-770 (ivacaftor) opens the defective channel gate of mutant CFTR in a phosphorylation-dependent but ATP-independent manner.* J Biol Chem, 2012. **287**(44): p. 36639-49.

41. Rowe, S.M. and A.S. Verkman, *Cystic fibrosis transmembrane regulator correctors and potentiators.* Cold Spring Harb Perspect Med, 2013. **3**(7).

42. Dalemans, W., et al., *Altered chloride ion channel kinetics associated with the delta F508 cystic fibrosis mutation.* Nature, 1991. **354**(6354): p. 526-8.

43. Denning, G.M., et al., *Processing of mutant cystic fibrosis transmembrane conductance regulator is temperature-sensitive.* Nature, 1992. **358**(6389): p. 761-4.

44. Du, K., M. Sharma, and G.L. Lukacs, *The DeltaF508 cystic fibrosis mutation impairs domain-domain interactions and arrests post-translational folding of CFTR.* Nat Struct Mol Biol, 2005. **12**(1): p. 17-25.

45. Lin, S., et al., *Identification of synergistic combinations of F508del cystic fibrosis transmembrane conductance regulator (CFTR) modulators.* Assay Drug Dev Technol, 2010. **8**(6): p. 669-84.

46. Kerr, W.G. and J.J. Mule, *Gene therapy: current status and future prospects.* J Leukoc Biol, 1994. **56**(2): p. 210-4.

47. Driskell, R.A. and J.F. Engelhardt, *Current status of gene therapy for inherited lung diseases.* Annu Rev Physiol, 2003. **65**: p. 585-612.

48. O'Connor, T.P. and R.G. Crystal, *Genetic medicines: treatment strategies for hereditary disorders.* Nat Rev Genet, 2006. **7**(4): p. 261-76.

49. Coutelle, C. and R. Williamson, *Liposomes and viruses for gene therapy of cystic fibrosis.* J Aerosol Med, 1996. **9**(1): p. 79-88.

50. Gao, X. and L. Huang, *Cationic liposome-mediated gene transfer.* Gene Ther, 1995. **2**(10): p. 710-22.

51. Avalosse, B., et al., *Method for concentrating and purifying recombinant autonomous parvovirus vectors designed for tumour-cell-targeted gene therapy.* J Virol Methods, 1996. **62**(2): p. 179-83.

52. Ziady, A.G. and P.B. Davis, *Current prospects for gene therapy of cystic fibrosis.* Curr Opin Pharmacol, 2006. **6**(5): p. 515-21.

53. Palu, G., R. Bonaguro, and A. Marcello, *In pursuit of new developments for gene therapy of human diseases.* J Biotechnol, 1999. **68**(1): p. 1-13.

54. Pickles, R.J., et al., *Limited entry of adenovirus vectors into well-differentiated airway epithelium is responsible for inefficient gene transfer.* J Virol, 1998. **72**(7): p. 6014-23.

55. Liu, X. and J.F. Engelhardt, *The glandular stem/progenitor cell niche in airway development and repair.* Proc Am Thorac Soc, 2008. **5**(6): p. 682-8.

56. Escors, D. and K. Breckpot, *Lentiviral vectors in gene therapy: their current status and future potential.* Arch Immunol Ther Exp (Warsz), 2010. **58**(2): p. 107-19.

57. Mann, R., R.C. Mulligan, and D. Baltimore, *Construction of a retrovirus packaging mutant and its use to produce helper-free defective retrovirus.* Cell, 1983. **33**(1): p. 153-9.

58. Ryser, M.F., et al., *Gene therapy for chronic granulomatous disease.* Expert Opin Biol Ther, 2007. **7**(12): p. 1799-809.

59. Kim, S.H., S. Kim, and P.D. Robbins, *Retroviral vectors.* Adv Virus Res, 2000. **55**: p. 545-63.

60. Bukrinsky, M.I., et al., *A nuclear localization signal within HIV-1 matrix protein*

that governs infection of non-dividing cells. Nature, 1993. **365**(6447): p. 666-9.

61. Gallay, P., et al., *HIV-1 infection of nondividing cells through the recognition of integrase by the importin/karyopherin pathway.* Proc Natl Acad Sci U S A, 1997. **94**(18): p. 9825-30.

62. Gallay, P., et al., *HIV-1 infection of nondividing cells: C-terminal tyrosine phosphorylation of the viral matrix protein is a key regulator.* Cell, 1995. **80**(3): p. 379-88.

63. Frankel, A.D. and J.A. Young, *HIV-1: fifteen proteins and an RNA.* Annu Rev Biochem, 1998. **67**: p. 1-25.

64. Freed, E.O., *HIV-1 replication.* Somat Cell Mol Genet, 2001. **26**(1-6): p. 13-33.

65. Landau, N.R., K.A. Page, and D.R. Littman, *Pseudotyping with human T-cell leukemia virus type I broadens the human immunodeficiency virus host range.* J Virol, 1991. **65**(1): p. 162-9.

66. Naldini, L., et al., *In vivo gene delivery and stable transduction of nondividing cells by a lentiviral vector.* Science, 1996. **272**(5259): p. 263-7.

67. Ramezani, A., T.S. Hawley, and R.G. Hawley, *Lentiviral vectors for enhanced gene expression in human hematopoietic cells.* Mol Ther, 2000. **2**(5): p. 458-69.

68. Zufferey, R., et al., *Multiply attenuated lentiviral vector achieves efficient gene delivery in vivo.* Nat Biotechnol, 1997. **15**(9): p. 871-5.

69. Dull, T., et al., *A third-generation lentivirus vector with a conditional packaging system.* J Virol, 1998. **72**(11): p. 8463-71.

70. Miyoshi, H., et al., *Development of a self-inactivating lentivirus vector.* J Virol, 1998. **72**(10): p. 8150-7.

71. Zufferey, R., et al., *Self-inactivating lentivirus vector for safe and efficient in vivo gene delivery.* J Virol, 1998. **72**(12): p. 9873-80.

72. Fuller, M. and D.S. Anson, *Helper plasmids for production of HIV-1-derived vectors.* Hum Gene Ther, 2001. **12**(17): p. 2081-93.

73. Koldej, R., et al., *Optimisation of a multipartite human immunodeficiency virus based vector system; control of virus infectivity and large-scale production.* J Gene Med, 2005. **7**(11): p. 1390-9.

74. Zufferey, R., et al., *Woodchuck hepatitis virus posttranscriptional regulatory element enhances expression of transgenes delivered by retroviral vectors.* J Virol, 1999. **73**(4): p. 2886-92.

75. Schlegel, R., et al., *Inhibition of VSV binding and infectivity by phosphatidylserine: is phosphatidylserine a VSV-binding site?* Cell, 1983. **32**(2): p. 639-46.

76. Hamaguchi, I., et al., *Lentivirus vector gene expression during ES cell-derived hematopoietic development in vitro.* J Virol, 2000. **74**(22): p. 10778-84.

77. May, C., et al., *Therapeutic haemoglobin synthesis in beta-thalassaemic mice expressing lentivirus-encoded human beta-globin.* Nature, 2000. **406**(6791): p. 82-6.

78. Till, J.E. and C.E. Mc, *A direct measurement of the radiation sensitivity of normal mouse bone marrow cells.* Radiat Res, 1961. **14**: p. 213-22.

79. Korbling, M. and Z. Estrov, *Adult stem cells for tissue repair - a new therapeutic concept?* N Engl J Med, 2003. **349**(6): p. 570-82.

80. Weissman, I.L., *Stem cells: units of development, units of regeneration, and units in evolution.* Cell, 2000. **100**(1): p. 157-68.

81. Weissman, I.L., D.J. Anderson, and F. Gage, *Stem and progenitor cells: origins,*

phenotypes, lineage commitments, and transdifferentiations. Annu Rev Cell Dev Biol, 2001. **17**: p. 387-403.

82. O'Dea, S. and D.J. Harrison, *CFTR gene transfer to lung epithelium--on the trail of a target cell.* Curr Gene Ther, 2002. **2**(2): p. 173-81.

83. Engelhardt, J.F., *Stem cell niches in the mouse airway.* Am J Respir Cell Mol Biol, 2001. **24**(6): p. 649-52.

84. Borthwick, D.W., et al., *Evidence for stem-cell niches in the tracheal epithelium.* Am J Respir Cell Mol Biol, 2001. **24**(6): p. 662-70.

85. Strebhardt, K. and A. Ullrich, *Paul Ehrlich's magic bullet concept: 100 years of progress.* Nat Rev Cancer, 2008. **8**(6): p. 473-80.

86. Rando, T.A., *Stem cells, ageing and the quest for immortality.* Nature, 2006. **441**(7097): p. 1080-6.

87. Stripp, B.R., *Hierarchical organization of lung progenitor cells: is there an adult lung tissue stem cell?* Proc Am Thorac Soc, 2008. **5**(6): p. 695-8.

88. Rawlins, E.L. and B.L. Hogan, *Epithelial stem cells of the lung: privileged few or opportunities for many?* Development, 2006. **133**(13): p. 2455-65.

89. Reynolds, S.D. and A.M. Malkinson, *Clara cell: progenitor for the bronchiolar epithelium.* Int J Biochem Cell Biol, 2010. **42**(1): p. 1-4.

90. Boers, J.E., A.W. Ambergen, and F.B. Thunnissen, *Number and proliferation of basal and parabasal cells in normal human airway epithelium.* Am J Respir Crit Care Med, 1998. **157**(6 Pt 1): p. 2000-6.

91. Ghosh, M., et al., *A Single Cell Functions as a Tissue-Specific Stem Cell and the In Vitro Niche-Forming Cell.* Am J Respir Cell Mol Biol, 2010.

92. Hong, K.U., et al., *Basal cells are a multipotent progenitor capable of renewing the bronchial epithelium.* Am J Pathol, 2004. **164**(2): p. 577-88.

93. Reynolds, S.D., et al., *Lung epithelial healing: a modified seed and soil concept.* Proc Am Thorac Soc, 2012. **9**(2): p. 27-37.

94. Ghosh, M., et al., *Context-Dependent Differentiation of Multipotential Keratin 14-Expressing Tracheal Basal Cells.* Am J Respir Cell Mol Biol, 2010.

95. Mitomo, K., et al., *Toward gene therapy for cystic fibrosis using a lentivirus pseudotyped with sendai virus envelopes.* Mol Ther. **18**(6): p. 1173-82.

96. Limberis, M., et al., *Recovery of airway cystic fibrosis transmembrane conductance regulator function in mice with cystic fibrosis after single-dose lentivirus-mediated gene transfer.* Hum Gene Ther, 2002. **13**(16): p. 1961-70.

97. Kremer, K.L., et al., *Gene delivery to airway epithelial cells in vivo: a direct comparison of apical and basolateral transduction strategies using pseudotyped lentivirus vectors.* J Gene Med, 2007. **9**(5): p. 362-8.

98. Stocker, A.G., et al., *Single-dose lentiviral gene transfer for lifetime airway gene expression.* J Gene Med, 2009. **11**(10): p. 861-7.

99. Cmielewski, P., D.S. Anson, and D.W. Parsons, *Lysophosphatidylcholine as an adjuvant for lentiviral vector mediated gene transfer to airway epithelium: effect of acyl chain length.* Respir Res, 2010. **11**: p. 84.

100. Farrow, N., et al., *Airway gene transfer in a non-human primate: Lentiviral gene expression in marmoset lungs.* Sci Rep, 2013. **3**: p. 4.

101. McQualter, J.L., et al., *Evidence of an epithelial stem/progenitor cell hierarchy in the adult mouse lung.* Proc Natl Acad Sci U S A, 2010. **107**(4): p. 1414-9.

102. Sinn, P.L., E.R. Burnight, and P.B. McCray, Jr., *Progress and prospects: prospects of repeated pulmonary administration of viral vectors.* Gene Ther, 2009. **16**(9): p. 1059-65.

103. Johnson, L.G., et al., *Pseudotyped human lentiviral vector-mediated gene transfer to airway epithelia in vivo.* Gene Ther, 2000. **7**(7): p. 568-74.

104. Ruoslahti, E., *RGD and other recognition sequences for integrins.* Annu Rev Cell Dev Biol, 1996. **12**: p. 697-715.

105. Morizono, K., et al., *Redirecting lentiviral vectors by insertion of integrin-tageting peptides into envelope proteins.* J Gene Med, 2009. **11**(7): p. 549-58.

106. Tagalakis, A.D., et al., *Integrin-targeted nanocomplexes for tumour specific delivery and therapy by systemic administration.* Biomaterials, 2011. **32**(5): p. 1370-6.

107. Leigh, M.W., et al., *Cell proliferation in bronchial epithelium and submucosal glands of cystic fibrosis patients.* Am J Respir Cell Mol Biol, 1995. **12**(6): p. 605-12.

108. Voynow, J.A., et al., *Basal-like cells constitute the proliferating cell population in cystic fibrosis airways.* American journal of respiratory and critical care medicine, 2005. **172**(8): p. 1013-8.

109. Ghosh, M., et al., *Context-dependent differentiation of multipotential keratin 14-expressing tracheal basal cells.* Am J Respir Cell Mol Biol, 2011. **45**(2): p. 403-10.

110. Rock, J.R., S.H. Randell, and B.L. Hogan, *Airway basal stem cells: a perspective on their roles in epithelial homeostasis and remodeling.* Dis Model Mech, 2010. **3**(9-10): p. 545-56.

111. Hilliard, T.N., et al., *Nasal abnormalities in cystic fibrosis mice independent of infection and inflammation.* Am J Respir Cell Mol Biol, 2008. **39**(1): p. 19-25.

112. Hajj, R., et al., *Human airway surface epithelial regeneration is delayed and abnormal in cystic fibrosis.* J Pathol, 2007. **211**(3): p. 340-50.

113. Danel, C., et al., *Quantitative assessment of the epithelial and inflammatory cell populations in large airways of normals and individuals with cystic fibrosis.* Am J Respir Crit Care Med, 1996. **153**(1): p. 362-8.

114. Snouwaert, J.N., et al., *An animal model for cystic fibrosis made by gene targeting.* Science, 1992. **257**(5073): p. 1083-8.

115. Zhou, L., et al., *Correction of lethal intestinal defect in a mouse model of cystic fibrosis by human CFTR.* Science, 1994. **266**(5191): p. 1705-8.

116. Mery, S., et al., *Nasal diagrams: a tool for recording the distribution of nasal lesions in rats and mice.* Toxicol Pathol, 1994. **22**(4): p. 353-72.

117. Grubb, B.R., R.N. Vick, and R.C. Boucher, *Hyperabsorption of Na+ and raised Ca(2+)-mediated Cl- secretion in nasal epithelia of CF mice.* Am J Physiol, 1994. **266**(5 Pt 1): p. C1478-83.

118. Grubb, B.R. and R.C. Boucher, *Pathophysiology of gene-targeted mouse models for cystic fibrosis.* Physiol Rev, 1999. **79**(1 Suppl): p. S193-214.

119. Hyde, S.C., et al., *Correction of the ion transport defect in cystic fibrosis transgenic mice by gene therapy.* Nature, 1993. **362**(6417): p. 250-5.

120. MacVinish, L.J., et al., *Normalization of ion transport in murine cystic fibrosis nasal epithelium using gene transfer.* Am J Physiol, 1997. **273**(2 Pt 1): p. C734-40.

121. Rogers, D.F., *Airway goblet cells: responsive and adaptable front-line defenders.* Eur Respir J, 1994. **7**(9): p. 1690-706.

122. Kreda, S.M., C.W. Davis, and M.C. Rose, *CFTR, mucins, and mucus obstruction in cystic fibrosis.* Cold Spring Harb Perspect Med, 2012. **2**(9): p. a009589.

123. Larson, J.E. and J.C. Cohen, *Developmental paradigm for early features of cystic fibrosis.* Pediatr Pulmonol, 2005. **40**(5): p. 371-7.

124. Mall, M., et al., *Increased airway epithelial Na+ absorption produces cystic fibrosis-like lung disease in mice.* Nat Med, 2004. **10**(5): p. 487-93.

125. Nakamura, H., et al., *Neutrophil elastase in respiratory epithelial lining fluid of individuals with cystic fibrosis induces interleukin-8 gene expression in a human bronchial epithelial cell line.* J Clin Invest, 1992. **89**(5): p. 1478-84.

126. Andersson, E.R., R. Sandberg, and U. Lendahl, *Notch signaling: simplicity in design, versatility in function.* Development, 2011. **138**(17): p. 3593-612.

127. Tsao, P.N., et al., *Notch signaling controls the balance of ciliated and secretory cell fates in developing airways.* Development, 2009. **136**(13): p. 2297-307.

128. Guseh, J.S., et al., *Notch signaling promotes airway mucous metaplasia and inhibits alveolar development.* Development, 2009. **136**(10): p. 1751-9.

129. Cmielewski, P., et al., *Transduction of ferret airway epithelia using a pre-treatment and lentiviral gene vector.* BMC Pulm Med, 2014. **14**(1): p. 183.

130. Farrow, N., et al., *Airway gene transfer in a non-human primate: lentiviral gene expression in marmoset lungs.* Sci Rep, 2013. **3**: p. 1287.

131. Sun, X., et al., *Disease phenotype of a ferret CFTR-knockout model of cystic fibrosis.* J Clin Invest, 2010. **120**(9): p. 3149-60.

132. Thomson, A. and A. Harris, *Cystic Fibrosis.* 4th edition ed. 2008, New York: Oxford University Press.

133. Goor, F., S. Hadida, and P. Grootenhuis, *Pharmacological rescue of mutant CFTR function for the treatment of cystic fibrosis*

Curr Top Med Chem, 2008. **3**(19).

134. Jackson, A.D., et al., *Validation and use of a parametric model for projecting cystic fibrosis survivorship beyond observed data: a birth cohort analysis.* Thorax, 2011. **66**(8): p. 674-9.

135. Potash, A.E., et al., *Adenoviral gene transfer corrects the ion transport defect in the sinus epithelia of a porcine CF model.* Mol Ther, 2013. **21**(5): p. 947-53.

136. Crystal, R.G., et al., *Administration of an adenovirus containing the human CFTR cDNA to the respiratory tract of individuals with cystic fibrosis.* Nat Genet, 1994. **8**(1): p. 42-51.

137. Liu, C., et al., *Lentiviral airway gene transfer in lungs of mice and sheep: successes and challenges.* J Gene Med, 2010. **12**(8): p. 647-58.

138. Wong, E.S., et al., *Correction of methylmalonic aciduria in vivo using a codon-optimized lentiviral vector.* Hum Gene Ther, 2014. **25**(6): p. 529-38.

139. Lloyd, M., *Health, Husbandry and Diseases.* 1st ed. 1999, Oxford: WileyBlackwell.

140. Gau, P., et al., *Air-assisted intranasal instillation enhances adenoviral delivery to the olfactory epithelium and respiratory tract.* Gene Ther, 2011. **18**(5): p. 432-6.

141. Nakata, M., T. Itou, and T. Sakai, *Quantitative analysis of inflammatory cytokines expression in peripheral blood mononuclear cells of the ferret (Mustela putorius furo) using real-time PCR.* Vet Immunol Immunopathol, 2009. **130**(1-2): p. 88-91.

142. Cao, H., et al., *Efficient gene delivery to pig airway epithelia and submucosal glands using helper-dependent adenoviral vectors.* Mol Ther Nucleic Acids,

2013. **2**: p. e127.

143. Koehler, D.R., et al., *Aerosol delivery of an enhanced helper-dependent adenovirus formulation to rabbit lung using an intratracheal catheter.* J Gene Med, 2005. **7**(11): p. 1409-20.

144. Johnson-Delaney, C.A. and S.E. Orosz, *Ferret respiratory system: clinical anatomy, physiology, and disease.* Vet Clin North Am Exot Anim Pract, 2011. **14**(2): p. 357-67, vii.

145. Donnelley, M., et al., *Synchrotron phase-contrast X-ray imaging reveals fluid dosing dynamics for gene transfer into mouse airways.* Gene Ther, 2012. **19**(1): p. 8-14.

146. Smith, D., et al., *The selection of marmoset monkeys (Callithrix jacchus) in pharmaceutical toxicology.* Lab Anim, 2001. **35**(2): p. 117-30.

147. Hibino, H., et al., *The common marmoset as a target preclinical primate model for cytokine and gene therapy studies.* Blood, 1999. **93**(9): p. 2839-48.

148. t'Hart, B.A., et al., *Gene therapy in nonhuman primate models of human autoimmune disease.* Gene Ther, 2003. **10**(10): p. 890-901.

149. Deisboeck, T.S., et al., *Development of a novel non-human primate model for preclinical gene vector safety studies. Determining the effects of intracerebral HSV-1 inoculation in the common marmoset: a comparative study.* Gene Ther, 2003. **10**(15): p. 1225-33.

150. Hanazono, Y., K. Terao, and K. Ozawa, *Gene transfer into nonhuman primate hematopoietic stem cells: implications for gene therapy.* Stem Cells, 2001. **19**(1): p. 12-23.

151. Parsons, D.W., *Airway gene therapy and cystic fibrosis.* J Paediatr Child Health, 2005. **41**(3): p. 94-6.

152. Stick, S.M. and P.D. Sly, *Exciting new clinical trials in cystic fibrosis: infants need not apply.* Am J Respir Crit Care Med, 2011. **183**(12): p. 1577-8.

153. Stocker, A.G., et al., *Single-dose lentiviral gene transfer for lifetime airway gene expression.* J Gene Med, 2009. **11**(10): p. 861-7.

154. Kobinger, G.P., et al., *Filovirus-pseudotyped lentiviral vector can efficiently and stably transduce airway epithelia in vivo.* Nat Biotechnol, 2001. **19**(3): p. 225-30.

155. Tarantal, A.F., et al., *Lentiviral vector gene transfer into fetal rhesus monkeys (Macaca mulatta): lung-targeting approaches.* Mol Ther, 2001. **4**(6): p. 614-21.

156. Rawlins, E.L. and B.L. Hogan, *Ciliated epithelial cell lifespan in the mouse trachea and lung.* Am J Physiol Lung Cell Mol Physiol, 2008. **295**(1): p. L231-4.

157. Rock, J.R., et al., *Basal cells as stem cells of the mouse trachea and human airway epithelium.* Proc Natl Acad Sci U S A, 2009. **106**(31): p. 12771-12775.

158. Wilson, A.A., et al., *Amelioration of emphysema in mice through lentiviral transduction of long-lived pulmonary alveolar macrophages.* Journal of Clinical Investigation, 2010. **120**(1): p. 379-389.

159. Hyde, S., et al., *Multiple Doses Of Lipid-Mediated Gene Therapy Nebulised To The Mouse Lung Show Robust And Sustained Cftr Expression.* Pediatric Pulmonology 2011. **46**(S34): p. 281.

160. Lundwall, A., et al., *Rapidly evolving marmoset MSMB genes are differently expressed in the male genital tract.* Reprod Biol Endocrinol, 2009. **7**: p. 96.

161. Hoffmann, R., et al., *Distribution of ciliated epithelial cells in the trachea of common marmosets (Callithrix jacchus).* J Med Primatol, 2014. **43**(1): p. 55-8.

162. Hoffmann, R.M., F.J. Kaup, and M. Bleyer, *Atypical cilia in the respiratory tract of common marmosets (Callithrix jacchus) with and without concurrent lung disease.* Exp Lung Res, 2013. **39**(9): p. 410-4.

163. Donnelley, M., et al., *A new technique to examine individual pollutant particle and fibre deposition and transit behaviour in live mouse trachea.* J Synchrotron Radiat, 2010. **17**(6): p. 719-29.

164. Morgan, K.S., D.M. Paganin, and K.K. Siu, *Quantitative x-ray phase-contrast imaging using a single grating of comparable pitch to sample feature size.* Opt Lett, 2011. **36**(1): p. 55-7.

165. Morgan, K.S., D.M. Paganin, and K.K. Siu, *Quantitative single-exposure x-ray phase contrast imaging using a single attenuation grid.* Opt Express, 2011. **19**(20): p. 19781-9.